The Role of the Histone Demethylase KDM5A in Cellular Differentiation

BY

MICHAEL LOUIS BESHIRI
B.A. Assumption College, 1999

THESIS

Submitted as partial fulfillment of the requirements
for the degree of Doctor of Philosophy in Biochemistry and Molecular Genetics
in the Graduate College of the
University of Illinois at Chicago, 2014

Chicago, Illinois

Defense Committee:

Elizaveta Benevolenskaya, Chair and Advisor
Pradip Raychaudhuri
Toru Nakamura
Vadim Gaponenko
Qun-Tian Wang, Biological Sciences

This thesis is dedicated to my wife Anjali, whose personal sacrifice, remarkable patience, and unwavering support made this possible.

ACKNOWLEDGEMENTS

I would like to thank my friends in the lab, both past and present members for their friendship and their contributions to this work: Reni Váraljai, Dr. Katie Holmes, Sasha Vilkova, and Bill Richter. It has been a pleasure to work with them over the years. I would like to thank Dr. Khademul Islam for his collaborative efforts in this work. I would like to thank my family for their support throughout this endeavor.

MLB

TABLE OF CONTENTS

CHAPTER PAGE

TABLE OF CONTENTS (continued)

LIST OF TABLES

LIST OF FIGURES

FIGURE PAGE

LIST OF FIGURES (continued)

FIGURE PAGE

LIST OF ABBREVIATIONS

H3	Histone 3
H4	Histone 4
H3K4	Histone 3 Lysine 4
H3K4me3	Trimethylated Histone 3 Lysine 4
H3K4me2	Dimethylated Histone 3 Lysine 4
H3K4me1	Monomethylated Histone 3 Lysine 4
H3K27me3	Trimethylated Histone 3 Lysine 27
H3K9me3	Trimethylated Histone 3 Lysine 9
HMT	Histone Methyltransferase
HDM	Histone Demethylase
RIZ	Retinoblastoma Interacting Zinc Finger
KDM5A	Lysine-specific Demethylase 5A
JARID1A	Jumonji AT-rich Interactive Domain 1A
RBP2	Retinoblastoma Binding Protein 2
LID	Little Imaginal Discs
LSD1	Lysine-specific Demethylase 1
FAD	Flavin Adenine Dinucleotide
PHD	Plant Homeodomain
MBT	Malignant Brain Tumor Domain
CW	Cystein-Tryptophan domain
PWWP	Proline-Tryptophan-Tryptophan-Proline domain
JmjC	Jumonji C-terminal domain

LIST OF ABBREVIATIONS (continued)

JmjN	Jumonji N-terminal domain
ARID	AT-rich interacting domain
Jhd2	Jumonji Domain Histone Demethylase 2
JMJD2A	Jumonji Domain 2A
EdU	5-ethynyl-2'-deoxyuridine
DAPI	4',6-diamidino-2-phenylindole
ETC	electron transport chain
ROS	reactive oxygen species
NAC	N-acetylcysteine
IGF1	Insulin-like growth factor 1
siRNA	small interfering RNA
shRNA	short hairpin RNA
mES	mouse embryonic stem cells
ChIP	chromatin immunoprecipitation
ATP	adenosine triphosphate
SAHF	senescence associated heterochromatic foci
TUNEL	terminal deoxynucleotidyl transferase dUTP nick end labeling
CKD	cyclin-dependent kinase
SEM	standard error of the mean
ECAR	extracellular acidification rate
DMEM	Dulbecco’s modified eagle medium

LIST OF ABBREVIATIONS (continued)

FBS	fetal bovine serum
PBS	phosphate buffered saline
TE	Tris EDTA
PCR	polymerase chain reaction
FCCP	carbonylcyanide p-trifluoromethoxyphenylhydrazone
H_2DCFDA	2’-7’-dichlorodiydrofluorescein diacetate
DCF	2’,7’-dichlorofluorescein
DM	differentiation media
C[t]	threshold cycle
PFU	plaque-forming units
DKO	double knockout
GO	gene ontology
GOBP	gene ontology biological process
GOCC	gene ontology cellular component

SUMMARY

The retinoblastoma tumor suppressor pRB is required for differentiation of several tissues. pRB is a transcriptional regulator. It functions as both transcriptional activator and repressor by interacting with a multitude of co-regulators. It has been shown that the lysine-specific histone demethylase KDM5A is a critical co-regulator in RB-mediated differentiation. In *RB1* null cells, the additional loss of the *KDM5A* gene can restore features of the differentiated phenotype indicating an antagonistic relationship with pRB. However it is also known that KDM5A can cooperate with members of the RB family to repress cell cycle genes during differentiation. The mechanism by which the loss of KDM5A rescues differentiation has not been determined, and the details of KDM5A cooperation with the RB family to repress cell cycle genes during differentiation have not been fully explored. The current model based on previous works proposes that KDM5A negatively regulates a set of genes by demethylation of trimethylated histone 3 on lysine 4 (H3K4me3) and that these genes must be upregulated to allow differentiation to proceed. pRB promotes differentiation at least in part by relieving the repressive effect of KDM5A on this gene set. Simultaneously KDM5A binds to a set of cell cycle genes as differentiation progresses to drive the requisite cell cycle withdrawal in cooperation with the RB family proteins.

The work presented here further explores this model to determine the mechanism of regulation of differentiation, and the requirement for KDM5A demethylase function during differentiation and cell cycle exit. I have used the myogenic model of differentiation with mouse embryonic fibroblasts from WT, *Rb1*$^{-/-}$, *Kdm5a*$^{-/-}$, and double

knockout mice (DKO) to identify the critical genes during differentiation to be a large set that codes for components of the mitochondria. These genes are direct targets of both pRB and KDM5A. They are deregulated by the loss of *Rb1*$^{-/-}$ and rescued by the additional loss of *Kdm5a*. Accordingly the mitochondrial phenotype mirrors the expression pattern of these genes. Mitochondrial biogenesis and function are defective in *Rb1*$^{-/-}$ MEFs induced to differentiate. Additional loss of *Kdm5a* in the DKOs rescues these defects. Additionally I show that a functional catalytic domain is required for KDM5A function in cell cycle withdrawal and differentiation.

I. INTRODUCTION

A. Cellular differentiation in cancer

Deregulation of differentiation and the cellular pathways that control it is intimately associated with cancer [1-4]. The details of this deregulation are not fully understood, but it is known that inappropriate, chromatin-mediated repression and derepression of genomic regions is involved [5]. It is plausible that if cell type specific genes are ectopically activated or repressed due to the state of chromatin in their genomic environment, the differentiation state of the cell could be altered [6-8]. Differentiation and cell cycle exit are tightly linked [4, 9]. Preventing a progenitor cell from differentiating may keep it in a state of proliferation [10]. Alternatively, a mature cell may regress by a process termed dedifferentiation, back to a proliferating precursor and possibly pluripotency [11]. A thorough knowledge of the molecular mechanisms that set the fixed patterns of expression during lineage commitment is required to fully understand the role that deregulation of differentiation plays in cancer and to identify potential targets for therapeutic intervention.

B. KDM5A and pRB during differentiation

The focus of this work is primarily related to the function of the retinoblastoma protein (pRB) as a positive regulator of differentiation, with a particular interest in the role of the lysine-specific histone demethylase 5A (KDM5A) within the RB pathway. This includes regulation of permanent cell cycle withdrawal during terminal differentiation and

regulation of the overt features of differentiation in general such as expression of tissue-specific markers and the morphological changes associated with a given cell type.

KDM5A was first identified in 1991 in a screen for proteins that interact with pRB [12]. So it is fitting that KDM5A operates as part of the pRB pathway in numerous capacities and cellular contexts [13-17]. pRB is a hub of cellular regulation. It directs control over multiple cellular processes through interactions with several proteins [18, 19]. pRB regulates the cell cycle, senescence, apoptosis, autophagy, metabolism and differentiation, all of which are deregulated in cancer [20].

pRB is a member of what is called the “pocket protein” family of proteins named after the so-called pocket domain shared by the family members [21]. Besides pRB there are two other pocket proteins: p107 and p130 [22]. There is a high degree of conservation within the shared pocket domain of these three proteins, but much less so outside of this domain, particularly with respect to pRB [23]. The two proteins, p107and p130, are more closely related to each other (50% overall sequence homology) than they are to pRB, where they share about 30% sequence homology [23]. Therefore it is not surprising that there is only a limited capacity for p107 or p130 to compensate for the loss of pRB function in the cell [19, 24].

RB1 was the first gene to be identified as a tumor suppressor, and either the *RB1* locus itself or components of its upstream regulatory pathway are mutated in more than 80% of human cancers [25-27]. Upstream mutations include loss of function of $p16^{INK_4A}$, a positive regulator of pRB, and amplification of Cyclin D1 a negative regulator of pRB [28]. Despite decades of research that have gone into understanding pRB function, it is still far from clear as to how exactly pRB is able to suppress tumor formation, and why

disruption of this pathway is such a critical step in tumorigenesis [29]. It is best known and best understood as a negative regulator of the cell cycle, in complex with E2F transcription factors [30]. Activating E2Fs 1,2 and 3 localize to cell cycle genes and activate transcription, driving the transition from G1 to S phase [31]. Hypophosphorylated pRB is recruited to E2F target genes by interacting with the E2F proteins [27]. At the target genes pRB induces transcriptional repression by blocking the E2F transactivation domain and by direct recruitment of co-repressors such as histone deacetylase (HDAC) enzymes [27]. Phosphorylation of pRB by cyclin-dependent kinases (CDKs) in complex with Cyclins causes pRB to dissociate from the complex with E2F allowing transcriptional activation [27].

There is no doubting the importance of pRB in cancer [32]. Development of a treatment that targets the RB pathway could have a great impact on cancer therapy. The challenges associated with such a treatment are many. They lie in the diverse cellular roles of pRB protein; the fact that pRB is inactivated in cancer means that a treatment would have to somehow reactivate pRB; and the numerous ways in which the pathway is affected, means that an effective RB-directed treatment in one cancer type may not work in another [32]. One promising approach is to target the negative regulators of pRB - the cyclin-dependent kinases that phosphorylate pRB [33]. Development of inhibitors of CDKs is currently underway, however; other options must be pursued for several reasons [34].

Although the role of CDKs in pRB regulation has been known for decades a viable drug is yet to reach the market, and there is no guarantee that this approach will be successful. Data derived from knockout mice and in vitro cell studies have revealed

the ability of cells to proliferate in the absence of CDK2 and 4 or CDK4 and 6, and in the absence of the CDK binding partners: Cyclins D1-3 [35-38]. Additionally, the inhibitory nature of phosphorylation on pRB has been studied mostly in the context of the cell cycle, where phosphorylation events disrupt the complex of pRB with E2F1 [30]. However, it is less clear if phosphorylation equally affects other important aspects of pRB function. For example it has been shown that phosphorylated pRB *is* able to interact with E2F1 in a pro-apoptotic complex after cells undergo DNA damage [39]. Preventing phosphorylation in this condition may have an undesirable effect on health. Additionally, if phosphorylated pRB is functional in this process, then it is conceivable that it may also be functional in other processes in which it operates. Also, while in most cases it is the upstream regulatory pathway that is deregulated in cancer, *RB1* itself is affected in about one third of all cancers, and so targeting the upstream pathway would likely be ineffective in those situations [40]. We must consider that the RB pathway is deregulated by these different and mutually exclusive mechanisms for a reason [28]. Deregulation of particular components of the RB pathway are preferentially selected in a given cancer type [28]. This is true even for different cancers that affect the same organ [28]. For example, small-cell lung cancer features the loss of pRB (> 90%), while non-small-cell lung cancer is primarily associated with loss of $p16^{INK_4A}$ [28]. In both cancers it is one or the other that is affected, but not both [28]. For the reasons described above, targeting the RB pathway will likely require context-specific approaches depending on the type of cancer and the particular component of the RB pathway that is affected.

As our understanding of pRB function progresses, it is becoming more and more evident that its importance as a tumor suppressor stems from its pleiotropic role as a

regulator of several cellular processes [32]. Besides cell cycle regulation, pRB has been implicated as critical to senescence, apoptosis, autophagy, differentiation, and most recently metabolism [34, 39-48]. It must be taken into consideration that the ability of pRB to act as a tumor suppressor is not limited to its role simply as a cell cycle regulator, and so other aspects of pRB function need also be considered [13, 17, 49].

Regulation of differentiation is emerging as a key function of the pRB protein for its ability to suppress tumor formation [13, 17, 49]. pRB is a positive regulator of several differentiation programs [32]. The current list of cell types that depend on pRB for proper differentiation includes skeletal muscle cells, adipocytes, neurons, osteocytes, erythrocytes, granulocytes, monocytes, lens cells, keratinocytes, and retinal rod photoreceptors [9, 32]. pRB is also required for placental development [50]. *Rb1*$^{-/-}$ mice die by day E15.5 due to placental abnormalities [50-53]. *Rb1* null embryos that are provided with a wild type placenta survive to birth but die soon after [50].

Studies using *RB1* mutants first revealed the significance of regulation of differentiation for the function of pRB as a tumor suppressor [49]. There are two classes of RB-mutations: highly penetrant and partially penetrant (Fig. 1). Most of the mutations that affect pRB occur within the pocket domain of the protein (Fig. 1). The majority of cases of hereditary retinoblastoma are caused by mutations that exhibit high penetrance with high expressivity. Carriers of mutant *RB1* develop the disease at a rate of 80-90% and in most cases develop multiple, bilateral tumors [54]. However certain naturally occurring mutations to the *RB1* gene exist that produce a protein with limited function (Fig. 1). These mutations demonstrate lower penetrance [54]. Interestingly it has been shown that these mutant forms of pRB are unable to interact with E2Fs and

unable to block cell cycle progression when reintroduced into *Rb1*$^{-/-}$ cells [49]. They are however able to promote differentiation [49]. On the other hand, the highly penetrant mutants have lost the capacity for regulation of both the cell cycle and differentiation [49]. These observations suggest that loss of pRB causes retinoblastoma due to its role as a negative regulator of the cell cycle and as a positive regulator of differentiation. It is also noteworthy that mutations rarely occur in the E2F genes in cancer, adding another level of support to the notion that pRB tumor suppression consists of more than regulation of the cell cycle [55]. It is therefore imperative that multiple approaches to targeting the RB pathway be implemented in order to reach the objective of successful therapeutic intervention.

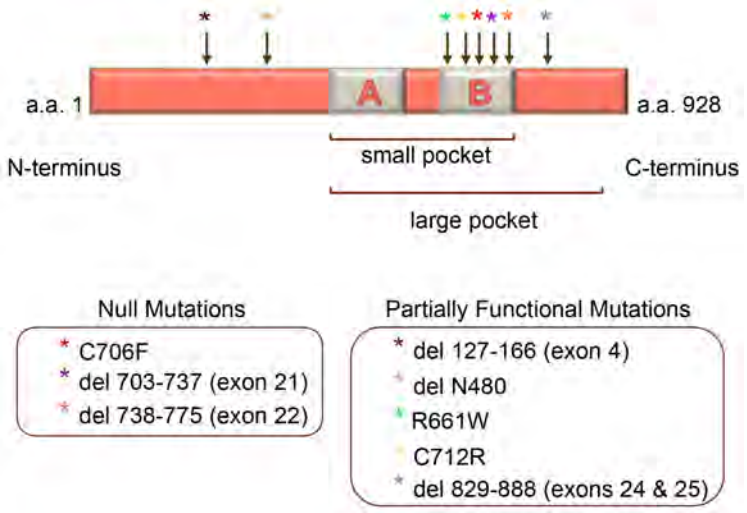

Figure 1. Mutations of the retinoblastoma tumor suppressor, pRB.

pRB is a 928 amino acid (a.a.) protein. The majority of its interactions with other proteins occur in the large pocket region. Within the large pocket is the small pocket region composed domains A and B. Several of the known mutations of the pRB protein are shown above. Mutations of pRB come in two categories: (1) Null mutations that entirely eliminate pRB function. These include a conversion of cysteine 706 to phenylalanine; deletion of a.a. 703-737 within exon 21; and deletion of 738-775 within exon 22. (2) Partially functional mutations where pRB retains some of its functional capacity. These include deletion of a.a. 127-166 of exon 4; deletion of asparagine 480; a conversion of arginine 661 to tryptophan; a conversion of cysteine 712 to arginine; and deletion of a.a. 829-888 spanning exons 24 and 25. References for figure 1: [54, 56].

As described above, regulation of differentiation has been shown to be a key factor in tumor suppression by pRB [9, 19, 23, 43, 52, 57, 58]. It therefore follows that it may be possible to exploit this aspect of pRB function to treat cancer. Unfortunately, little is known about how pRB regulates differentiation. It is known to be required for proper execution of several differentiation programs [9, 32]. For example, deletion of *Rb1* in myoblasts results in their failure to complete terminal differentiation [57]. Unlike its role in cell cycle regulation, pRB is involved in activating transcription during differentiation [32]. Some clues as to its function in promoting differentiation come from studies showing that several tissue-specific transcription factors require *RB1* to activate transcription: these include MYOD in myogenic differentiation, RUNX2 in osteogenic differentiation, NF-IL6 in monocyte, macrophage and adipogenic differentiation, and C/EBP in adipogenesis [23, 30, 59]. Currently it is not clear how pRB activates transcription. Some data suggests that it may directly cooperate with these factors to augment their positive transcriptional activities; while other data support and alternative scenario, where it may indirectly activate transcription by inhibiting negative regulators [23, 32]. It is possible that pRB may activate transcription by both of these proposed mechanisms.

A study published in 2005 indicated that the H3K4 histone demethylase KDM5A is a critical downstream component of the RB pathway regulating differentiation [17]. The role of KMD5A in pRB-mediated differentiation was not tissue specific, but broadly implicated in the regulation of differentiation of several tissue-types, pointing to the importance of this protein to the general function of the pathway[17]. Specifically, KDM5A was identified in a screen for pRB-interacting proteins that retain the ability to

complex with the low penetrant pRB mutants [17]. These are the same pRB mutants that were shown to be unable to regulate the cell cycle while retaining their pro-differentiation capacity [49, 54]. They showed that the pRB-KDM5A interaction occurred only in cells induced to differentiate but not in proliferating progenitors [17]. Importantly, they also showed that by knocking down *Kdm5a* in *Rb1*$^{-/-}$ MEFs they could rescue the expression of late markers of differentiation when the MEFs were induced to differentiate down the myogenic or adipogenic lineages [17]. Also, knockdown of *KDM5A* in the Saos2, *RB1* null osteogenic cell line resulted in the expression of markers of osteogenic differentiation, and a senescent phenotype [17]. Overall the effect of knocking down *KDM5A* mimicked, both the overall phenotype and the underlying gene expression patterns that are observed upon reintroduction of WT pRB into these cells [17]. The results of this study suggested a model where KDM5A represses a set of genes that are required for differentiation in order to maintain an undifferentiated state (Fig. 2) [17, 60]. pRB then promotes differentiation by relieving the repressive effect of KDM5A on these genes either by modifying KDM5A function somehow, or by physically removing KDM5A from the chromatin, possibly through a direct interaction (Fig. 2) [17, 60]. So that the reason *RB1*$^{-/-}$ cells are defective in their ability to differentiate is because pRB is not available to stop KDM5A from blocking differentiation [17, 60].

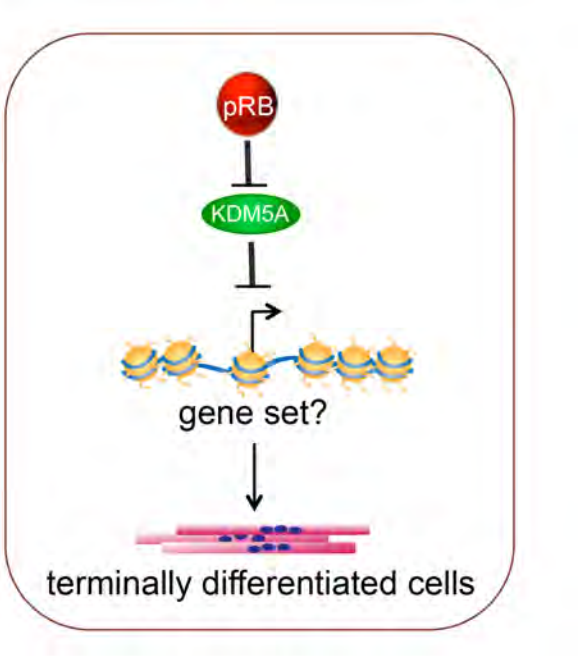

Figure 2. Potential model for pRB and KDM5A regulation of differentiation.

KDM5A represses transcription of a set of genes in undifferentiated cells. Upregulation of these genes is necessary for differentiation to occur. This upregulation in WT cells is achieved when pRB relieves the repressive effect of KDM5A, possibly through a direct interaction. This model predicts that *RB1*$^{-/-}$ cells do not differentiate because pRB is not available to challenge repression by KDM5A. The requirement for pRB can be bypassed by knocking down *KDM5A* in *RB1*$^{-/-}$ cells resulting in a rescue of the phenotype. Reference for figure 2: [17].

Interestingly, in addition to its antagonistic relationship with pRB and acting in general as a negative regulator of differentiation, a second role for KDM5A in RB-mediated differentiation has been identified [15, 16, 61]. In this case however, KDM5A works in cooperation with the pocket protein family, specifically p130 and E2F4 to shut down expression of cell cycle genes to promote cell cycle-withdrawal during terminal differentiation [15, 16, 61]. In a hematopoietic model KDM5A was shown to bind to cell cycle-related E2F target genes in a manner that was temporally correlated to the progression of differentiation and gene silencing [15]. In another study, we found that KDM5A independently colocalized with a p130/E2F4 complex at cell cycle gene promoters during differentiation (Fig. 3) [16]. KDM5A promoted transcriptional repression by demethylating H3K4me3 [16]. The p130/E2F4 complex was required for histone deacetylation at the promoter, consistent with previous work showing that localization of HDACs required p130 and E2F4 [62].

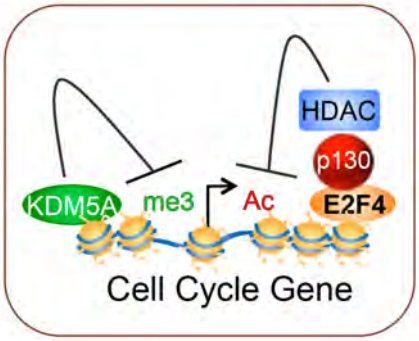

Figure 3. Model of how KDM5A cooperatively represses cell cycle genes during differentiation.

KDM5A colocalizes with the RB-family protein p130, and E2F4 at cell cycle gene promoters during differentiation. KDM5A represses transcription by demethylation of H3K4me3. The p130/E2F4 complex is required for deacetylation of histone 3.

References for figure 3: [15, 16].

The significance of the relationship between pRB and KDM5A in carcinogenesis is evident from *in vivo* mouse studies. Deletion of both *Rb1* alleles is embryonic lethal but, $Rb1^{+/-}$ mice develop thyroid and pituitary tumors due to the stochastic loss of heterozygosity at the *Rb1* locus [51]. Importantly, when *Kdm5a* is also deleted in $Rb1^{+/-}$;$Kdm5a^{-/-}$ mice, tumor formation is suppressed and survival of the mice is extended [13]. The fact that loss of *Kdm5a* in addition to *Rb1* has an anti-tumorigenic effect despite the role of KDM5A to promote cell cycle withdrawal (Fig. 3), suggests that its other role as a negative regulator of differentiation (Fig. 2) is somehow dominant with respect to tumor formation.

In order to understand how KDM5A operates in the RB pathway during differentiation, it is important to have a general knowledge KDM5A structure and function. Although KDM5A was first discovered in 1991, it was largely overlooked for more than a decade, until it was shown to be a key component of RB-mediated differentiation [12, 17]. In 2007 it was determined to be an epigenetic regulator with a capacity for histone demethylation [63, 64]. This is significant, as epigenetic regulation is burgeoning as a field of study, and it is one that has implications for development, differentiation and cancer [65-71].

The function of pRB as a tumor suppressor is tied to its role as a regulator of differentiation [49]. The means by which pRB regulates differentiation is at least in part through a relationship with KDM5A [17]. This is a complex relationship that includes two opposing roles for KDM5A in the pRB pathway during differentiation. One as a positive regulator, where it acts to promote cell cycle withdrawal in cooperation with the RB family and, second as a negative regulator, where it acts in opposition to pRB to

maintain the undifferentiated state [15, 16, 61]. What is not yet clear is how exactly does pRB promote differentiation? What are the critical set(s) of genes that are involved? What is the specific role of KDM5A? We know from earlier work that it is a negative regulator in opposition to pRB, but again, what are the critical genes and what is the mode of regulation?

C. Epigenetic regulation

1. Epigenetic regulation and differentiation

All somatic cells contain the same DNA sequence (with the exception of somatic recombination and hypermutation in particular DNA regions in certain immune cells), yet differentiation yields a high degree of cellular specialization that is visible in both function and morphology [72]. How does this happen? Epigenetic regulation has been shown to play a prominent role in differentiation [65-67]. As a term epigenetics was first coined in 1942, and as a field it was an early link between developmental biology and genetics [73, 74]. Currently epigenetics is closely associated with the molecular mechanisms that control gene expression during and after development [67, 69-71, 73-75]. In many cases this involves chemical modifications to the DNA itself or the histones around which the DNA is wrapped [76]. These epigenetic modifications to the DNA and histones, directly or indirectly alter the state of chromatin to affect gene expression [73]. This in turn allows for different global expression patterns that are the driving force of specialization [67]. Transcriptionally permissive euchromatin is in general more open and accessible to transcriptional regulators, while the transcriptionally repressive

heterochromatin is more compacted and less accessible [77, 78]. These states of compaction are however not static and are subject to change to suit the needs of the cell whether it be and adaption to external stimuli or induction of differentiation [7, 69, 75]. Additionally chromatin possesses another layer of regulatory function - that of its organization within chromosomal territories and its association with the nuclear envelope [79, 80]. This nuclear architecture is thought to regulate gene expression by strategically positioning chromatin in regions where it may interact with transcriptional regulating proteins [80]. These dynamic properties of chromatin are essential to the transcriptional flexibility required to create hundreds of specialized cell types from a single genome [81].

2. Histone lysine methylation

The various epigenetic modifications to the chromatin determine its physical state [82]. Such modifications arise from DNA methylation, covalent post-translational modification of histones, incorporation of histone variants into nucleosomes, ATP-dependent remodeling, and the actions of various noncoding RNAs [67].

Covalent but reversible post-translational modification of histone tails is a critical, if not fully understood, mode of epigenetic regulation [67]. It plays a major role in the maintenance of stem cell chromatin and the dynamic alterations that occur as cells undergo differentiation [67]. Several of these modifications are known: methylation, phosphorylation, acetylation, ubiquitination are four examples [83]. Of primary interest to this work, is the methylation of lysine residues. This modification occurs by the addition of one, two, or three methyl groups to the ε-amino group of the lysine residue [83, 84]. Unlike some other well studied modifications, acetylation for example, which weakens

the association of DNA to the histones by affecting the charge of the histone, methylation is not known to directly affect the chromatin state on its own [76]. Rather it serves as a docking factor to recruit certain effector proteins to the chromatin [85, 86]. It can also act as a blocking factor to prevent the binding of other effectors [85, 86]. Also in contrast to acetylation, which is only associated with transcriptional activation, methylation may be involved in activation or repression [76]. The position of the amino acid within the sequence of the histone tail and the number of methyl groups attached, define the function of the mark [86]. For example H3K4me3 is found at the promoters of genes and is associated with active transcription while H3K27me3 is associated with repressed transcription [77, 78, 87].

There is only a subtle, physical difference between H3K4me3 and H3K27me3, yet their functional outcomes could not be more polarized. How is this so? How can such minor variations to the relatively large histones, have such impressive and opposite, outputs? The proteins that “read and write” and “erase” these modifications are in this regard, at least as important as the marks themselves.

3. Histone lysine modifying proteins

There are three types of proteins associated with histone methylation. They can be generally classified as “writers”, “erasers”, and “readers” [84, 88]. Writing is carried out by the histone methyltransferase enzymes (HMTs). Lysine-specific methyltransferases deposit one, two or three methyl groups to lysine residues on histones H3 and H4 [89, 90]. There are several mammalian HMTs with different specificities and therefore different functions. All but one HMT fall into the large family of SET (Su(var)3-9 Enhancer of Zeste) domain-containing enzymes [91-93]. They carry

out methylation through the highly conserved SET domain [94]. This large family is further subdivided into four smaller groups: SET1, SET2, SUV39 (suppressor of variegation histone 3 lysine 9), and RIZ (retinoblastoma interacting zinc finger) [89].

Previously believed to be permanent, histone methylation has within the last decade been shown to be quite reversible [95-99]. The proteins responsible for "erasing" the methyl mark are the histone demethylases (HDMs). In the case of methylated lysine, several enzymes have been found to act as specific demethylases [100]. The first discovered enzyme of this category was the lysine-specific histone demethylase, LSD1 [98]. It can remove the mono- and dimethylated state of H3K4 and H3K9 via an amine oxidation reaction using flavin adenine dinucleotide (FAD) as a cofactor [98, 100, 101]. Since then a large superfamily of Jumonji C domain (JmjC) enzymes have been identified as histone demethylases, with the capacity to remove all three states of lysine methylation [100, 102-105]. KDM5A belongs to this JmjC domain containing of histone demethylases [63, 64].

The JmjC domain is enzymatic. It can catalyze the removal of methylation through a hydroxylation reaction that requires Fe(II) and α-ketoglutarate (αKG) as cofactors [100]. The reaction is thought to occur as follows: The JmjC domain first binds to Fe(II) which then binds αKG and an O_2 molecule [100]. This leads to the oxidative decarboxylation of αKG that generates CO_2, succinate and Fe(IV), also known as ferryl [100]. Ferryl is a highly reactive form of iron with an oxidation number of 4 [106]. Ferryl is thought to then oxidize the carbon of a methyl group bound to the ε-nitrogen of the lysine resulting in an unstable carbinolamine that quickly degrades to release formaldehyde [100].

Many proteins such as KDM5A interact with chromatin by binding directly to modified-histone tails [10, 84, 86]. This is the “reading” capacity [88] [84]. This group is largely represented by epigenetic regulators, the “writers”, “erasers” and the chromatin remodelers, but the ability to read histone marks is also found in proteins that regulate transcription, DNA damage repair, recombination, replication, and RNA processing [86]. These proteins are recruited to the chromatin by directly binding to specifically modified histones through one of several known domains [84, 86]. It is not uncommon for reader proteins to have multiple reader domains with different specificities [86]. Additionally, some proteins with “reading” capacity, including KDM5A, also have DNA-binding domains that contribute to the specificity of binding [86, 107]. In the case of methylated lysine, there are several known reader domains: PHD (plant homeodomain), Tudor domain, WD40 (tryptophan-aspartic acid repeat domain), chromodomain, MBT (malignant brain tumor domain), ankyrin repeats, zf-CW (cysteine-tryptophan domain), and PWWP (proline-tryptophan-tryptophan-proline domain) (Table I) [86]. These methyl-binding domains are highly specific. They can discriminate, not only between different methylated lysines on the same histone tail, but in some cases, by the number of methyl groups on the same residue [86, 108]. This specificity is derived from three factors: (1) the number of methyl groups (2) the position of the modified lysine within the histone (3) interaction with flanking sequence amino acids [86]. In addition to its “erasing” function, KDM5A possesses “reading” capacity through its PHD domains [10, 100].

Domain	Methylated Histone and Amino Acid Residues that are Recognized
PHD	H3K4, H3K9
Tudor	H3K4, H3K9, H3K79, H4K20
WD40	H3K9, H3K27, H4K20, H1K26
Chromo	H3K4, H3K9, H3K23, H3K27, H3K36
MBT	H3K4, H4K20, H1K26
Ankyrin Repeats	H3K9
Zf-CW	H3K4
PWWP	H3K36, H4K20

Table I. Domains that bind to methylated histones.

Left column is the name of the domain. Right column is the specific Histone(s) and Lysine residue(s) that is/are recognized. Table I reference: [86].

D. KDM5A structure

KDM5A is also known as JARID1A (Jumonji AT Rich Interactive Domain 1A) and RBP2 (Retinoblastoma-Binding Protein 2). It is one of four members of the KDM5 histone demethylase family of proteins that also includes KDM5B, KDM5C and KDM5D. This group belongs to the larger family of JmjC domain-containing demethylase enzymes [100]. Within the KDM5 family, KDM5C and KDM5D are highly homologous, sex chromosome-specific, and are the least well studied. KDM5A and KDM5B share a high degree of sequence homology but exhibit different cellular roles [88]. This family of proteins (along with the LSD1 demethylase) is responsible for the removal of methylation from histone 3 on lysine 4. Unlike LSD1, KDM5 enzymes are able to demethylate all three methylation states of H3K4 in vivo [63].

The *KDM5A* gene is located on chromosome 12 in humans (12p13.33). The protein product is made up of 1,690 amino acids (a.a.) (Ensembl). Structurally, KDM5A contains several known domains (Fig. 4).

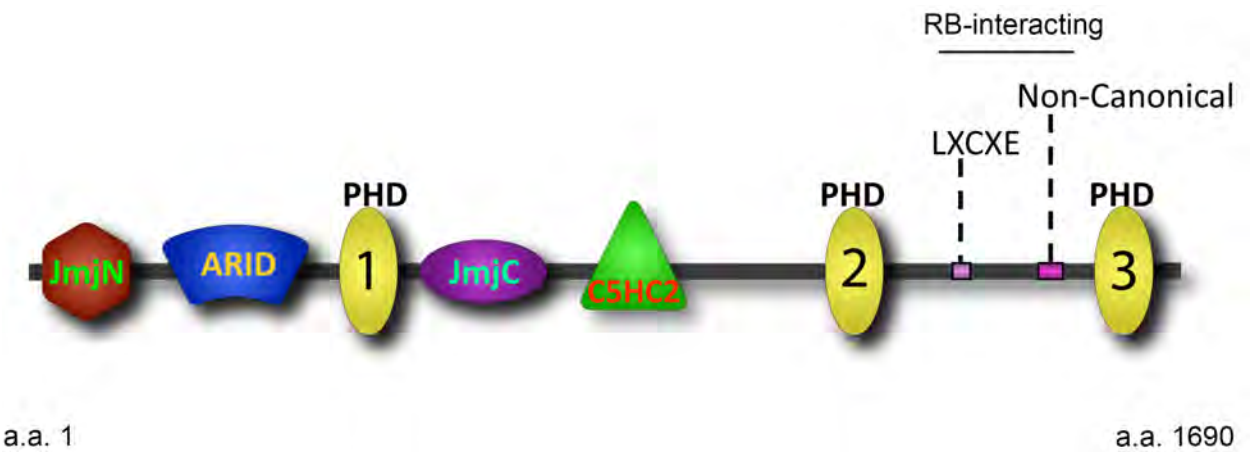

Figure 4. Domain structure of KDM5A.

KDM5A contains 1690 amino acids (a.a.). JmjN (Jumonji N-terminal domain (a.a. 20-53)) has unknown function but may interact with and be required from JmjC catalytic activity. ARID (AT-Rich Interacting Domain (a.a. 82-170)) is a DNA binding domain with specificity for the sequence CCGCCC. JmjC (Jumonji C-terminal domain (a.a. 470-586)) is the catalytic domain. C5HC2 (a.a. 676-728) is a zinc finger domain with unknown function. PHD1-3 (PHD1 a.a. 295-342; PHD2 a.a. 1163-1217; PHD3 a.a. 1607-1661) are Plant Homeo Domains. PHD domains are known to bind to methylated lysines. LXCXE (a.a. 1373-1377) is a canonical RB-interacting domain found in several RB-interacting proteins. The Non-Canonical domain is a second less well-defined RB-interacting domain. Its exact location in the sequence is unknown but is located between a.a. 1457-1558. References for figure 4: [100, 109].

The JmjC domain is the catalytic demethylase domain (Fig. 4). It is highly conserved across several species including both fission and budding yeast, *Caenorhabditis elegans*, *Drosophila melanogaster*, mice and humans [110].

KDM5A has three PHD domains (Fig. 4). PHD domains are known to bind to methylated lysines on histone tails [86]. They are frequently found on chromatin-binding epigenetic regulators [10, 108]. The third PHD domain of KDM5A has been shown to bind directly and specifically to H3K4me3 and with a lower affinity to H3K4me2, but not to H3K4me1 or H3K4me0, and not to other H3 methylated lysines: K9, K27, K36, or K79 [10]. PHD3 of KDM5A is likely involved in recruitment of the KDM5A protein to its target locations on the chromatin [10]. The binding capacity/specificity of the other two PHD domains has not been determined.

The AT-rich interacting domain (ARID) domain of KDM5A is a DNA binding domain that has been shown to have specificity for the CCGCCC motif (Fig. 4). Its role in recruitment of KDM5A to its target locations has not been studied in depth to this point [107].

Additionally, KDM5A has two other known domains with less clearly defined roles. **1)** A JmjN domain and a C5HC zinc finger domain (Fig. 4). The full function of the JmjN domain is not understood, however; it is known that this domain in the budding yeast ortholog Jumonji Domain Histone Demethylase 2 (Jhd2) is required for the demethylase activity of the JmjC domain [111]. Further, the JmjN domain of the human Jumonji Domain 2A (JMJD2A) demethylase protein has been shown by crystal structure to interact directly with the JmjC domain [112]. **2)** A C5HC zinc finger domain (Fig. 4).

Less is known about this domain, but it has been identified in other chromatin modifying proteins [113, 114].

Finally, KDM5A has two pRB-interacting domains (Fig. 4): a canonical LXCXE domain at amino acids 1373 - 1377, and a second non-canonical domain whose exact sequence has not been determined but is located somewhere between amino acids 1457 - 1558 [115].

In summary, KDM5A is a large protein with several domains. Although the full range of KDM5A's role in the cell is currently unknown, its numerous and varied domain structures and its capacity for multiple protein:protein interactions, are likely to be the key to KDM5A's diversity of function. Interesting questions with regards to differentiation are what is the requirement of the demethylase domain, and how is the specificity of function for KDM5A regulated? Possible mechanisms include post-translational modification, protein interactions, and DNA and histone-binding domains. In this work, I look at the requirement of a functional JmjC domain for differentiation, and briefly at post-translational modification of KDM5A.

E. KDM5A function in transcriptional regulation

KDM5A is widely expressed in adult human tissues (EMBL-EBI expression atlas database). It has also been shown to be expressed in mouse ES cells and to bind and regulate expression of developmental genes [13, 64, 116]. KDM5A is interesting in that it is known to act as both a transcriptional repressor and activator with functions in multiple biological processes [13-17, 63, 64, 116-125]. As a histone demethylase that removes H3K4me3, a mark associated with transcriptional activation, KDM5A is

generally considered to be a transcriptional repressor. Multiple publications have shown that it does in fact repress transcription by demethylation of H3K4 in several different contexts [13-17, 63, 64, 110, 116-120].

It is therefore somewhat counterintuitive that KDM5A and its orthologs in flies and yeast have also been shown to be involved in transcriptional activation in other specific contexts [17, 121-125]. How it is able to activate transcription is not entirely clear but there are a number of publications that offer insights into this mechanism [17, 121-125]. In both *Drosophila* and fission yeast, the KDM5A ortholog was shown to directly interact with transcriptional activator proteins [122-125]. These interactions occurred in the JmjC domain resulting in an inhibition of its demethylase function [122-125]. In mammals and *Drosophila*, it was recently found that KDM5A was recruited to target gene promoters by transcription factors that control circadian rhythm [121]. At the target gene it inhibited the function of transcriptionally repressive HDACs that were also bound to the same promoter [121].

Evidence exists, demonstrating that KDM5A is involved in both activation and repression of different genes during differentiation [13, 17]. Despite these observations of duality, it seems that ability to block differentiation in the absence of pRB is due to the transcriptional repressive function [17].

F. The myogenic model system

KDM5A is an integral component of the pRB pathway that operates during differentiation [13, 15-17, 61]. The goal of this thesis work has been to further understand the role of KDM5A in the pRB pathway as it relates to differentiation. How

does the loss of *KDM5A* rescue defects in differentiation caused by loss of *RB1*? More specifically, what are the genes and molecular pathways that are regulated by KDM5A and pRB during differentiation: what genes are deregulated by the loss of *RB1,* and is expression restored by the additional loss of *KDM5A*? How does the loss of *KDM5A* affect other processes, like cell cycle, and apoptosis during differentiation? Does regulation of differentiation by KDM5A require its histone demethylase function?

In order to study the dynamic roles of KDM5A and pRB during cellular differentiation I have used the myogenic model. Myogenesis is a frequently used and well-characterized model system used for the study of differentiation [126]. It has been employed to study differentiation in contexts including but not limited to transcriptional regulation of differentiation, cell cycle withdrawal that occurs during differentiation, as well as differentiation specifically related to pRB, and to characterize global epigenetic changes that occur during differentiation [8, 57, 61, 126-128]. It has the benefits of having a fairly well characterized transcriptional network; several well known myogenic markers; drastic, easily visualized morphological changes; myoblast cell lines that are easily induced to differentiate; and the fact that mouse embryonic fibroblasts (MEFs) can be reprogrammed to differentiate down this lineage [57, 126, 129, 130]. MEFs are advantageous in that they are primary cells and can be extracted from knockout mice to yield cells with a knockout genotype that can be studied *in vitro*.

Myogenic differentiation of myoblasts or MEFs *in vitro* results in the formation of terminally differentiated myotubes (Fig. 5) [129]. Myotubes are large multinucleated, tube-like cells [130]. Multinucleation is due to the fusion of myoblasts during the differentiation process [130]. The tube-like morphology is a functional necessity of

muscle contraction and is caused by the ordered arrangement of cytoskeletal proteins [131].

Myogenesis in nature is driven by the myogenic regulatory factors (MRFs) (Fig. 5) [132]. These are a family of four basic-helix-loop-helix transcription factors that includes MYOD and Myogenin (MYOG) [132]. Along with the MEF2 (Myocyte Enhancer Factor-2) family of transcriptional regulators, they are at the center of a large transcriptional network, working in cooperation to drive cell fate specification and lineage commitment, followed terminal differentiation (Fig. 5) [126]. *MYOD* is expressed in the mesodermal germ layer where it directs myogenic lineage commitment [133, 134]. This is followed by expression of *MYOG* and *MEF2*, which are required to complete terminal differentiation [133, 134]. Ectopic expression of MYOD or myogenin, but not MEF2, is sufficient to reprogram fibroblasts into myotubes [134].

Myogenesis can be divided into early and late-stage differentiation (Fig. 5) [126, 132, 133, 135]. Each is associated with stage-specific features that can be used to distinguish between events occurring early during myogenesis and those occurring late [126, 132, 133, 135]. Expression of MYOD occurs in the undifferentiated, uncommitted cells. MYOD activity is kept in check by growth factors that activate CDK/Cyclin D1 activity [136]. This complex phosphorylates MYOD to keep it inactive to maintain the undifferentiated state [136]. Because of this, in vitro differentiation is induced in media containing low serum levels.

Upon serum withdrawal and activation of MYOD, the cells begin the process of early differentiation to form committed myoblasts [137]. Myoblasts upregulate a second critical transcription factor: myogenin [133, 134]. Myogenin is not only a commonly used

molecular marker of early differentiation but is also required for the downstream completion of terminal differentiation [133, 134, 138]. There are several distinct steps between the myoblast stage and the formation of mature myotubes (Fig. 5) [139]. Myoblasts undergo further differentiation into myocytes [139]. Myocytes are mononucleated and have an elongated spindle-like morphology [139]. These cells are motile and move into contact with each other where they ultimately fuse together [139].

The initial fusion events result in the formation of nascent myotubes (Fig. 5). These cells have a tubular morphology but contain only a few nuclei and are smaller than mature myotubes [139]. The nascent myotubes undergo further fusion events either with other nascent myotubes or with myocytes to ultimately form the mature myotube [139]. Mature myotubes are characterized by a high degree of Multinucleation (Fig. 5). They can contain up to several hundred nuclei [138]. Additionally they can be identified by expression of molecular markers such as the structural protein, myosin heavy chain (MYHC) [138].

Cell cycle withdrawal occurs during the terminal differentiation process, after the formation of committed myoblasts marked by expression of myogenin [9, 140-142]. The process requires pRB but not the other pocket proteins, p107 or p130 [127]. Not coincidentally, expression of *RB1* is upregulated by MYOD and there is an increase of the active, unphosphorylated form of pRB in the committed myoblasts [142, 143]. pRB promotes cell cycle withdrawal by repression cell cycle genes (Fig. 5) [9]. It has been shown to recruit epigenetic repressors such as HDAC1 and the SWI/SNF chromatin remodeling complex to cell cycle promoters [144].

As described above in section B of this introduction, pRB is required for proper activation of the differentiation program in a manner that is independent of its requirement to drive cell cycle exit, but he mechanism by which pRB acts, to potentiate the myogenic program, is not clear [9]. In addition to the epigenetic changes that repress cell cycle genes, it is also known that there is, in general large-scale-changes to the chromatin landscape that underlies the activation of tissue specific genes and repression of non-lineage genes [8, 128]. There is an increase of H3K4me3 at the promoters of genes that are upregulated during myogenesis [8]. pRB has been shown to interact directly with the H3K4me3 demethylase KDM5A; and KDM5A has been shown to work in opposition to pRB to repress gene transcription and differentiation in general (Fig. 5) [12, 17].

In my studies I have used the myogenic model to further characterize the nature of the relationship between pRB and KDM5A and to better understand the genetic mechanism by which pRB and KDM5A control differentiation. I have used ectopic expression of *MYOD* by adenoviral vectors and lentiviral vectors to force myogenic differentiation of mouse embryonic fibroblasts (Fig. 6). Primarily I used MEFs of the following genotypes: WT, *Rb1*$^{-/-}$, *Kdm5a*$^{-/-}$, and *Kdm5a*$^{-/-}$*; Rb1*$^{-/-}$ (DKO) [13, 51, 63]. This model system has allowed me to examine the specific differences between these genotypes during differentiation that are associated with the loss of *Rb1*, *Kdm5a*, or both.

Figure 5. Model of myogenic differentiation.

Transcriptional activation of myogenic differentiation is driven by myogenic regulatory factors (MRFs): MYOD and Myogenin, in cooperation with the myocyte enhancer factor-2 (MEF2) family of transcription factors. The process requires the pRB tumor suppressor. pRB has a dual role of promoting cell cycle exit and promoting expression of the myogenic transcriptional program in cooperation with the myogenic factors. MYOD is expressed in the mesodermal germ layer to initiate lineage commitment and the formation of myoblasts. It upregulates the expression of pRB, myogenin, and MEF2. Myogenin and MEF2 work in cooperation with MYOD to direct the completion of terminal differentiation. This includes further differentiation of myoblasts into myocytes followed by myocyte fusion into nascent and finally mature myotubes. Myotubes are characterized as large multinucleated cells. They have a long tube-like morphology. They express muscle-specific markers (e.g. myosin heavy chain, MYHC) and permanently exit the cell cycle. KDM5A works in opposition to pRB acting in general as a negative regulator of myogenic differentiation. References for figure 5: [9, 15-17, 126, 129-134].

Figure 5

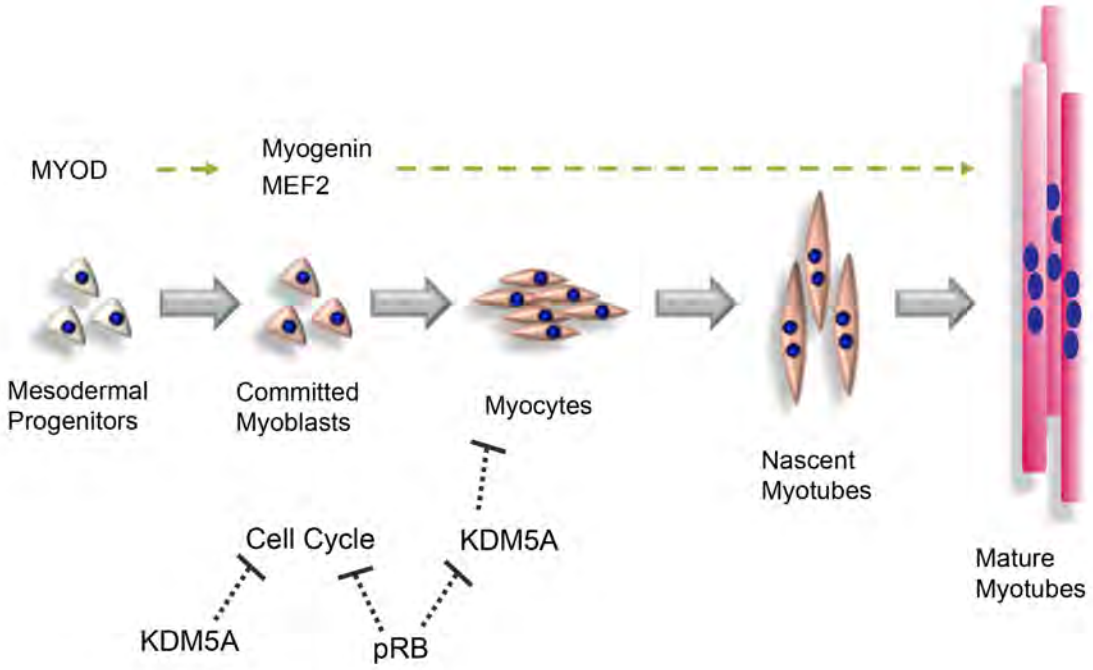
MYOD
Myogenin
MEF2
Mesodermal
Progenitors
Committed
Myoblasts
Myocytes
Nascent
Myotubes
Mature
Myotubes
Cell Cycle
KDM5A
KDM5A
pRB

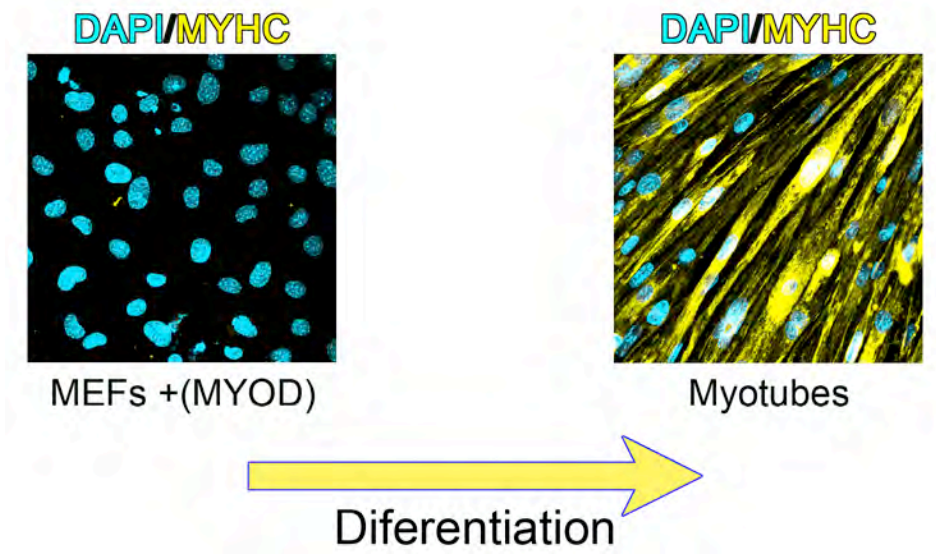

Figure 6. MEFs can be reprogrammed to differentiate into myotubes.

WT MEFs were transduced with Adeno-CMV-MYOD in differentiation media composed of DMEM, 2% horse serum, and insulin (10 µg/ml). At 72 hours post induction, cells show high expression of the late myogenic marker myosin heavy chain (MYHC), adopt a long tube-like morphology and become multinucleated due to cellular fusion. MYHC is yellow. DAPI-stained nuclei are blue.

II. MATERIALS AND METHODS

A. Cell Culture

Mouse embryonic fibroblasts (MEFs) were generated as described previously, [13]. MEFs were maintained in Dulbecco's Modified Eagle Medium (DMEM) (CellGro) containing 10% Fetal Bovine Serum (FBS) (HyClone). All cells were grown in 10% CO_2 in a humidified incubator at 37^{o}C. Stock cells were passaged weekly so that the confluence did not exceed 80%. For general differentiation of MEFs, the cells were first transduced to express MYOD by either Adenoviral or Lentiviral vector. The cells were then seeded to 100% confluence, 12 – 24 hours prior to induction. To induce differentiation, the growth media was replaced with differentiation media (DM): DMEM supplemented with 2% horse serum (Gibco) and 10 µg/ml insulin from bovine pancreas (Sigma).

C2C12 myoblast cells were maintained in DMEM containing 20% FBS. For induction of differentiation, the growth media was replaced with DM. All cells were grown in 10% CO_2 in a humidified incubator at 37^{o}C. Stock cells were passaged 3 times per week so that the confluence did not exceed 70%.

B. Transduction with viral vectors

Three different viral constructs were used for introduction of MYOD into MEFs. Cells were infected with either Adeno-CMV-MyoD or empty Adeno vectors (Vector BioLabs) for 18 hours, at multiplicity of infection of 1,000, or with Lenti-CMV-MyoD,

Lenti-CMV-MyoDER[T] (Addgene #26808 & #26809) or Lenti-CMV-empty. For lenti-viral constructs, cells were transduced for 18 hours, with 200 µl of 20x concentrated virus per 1 x 10^6 cells, in growth medium and containing polybrene (7 µg/mL). See section (C) in materials and methods for viral description, production and concentration. The number of cells and virus can be scaled up or down depending on the requirements of a given experiment. To induce differentiation, the growth medium was replaced with differentiation medium (DM) after 24 to 48 hours after transduction.

C. Generation of lentivirus

Viral packaging cells, Lenti-X 293T cell line, (Clontech # 632180) were seeded at 1.8 x 10^7 cells / 10 cm dish. The cell numbers can be scaled up or down for larger or smaller dishes based on the surface area of the dish. After 18 - 24 hours the cells were transfected with a combination of three plasmids in order to create lentiviral particles: (1) psPAX2 (Addgene deposited by Didier Trono) which is a plasmid containing viral packaging genes (2) pMD2.G (Addgene deposited by Didier Trono) which is a plasmid containing viral envelope genes (3) a plasmid containing the transgene of interest and a packaging signal. The cells were transfected using Lipofectamine 2000 reagent (Life Technologies #11668019). Plasmids were combined in 500 µl of OptiMEM serum-free media (Life Technologies # 11058021). 15 µg of psPAX2, 6 µg of pMD2.G, and 20 µg of expression vector. 60 µl of lipofectamine was mixed with 500 µl of OptiMEM and incubated at room temperature for 5 minutes. The plasmid solution was then combined with the lipofectamine solution, mixed and incubated at room temperature for 25 minutes. During the incubation time the growth media on the cells was removed and

replaced with 4 mL of OptiMEM. The transfection mixture was then added to the dish of cells and gently mixed. Cells were then incubated for 8 hours at 37^{o}C in 5% CO2 in a humidified incubator. After incubation the transfection media was removed and replaced with 5 mL of fresh OptiMEM. To harvest the virus, the media was collected at 48 hours post-transfection, stored overnight at 4^{o}C. Five mL of fresh OptiMEM was added to the cells. A second collection was taken after an additional 24 hours, and combined with the first collection in a 15 mL conical tube.

Confirmation of viral production was performed using Lenti-XGoStix (Clontech #631243) according to the manufacturer's specifications.

Cells and debris were removed from the collected virus-containing media by centrifugation at 1000 x g for 10 minutes. The viral supernatant was transferred to a new tube. The virus was concentrated using Lenti-X Concentrator (Clontech # 631232). 3.3 mL of concentrator (1/3 the volume of the collected viral media) was added to the viral media. The solution was mixed and incubated at 4^{o}C for 1 hour. The solution was then centrifuged at 1,500 x g for 45 minutes at 4^{o}C. The supernatant was removed and discarded. The pellet, containing virus was then re-dissolved to increase the concentration 20 times, in 500 µl of serum-free DMEM. The concentrated virus was then stored at -80^{o}C in single use aliquots.

D. Growing and fixing cells for immunofluorescence

Sixteen well, glass chamber slides (Lab-Tek #12565-110N) were pre-coated with a solution of 0.01% poly-D-lysine (Sigma # 4707) at a volume sufficient to cover the area of the well (75 µl), for 10 minutes. The solution was removed and the slides were rinsed once with sterile deionized H_2O. The H_2O was removed by aspiration and the

slides were dried at room temperature in a sterile laminar flow hood for 2 hours. After drying, the slides were then coated with fibronectin. Fibronectin (Sigma # F1141) was diluted to a concentration of 5 µg/mL in a 0.1% solution of gelatin. 100 µl of the fibronectin solution was added to each well. The slides were incubated for 3 hours at 37^{o}C in a 5% CO_2 humidified incubator. Following the incubation, the fibronectin solution was removed and the slides were rinsed once with phosphate buffered saline (PBS). Slides can be used immediately or stored long term at -20^{o}C.

For immunofluorescence, 2x10^{4} MEFs were seeded onto the coated chamber slides the day before infection. Differentiation was induced as described in section (A) of this materials and methods. After induction of differentiation for the indicated number of days, the cells were fixed and stained. For fixation, the media was removed and a solution of 10% formalin was added directly to the cells and incubated for 10 minutes at room temperature. After fixation, the formalin was removed and the cells were rinsed three times with PBS. Following the rinse steps the cells were permeablized and blocked with a solution of 0.5% Triton X-100 and 3% Bovine Serum Albumin (BSA) in PBS for 30 minutes at room temperature. The cells were then rinsed once with PBS. Primary antibodies were diluted in a solution of 1% BSA in PBS. The cells were incubated with the antibody solution for 2 hours at room temperature followed by 3 x fifteen-minute washes with PBS at room temperature. Secondary antibodies were diluted in a solution of 1% BSA in PBS. The cells were incubated with secondary antibody for 25 minutes at room temperature in the dark followed by 3 x fifteen-minute washes with PBS. Alternatively, if 4',6-diamidino-2-phenylindole (DAPI) was used to stain the nuclei, then the final three washes were as follows: 1 x fifteen-minute wash in

PBS followed by one 10 minute incubation with DAPI diluted 1:5,000 in PBS, followed by one final wash in PBS.

Slides were analyzed using either a fluorescent microscope (Zeiss Axioplan2) and images were acquired using AxioVision Version 4.1 software or a Zeiss LSM confocal microscope.

E. Immunofluorescent staining for myogenin

MEFs were transduced with Adeno-CMV-MYOD induced to differentiate as described in sections (A) and (B) of this materials and methods. Detection of myogenin was done with anti-myogenin antibody (Thermo Scientific, Clone F5D) at a 1:50 dilution. Cy3 labeled anti-mouse (Life Technologies) was used as the secondary antibody. Nuclei were stained with DAPI. Images were taken with the Zeiss Axioplan2 upright fluorescent microscope. Quantitation of myogenin-positive cells was performed by counting 4 microscope fields (40X power) per well, in triplicate wells. The percentage of all cells that were stained positive for myogenin was then determined. In the case of multinucleated cells, if multiple nuclei in the same cell were positive for myogenin, the cell was counted once.

F. Cell Cycle Analysis in Myotubes

MEFs were induced to differentiate for three days as described in sections (A) and (B) of this materials and methods. On day three, the cells were removed from differentiation media and put into DMEM/20% FBS for 12 hours to promote cell cycle reentry. After 12 hours, 5-ethynyl-2'-deoxyuridine (EdU) (Invitrogen #C10340) was

added to a 10 μM concentration into the culture media and the cells were incubated for an additional 12 hours. Cells were then fixed, permeablized and blocked as described in section (C) of this materials and methods. Immunofluorescent staining was done with mouse monoclonal anti-MYHC at a 1:300 dilution (Sigma, MY-32). Staining for EdU was done according to the manufacturer's protocol (Invitrogen) using reagents included in the EdU kit. Images were taken with a Zeiss Confocal microscope. The experiment was performed in triplicate. Cells were counted from three fields in each well (3 fields/well x 3 wells) for each genotype for a total of 9 fields per genotype.

G. TUNEL staining assays

MEFs were induced to differentiate for the designated period of time. Terminal deoxynucleotidyl transferase dUTP nick end labeling (TUNEL) staining was performed with the *In Situ* Cell Death Detection Kit (Roche #11684795910) according to the manufacturer's protocol. Quantification was done by counting the number of TUNEL-positive cells and determining the percentage that were TUNEL-positive out of the total cell number. Assays were done in triplicate. Images were taken with the Zeiss Axioplan2 upright fluorescent microscope using the 10x objective in order to visualize the maximal number of cells per field. >100 cells per replicate were counted and averaged. In the case of multinucleated cells, if multiple nuclei in the same cell were positive for TUNEL, the cell was counted once.

H. Purify myotubes for RNA-seq

WT and Rbp2$^{-/-}$;Rb1$^{-/-}$ MEFs were seeded on 6-well dishes coated with fibronectin. Two duplicate sets of 4 wells for each genotype (8 wells/genotype total) were seeded at 2.2 x 10^5 cells/well. The following day the cells were induced to differentiate by transduction with Adeno-MyoD (2.2 x 10^8 plaque-forming units, PFU) and switching to differentiation media (DM): DMEM (CellGro), 2% horse serum (Gibco), 10 µg/mL insulin (Sigma) and incubated overnight. After 24 hours, the DM containing Ad-MyoD was replaced with fresh DM. At 48 hours, ½ the media was removed and replaced with fresh DM. At 72 hours myotubes were purified as follows: the media was removed from the cells and kept aside. Cells in each of 4 wells for each genotype were trypsinized, resuspended and combined in 2 mL of growth media, DMEM and 10% FBS, into one well. The plate was left to sit undisturbed for 1 minute to allow the heavier myotubes to sink to the bottom leaving mostly undifferentiated MEFs suspended in the media. Then ¾ (1.5 mL) of the media containing mostly undifferentiated MEFs was carefully removed by pipette leaving differentiated myotubes on the bottom of the well. 1.5 mL of growth media was added back to the well and the cells were resuspended. This processes was repeated 2 more times to generate a purified population of myotubes. Cells were allowed to recover and reattach to the dish for 3 hours in growth media. After 3 hours the growth media was removed and replaced with the conditioned media that was set aside. Cells were then allowed to recover for 24 hours.

I. RNA-seq mRNA library preparation

RNA from purified wild type and double knockout myotubes was extracted with 400 µl Trizol (Invitrogen) but not precipitated. The aqueous phase containing the RNA was removed and one volume of 70% ethanol was added followed by purification on Qiagen RNeasy Micro (cat# 217084) column according to the Qiagen protocol. 1.5 µg of RNA from each sample was purified by two rounds of oligo-dT purification with Dynal oligo-dT beads (Invitrogen cat# 610.06) according to the manufacturer's protocol. Using the NEBNext mRNA Sample Prep Master Mix Set 1 (New England Biolabs (NEB) cat# E6110S), the purified RNA was fragmented for 5 minutes at 94^{o}C using 10X fragmentation buffer. First strand cDNA synthesis was performed with random primers (NEB) and Superscript II reverse transcriptase (Invitrogen). Second strand synthesis was done with 10X Second Strand Synthesis Reaction Buffer (NEB) and Second Strand Synthesis Enzyme Mix (NEB). Double stranded cDNA was purified with 1.8 volumes of AMPure XP Beads (Beckman Coulter) followed by end repair using NEBNext End Repair Enzyme Mix and Reaction Buffer (NEB). End-repaired DNA was cleaned up with 1.8 volumes of AMPure XP Beads followed by dA-Tailing using 10X NEBNext dA-Tailing Reaction Buffer and Klenow Fragment (3'>>>5' exo^{-}). dA-Tailed DNA was cleaned up with 1.6 volumes of AMPure XP Beads followed by adapter ligation using paired end (PE) adapters designed for Illumina sequencing: PE Adapter 1: GATCGGAAGAGCGGTTCAGCAGGAATGCCGAG; PE Adapter 2: ACACTCTTTCCCTACACGACGCTCTTCCGATCT Adapter-ligated DNA was cleaned up and size selected for a range of 250-300 bp using 1 volume of AMPure XP Beads. cDNA was enriched by polymerase chain reaction (PCR) - 15 cycles using Phusion

DNA Polymerase (NEB) and PE primers designed for Illumina sequencing. PE primer 1: AATGATACGGCGACCACCGAGATCTACACTCTTTCCCTACACGACGCTCTTCCGATCT; PE primer 2: CAAGCAGAAGACGGCATACGAGATCGGTCTCGGCATTCCTGCTGAACCGCTCTTCCGATCT. Enriched DNA was cleaned up with 1 volume AMPure XP Beads. Single-read sequencing for 36 bases was done on an Illumina Genome Analyzer II.

J. RNA-seq RiboMinus RNA library preparation

RNA from purified MEFs induced for myogenic differentiation was extracted with 400 µl Trizol (Invitrogen) but not precipitated. The aqueous phase containing the RNA was removed and one volume of 70% ethanol was added followed by purification on Qiagen RNeasy Micro (cat# 217084) column according to the Qiagen protocol. 1.7 µg of total RNA from each sample was processed using the RiboMinus Eukaryote Kit for RNA-Seq (Ambion cat#A10837-08) according to the manufacturer's protocol. Using the NEBNext mRNA Sample Prep Master Mix Set 1 (NEB cat# E6110S) the RiboMinus RNA was fragmented for 5 minutes at 94^{o}C using 10X fragmentation buffer (NEB). First strand cDNA synthesis was performed with random primers (NEB) and Superscript II reverse transcriptase (Invitrogen). Second strand synthesis was done with 10X Second Strand Synthesis Reaction Buffer (NEB) and Second Strand Synthesis Enzyme Mix (NEB). Double stranded cDNA was purified with 1.8 volumes of AMPure XP Beads (Beckman Coulter) followed by end repair using NEBNext End Repair Enzyme Mix and Reaction Buffer (NEB). End-repaired DNA was cleaned up with 1.8 volumes of AMPure XP Beads, redissolved in 17.5 µl of Tris buffer 10 mM pH 8. From this point the end-

repaired library was integrated into the standard TruSeq Illumina protocol at the step of "Adenylate 3' ends". Single-read sequencing for 40 bases was done on an Illumina HiSeq Analyzer.

K. Gene overlap analysis

Overlap analysis to identify common target genes was done using an online venn diagram generator "Venny" http://bioinfogp.cnb.csic.es/tools/venny/index.html.

L. Enrichment Analysis

Enrichment analysis for Gene Ontologies was done using GiTools v1.8.4. Gene lists were converted into binary matrices. The background gene list was created using all mouse genes (Ensembl release 5), excluding non-protein coding genes, excluding genes on the X and Y chromosomes. Gene ontologies for each gene in the background list were downloaded from the Gene Ontology Consortium (www.geneontology.org).

M. Electron Microscopy

MEFs +lenti-MyoDER[T] were seeded on 10 cm, fibronectin-coated dishes. WT, *Kdm5a*$^{-/-}$, Rb$^{-/-}$ at 5x10^{6}/dish and DKOs at 1x10^{7}. Induced to differentiate for 72 hours in DM and 100nM 4-hydroxy-tamoxifen. Prior to fixation, the cells were rinsed twice with 5 mL of serum-free DMEM pre-warmed to 37^{o}C. Cells were fixed for 5 minutes at room temperature in 5 mL of EM fixative (2% glutaraldehyde and 4% paraformaldehyde in 0.1 M sodium cacodylate buffer) pre-warmed to 37^{o}C. The cells were scraped and

transferred to 15 mL conical tubes. Spun at 1,000 rpm for 5 minutes at room temperature. Samples were transported on ice to The University of Chicago electron microscopy core facility for embedding, and imaging.

N. Quantification of mitochondria size

The area of the mitochondria was measured using NIH ImageJ 1.42q software. The manual trace tool was used to establish the area of each mitochondrion to be measured. The area was then determined with the measure tool. Measurements were taken for all mitochondria in each genotype and averaged. The data is shown as relative to the WT.

O. Measured rates of O_2 consumption and glycolysis

Coated 24-well Seahorse XF24 cell culture microplates (Seahorse Bioscience # 100777-004) with fibronectin as described in section (D) of this materials and methods. MEFs were seeded to 100% confluence according to previously optimized seeding densities for each genotype: WT at $5x10^4$ cells/well, $Kdm5a^{-/-}$ at $5x10^4$, $Rb^{-/-}$;$Kdm5a^{-/-}$ at $1x10^5$ cells/well, $Rb^{-/-}$ at $1x10^5$ cells/well. The cells were transduced overnight with Lenti-CMV-MyoD (2 µl of 20x virus/$1x10^4$ cells) for the 24hr condition or Lenti-CMV-empty vector for the 0hr condition, in growth medium and polybrene (7 µg/mL). The 0hr and 24hr differentiation conditions were induced by switching the cells to differentiation media for 24 hours. Each genotype and differentiation condition were set up in 4 replicates.

Rates of Oxygen consumption and glycolysis were measured simultaneously on a XF24 Extracellular Flux Analyzer (Seahorse Bioscience). The night before the experiment, XF24 Sensor Cartridge (Seahorse Bioscience #100850-001) was calibrated by adding 1 mL of XF24 calibrant solution (Seahorse Bioscience #100840-000) to each well of the cartridge and incubated at 37^{o}C overnight without CO_2.

On the day of the assay, the growth or differentiation media was removed from the cells and the cells were rinsed once with PBS. New media was added to all wells: DMEM supplemented with glucose (25 mM) (Sigma Aldrich #G8270), glutamine (4 mM) (Life Technologies #35050-061), and sodium pyruvate (1 mM) (Life Technologies #11360-070), but without the pH buffer sodium bicarbonate. The cells were then placed in a 37^{o}C incubator without CO_2 for 1 hour.

Three measurements of the basal rate of O_2 consumption were taken for each well, along with three measurements of the rate of glycolysis followed by three measurements of the maximal rate of O_2 consumption. Maximal rates were induced by injection of the ionophore, carbonylcyanide p-trifluoromethoxyphenylhydrazone (FCCP) at a final concentration of 0.5 μM.

The rates of O_2 consumption and glycolysis were averaged from each of the three measurements for each of the 4 replicates for every condition.

P. Culture conditions for ROS measurement

Cells were grown on 12-well plates coated with fibronectin as described in section (D) of this materials and methods. Transduced with lenti-CMV-MyoD or empty control as described in section (B) of this materials and methods. For the differentiated

condition, cells were induced to differentiate for 7 hours prior to measurement of ROS. The short differentiation time was necessary in order to run the assay on the fluorescence-activated cell sorting (FACS) machine, before fusion into myotubes. To measure reactive oxygen species (ROS) the cells were incubated in serum-free media with 10 μM 2'-7'-dichlorodiydrofluorescein diacetate (H_2DCFDA) (Life Technologies #D399) for exactly 30'. The cells were then washed once with PBS. After washing, the cells were trypsinized, followed by neutralization with PBS/FBS (10%). The cells were then spun at 700 x gravity for 5 minutes at room temperature to pellet. The supernatant was removed and the cells were resuspended in 200 μl of PBS/EDTA (1mM) and passed through mesh filter top tubes to remove any large clumps. The cells were then transferred to a 96 well plate that was loaded onto the FACS machine. ROS was measure by DCF fluorescence in 10,000 events for each condition in triplicate.

Q. Protocol for Mitotracker staining of myotubes

The protocol was adapted from the manufacturer's protocol (Life Technologies cat# M7512). Cells were grown and differentiated as described in sections (A) and (B) of this materials and methods. To stain, the media was removed, and the cells were rinsed twice in warm Serum-free DMEM. Mitotracker was added to the cells: Mitotracker Red CMXRos diluted 1:1,500 in serum-free DMEM. Incubated 45 minutes at 37^{o}C. The cells were then washed twice for 5 minutes in warm serum-free DMEM. The cells were then fixed in 10% formalin for 10' and then rinsed 3 times with PBS. Permeabilization and blocking was done in 0.5% Triton X-100 and 3% BSA in PBS. Cells were stained with DAPI as described in section (D) of this materials and methods. Images of

mitochondria were taken using Zeiss confocal LSM microscope at 40X and 100X magnification.

R. Antibodies

α-MyHC: Sigma MY-32; α-MYOG: DSHB F5D; α-H3K4me3: Millipore #07473; α-H3: total: Abcam #ab1791; α-Tubulin: Sigma; α-MYOD: Santa Cruz #sc-760 and sc-304, Pharmingen #554130; α-KDM5A: 2469 described in [16], and 1416 described in [17]; α-COXIV: Abcam #ab16056; α-FLAG: Sigma monoclonal #F1804, and polyclonal F7425; α-RB: Cell Signaling 4H1; phoshpo-IGF-1R: Abcam #ab38465; IGF-1R beta: Cell signaling #3018.

S. Phosphatase treatment of lysates

Cells were lysed in Lysis buffer (50 mM Tris pH 8, 450 mM NaCl, 0.5% NP-40). A protease inhibitor cocktail (Calbiochem # 539131) was included in all lysates. In the indicated lysates, a phosphatase inhibitor cocktail (Calbiochem # 524629) was added. λ-phosphatase (NEB # P0753S) treatment was performed where indicated for 25 minutes at 30^{o}C. 800 Units of λ-phosphatase per 200 µg of protein.

T. Creation of lentiviral constructs

Genes to be sublconed were amplified by PCR from either cDNA or plasmid DNA containing the gene of interest. Primers were designed with restriction sites for cloning into pENTR4-FLAG entry vector (Addgene #17423) [145].

The forward primer for cloning RB contained the NotI restriction site. The reverse primer contained the XhoI site. RB primer sequences: forward 5'-CTTGCGGCCGCAGGGTACCCATACGATGTTCCAGATTAC – 3'; reverse 5' – CTTCTCGAGTCATTTCTCTTCCTTGTTTGAGGTATC – 3'. The PCR reaction was performed using Elongase Enzyme Mix (Life Technologies #10480-028). RB PCR products were cut with NotI and XhoI (New England Biolabs) and purified with Qiagen MinElute Reaction Cleanup Kit (Qiagen #28204) according to the manufacturer's protocol.

The forward primer for cloning KDM5A and KDM5A mutants contained the NotI restriction site. The reverse primer contained the XbaI site. KDM5A primer sequences: forward 5' – CTTGCGGCCGCAGCGGGCGTGGGGCCGGGGGGCTAC – 3'; reverse 5' – ATCTAGACCTAACTGGTCTCTTTAAGATCCTCCATTG – 3'. The PCR reaction was performed using Elongase Enzyme Mix (Life Technologies #10480-028). KDM5A PCR products were cut with NotI and XbaI (New England Biolabs) and purified with Qiagen MinElute Reaction Cleanup Kit (Qiagen #28204) according to the manufacturer's protocol.

The entry vector was cut with NotI and XhoI or NotI and XbaI (New England Biolabs) to generate compatible ends for ligation of the RB or KDM5A PCR products respectively. Digested plasmid was gel purified (Qiagen #28704) according to the Qiagen protocol.

Genes in the entry vectors were recombined into pLenti-CMV-Hygro-DEST, lentiviral destination vector (Addgene #17454) (Fig. 7) [145]. The recombination reaction was done by mixing 150 ng of pLenti-CMV-Hygro-DEST plasmid with 72 ng of entry

vector containing the RB gene or 114 ng of entry vector containing KDM5A or KDM5A mutant and 2 µl of Gateway LR II Clonase Enzyme Mix (Life Technologies #11791-20) brought to a final volume of 10 µl in Tris-EDTA (TE) buffer (pH 8). The reaction was incubated at 25^{o}C overnight. The reaction was terminated by the addition of 1 µl of Proteinase K (Life Technologies #11791-20) incubated for 10 minutes at 37^{o}C.

A

B

Vector Features	Description
attB	Attachment B sites for recombination
PRE	Woodchuck post-translational element
PGK	Phosphoglycerate kinase promoter
Hygromycin	Mammalian selection marker
LTR	Long terminal repeats
SV40 pA	SV40 virus poly-A signal
Amp	Ampicillin resistance
pUC ori	Origin of replication
Ψ	HIV-1 psi packaging signal
RRE	HIV-1 Rev response element
cPPT	Central polypurine tract
CMV	Cytomegalovirus promoter

Figure 7. Vector Maps for lentiviral constructs.

A) Vector maps for lentiviral constructs to express KDM5A, KDM5A mutants and RB. Top left: KDM5A. Top right: KDM5AHE mutant. Bottom left: KDM5AFS mutant. Bottom right: RB. **(B)** List of vector features in the left column and descriptions in the right.

U. Chromatin Immunoprecipitation

Crosslinking was performed in cells, undifferentiated or differentiated, by adding formaldehyde directly to the culture media to a final concentration of 1% and incubating for 10 minutes at room temperature, followed by 2 rinses in cold PBS on ice. Cold LB1 buffer (Hepes-KOH 50mM pH 7.5, NaCl 140mM, EDTA 1mM, glycerol 10%, NP-40 0.5%, Triton X-100 0.25%) was added to the cells (1ml / 10 cm dish or 3 ml / 50 cm dish). The cells were scraped to detach and transferred to a 15 mL conical tube. The cells were then incubated for 20 minutes at 4^{o}C while rocking in the LB1 buffer. Following the incubation the cells were pelleted by spinning at 3,000 rpm for 20 minutes. The LB1 buffer was removed and the cells were resuspended in 3 mL of LB2 buffer (NaCl 200mM, EDTA 1mM, EGTA 0.5mM, Tris 10mM pH 8) and incubated while rocking for 10 minutes at room temperature. The cells were then pelleted and resuspended in 2.5 mL of LB3 buffer (NaCl 100mM, EDTA 1mM, EGTA 0.5mM, Tris 10mM pH 8, Na-Deoxycholate 0.1%, N-Lauroyl sarcosine 0.5%). Cells were sonicated to shear DNA to a peak size range of 1kb using a Branson 450 microtip sonicator at 60% amplitude. Triton X-100 was added to a concentration of 1% and mixed by vortex. The sonicated DNA solution was then equally divided into 1.5 mL microcentrifuge tubes and spun for 15 minutes at 13,000 rpm at 4^{o}C to pellet insoluble debris. Antibodies pre-bound to protein G Dynal magnetic beads (Invitrogen) were added to the DNA and immunoprecipitated overnight at 4^{o}C while rotating. The beads were washed on ice, six times in wash buffer (Hepes 50mM pH 7.6, EDTA 1mM, Na-Deoxycholate 0.7%, NP-40 1%, LiCl 0.5M) followed by one wash with TE/NaCl (50mM). The DNA was eluted in 100 µl of elution buffer (Tris 50mM pH8, EDTA 10mM, 1% SDS) by incubation at 65^{o}C for 15

minutes while mixing every 2 minutes. Following the elution step the beads were removed and discarded. Reverse crosslinking was performed by incubating at 65^{o}C overnight in elution buffer. Cells were treated with RNase A followed by Proteinase K. DNA was extracted by phenol:chloroform then ethanol precipitated and redissolved in 60 µl of TE.

V. qPCR

Quantitative PCR (qPCR) was performed on a BioRad CFX real time PCR machine. cDNA was generated from 0.5 µg of total RNA using the SuperScript VILO cDNA Synthesis Kit (Life Technologies #11754050) according to the manufacturer's protocol. For qPCR reactions, the cDNA was diluted 100 fold. PCR reactions included 1.25 µl of diluted cDNA, forward and reverse primers (1 µM each), and 2.5 µl of iQ SYBR Green Supermix (BioRad # 170-8882).

Quantitation was calculated using the ΔΔC(t) method [146]. Relative quantification was performed by normalizing to a reference gene: B2M. Absolute quantification was done using standard curves generated from known copy numbers of three different *Drosophila* RNA control transcripts, converted to cDNA (LD22368, LD05461, dE2F2). Five dilutions covering 3 orders of magnitude of each control cDNA were made and qPCR was performed in triplicate. The threshold cycle C[t] values from each cDNA control were averaged and used to generate the standard curve.

Control RNAs were spiked into the unknown sample RNA and processed into cDNA with the sample RNA. Copy numbers were determined with the following calculation: copy # =10^((C[t]-36.056)/-3.3806). The value 36.056 is the y intercept of

the standard curve and -3.3806 is the slope of the standard curve. C[t] values were derived for each gene of interest by qPCR. Absolute copy numbers were represented as relative fold difference compared to the WT 0hr condition.

W. Primers for qPCR and ChIP-qPCR

Gene	qPCR Forward Primer Sequence	qPCR Reverse Primer Sequence
Mfn2	AGCGACACATGGCTGAAGTGAATG	TGTTCCTGTGGGTGTCTTGAAGGA
Ndufs4	TGGTTCTGACCTTCAGTGCCAAAG	GGACTTGGGTTTCGGAACCTTCTT
Cox6b1	TGATGTCTCCGTGTGTGAGTGGTA	AGGAAATGTGCCTTCAGCTATGCG
Myh6	TGCCAAGCTGACCAAAGAG	GCGTGTTGACCTTGTCTTCT
Tnnc2	TACCTCAGCGAGGAGATGAT	CACGGTGCCCAACTCTTTA
Pitx2	AGCTGCTGGCTAGTGAAATG	ATAAGGGCCAGCAAGGAAAG
Pgc1α	GCTCGTACAGGTCATCAAGAAG	CTGCCATCTCAGGAAAGATCAG
Dnajc11	CGAGATCAGAGAGGAGTTTGAG	AAAGGTCAGTCGCATCTACTC
Tgm2	CTCCTGGAGAGGTGTGATTT	GCAGCACCAGTTTCTCTTG
Atp5a1	CTCAGAACAGTCAGACGCAAAG	CCAAAGCAGTATCTGGTGACAG
Uqcrc1	GATGCTGCGTGACATTTGC	ATCCGGTTGTAGTCTGGGA
Uqcrq	TACAGCTTGTCGCCCTTT	CCCATGTGTAGATCAGGTAGAC
Sdhb	GGGTTGTAGAGTGACCTTGAG	TGACACATAAGCGGGTCTG
Sdhd	CTGCCACACCATCATGAACT	CTTGTAGGTCGCCATCATCTTC
Coq7	GCAGCCGTGGATCGAATAA	CTGAATGACAGGGCCAACA
Prox1	CAAGGTTCAGAGCAGGATGT	CATACGAGTTCGCCCTCTTC
Myo18b	GAGGTGGTGTCAAGTGATAGTG	TGGGAGCTGATGACAGAGA
Tnni2	GCACCTGAAGAGTGTGATGC	GGGCAGTGTTCTGACAGGTA

Mef2c	AGGACAAGGAATGGGAGGAT	GCAGTGTTGAAGCCAGACAG
Orai1	CTACTTAAGCCGCGCCAAG	CCTGGTGGGTAGTCATGGTC
Sod2	GTGGGAGTCCAAGGTTCAGG	GTAGTAAGCGTGCTCCCACA
Vdac1	CGGGCCAAAGTGAACAACTCT	ATTGACGTTCTTGCCATCG
Glut4	TGGGAACACTCAACCAACTG	AGCAGTGGCCACAGGGTA
Esrrγ	GGAAGAATTCGTCACCCTCA	GGGCCTCATGTAACACATCC
Meis1	ATGATAGACCAGTCCAACCGAGCA	TGCCCATATTCATGCCCATTCCAC
Rttn	TTGCTGAGACCTGGGAAAGCAGTA	CGTGCTTCAAGAGCTGCCACTTTA
Recql4	TCTCCGTAAGCAGGTATGGAAGCA	CCGGAAACAAGTGTCCTTGTCTGT
Dact1	AACTCCTCCAACTCCGTGTTCAGT	CCGCCTTTACATTCCAACCATCCT
Aaas	ACGGGAATCCTGTCATCCTCCTTT	TGGAAAGTGATGAGCTGAGCTTGG
Setdb2	AAAGAGCCCGCTGTGGAAATGAAC	GGCGGCAGAATCTGAGCAAACAAA

Gene	**ChIP-qPCR Forward Primer Sequence**	**ChIP-qPCR Reverse Primer Sequence**
Uqcrq	GCCCTGGGACAGAAGATAGA	GAGCTCTGGAGGTAGAGGTG
Sdhd	GAGAACGCCCAGCTTTAAGA	GGCGGGACTTACTACATAACTG
Mfn2	CACCCTACAGCTTACGTCAT	CCTCAACCTTACCACTCCT
Opa1	CGTTCCTGTGGGTGGTTATT	CTCAGCAACAAGGGCATAGA
Ndufs4	CCTGGGAACCCTGAATGAATAG	CGAAGGGCAATGGCTACA
Cox6b1	GGGCTGAAGGATGGAGTAATAG	GTGTCCTGGAGCTAACCATTAT

X. Raw genomic data

ChIP-seq KDM5A. Gene Expression Omnibus (GEO) accession number GSE28343

ChIP-seq RB. GEO accession number GSE19898

RNA-seq data has been submitted to NCBI GEO to be made public.

Y. Quantification of global H3K4me3

Quantification of global H3K4me3 levels was performed using NIH ImageJ 1.42q software. Western blot images were scanned and saved as high-resolution TIFF files. Each band including background area was selected using the rectangular selection tool. A uniform total area was selected for each. Each selected area was analyzed and plotted as a histogram. Background was subtracted from each histogram and each peak was selected with the wand tool. The relative fold difference between each peak was calculated using the label peaks function.

III. RESULTS

A. Knockout of *Kdm5a* rescues differentiation in *Rb1*$^{-/-}$ MEFs

Knockdown of *Kdm5a* in *Rb1*$^{-/-}$ MEFs was shown to restore expression of the myogenic marker MyHC [17]. With the recent availability of *Kdm5a* knockout mice it is now possible to study the effect of complete ablation of *Kdm5a* gene expression on differentiation [63]. To study the differences in the dynamics of early differentiation due to the loss of *Rb1* and/or *Kdm5a*, I induced WT, *Kdm5a*$^{-/-}$, *Rb1*$^{-/-}$ and *Kdm5a*$^{-/-}$*; Rb1*$^{-/-}$ (DKO) to differentiate for 48 hours. The cells were then stained for the early marker of differentiation, myogenin (Fig. 8A). Myogenin expression was first detected 12 hours after induction, with nearly 100% of cells expressing by 36 hours in the WT condition, while only a small fraction of the *Rb1*$^{-/-}$ cells expressed myogenin by 48 hours (Fig. 8A and 8B). Expression in the Kdm5a$^{-/-}$ cells appears to be even more robust than in the WT cells. Importantly, the DKOs showed an expression pattern similar but not identical to WT (Fig. 8A and 8B). In fact upregulation of myogenin appears to occur slightly sooner in the DKOs than in WT cells (Fig. 8C). These results indicate that the loss of *Kdm5a* in the *Rb1*$^{-/-}$ background rescues expression of a key myogenic transcription factor that is required for terminal differentiation.

Figure 8. Loss of *Kdm5a* rescues expression of myogenin.

(A) Immunofluorescent detection of myogenin at seven time points over the first forty-eight hours after induction to differentiate. Cells were stained with an anti-Myogenin antibody and DAPI. **(B)** Quantification of myogenin-positive cells for each genotype at each of the seven time points. Bars indicate percentage of myogenin-positive cells out of the total cell population and represent the average of three independent experiments and the standard error. **(C)** The12hr time point from the quantification chart shown in (B) was isolated for clarity. Statistical significance for *Kdm5a*$^{-/-}$ and *Kdm5a*$^{-/-}$*;Rb1*$^{-/-}$ compared to WT is shown as p-values on the chart. P-values were determined by the Student's t-test.

Figure 8

A

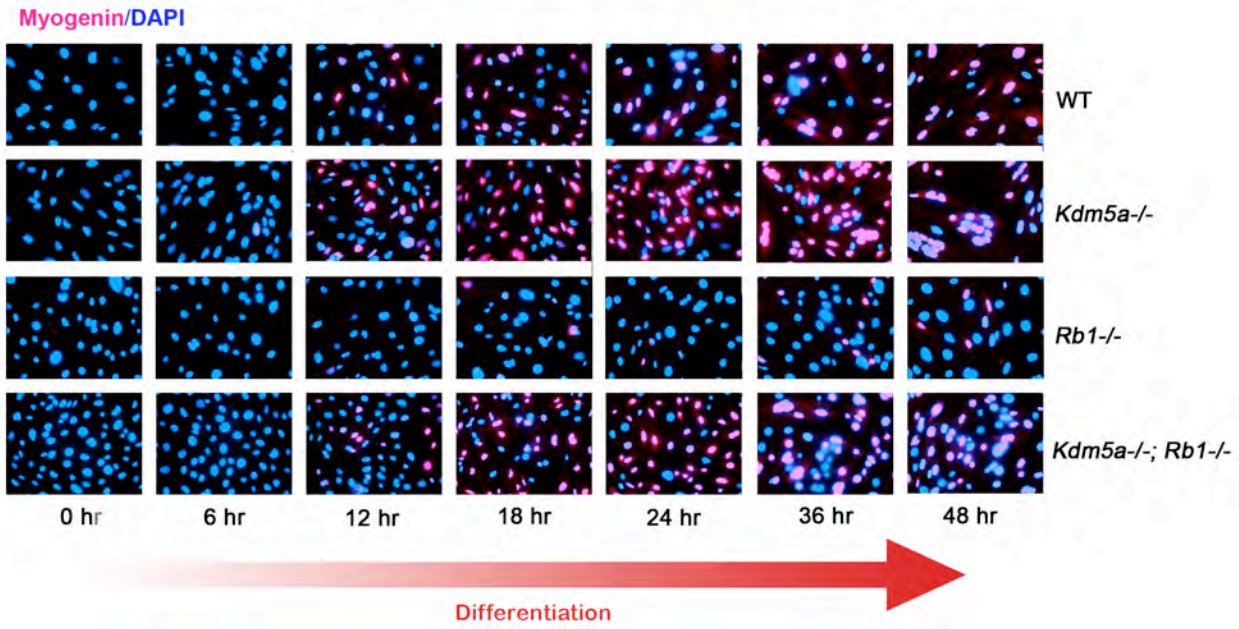
Myogenin/DAPI
WT
Kdm5a-/-
Rb1-/-
Kdm5a-/-; Rb1-/-
0 hr
6 hr
12 hr
18 hr
24 hr
36 hr
48 hr
Differentiation

B

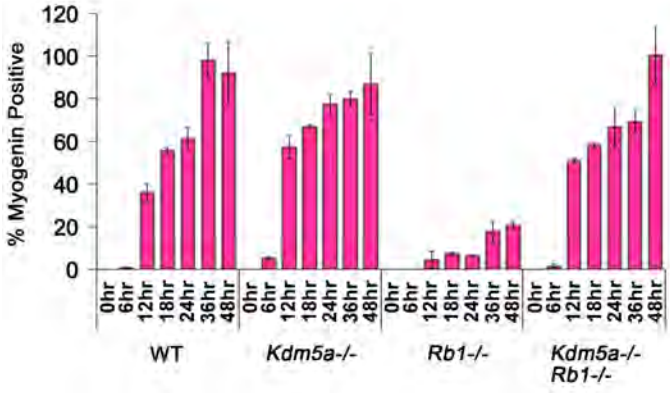
% Myogenin Positive
120
100
80
60
40
20
0
0hr
6hr
12hr
18hr
24hr
36hr
48hr
WT
Kdm5a-/-
Rb1-/-
Kdm5a-/-
Rb1-/-

C

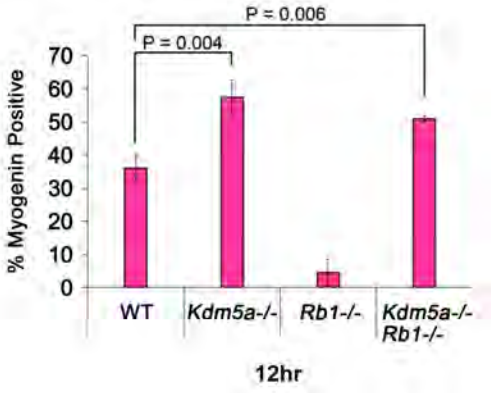
P = 0.006
P = 0.004
% Myogenin Positive
70
60
50
40
30
20
10
0
WT
Kdm5a-/-
Rb1-/-
Kdm5a-/-
Rb1-/-
12hr

In addition to the early events of differentiation, I also looked at expression of a late marker, myosin heavy chain (MYHC). Here I induced differentiation for 96 hours followed by immunofluorescence staining. Similar to the early marker, features of late myogenic differentiation were also rescued (Fig. 9A). Consistent with previous reports, *Rb1* knockouts were generally defective for late differentiation (Fig. 9A and 9B) [57]. They showed limited expression of MYHC and were primarily small and mononucleated. The small percentage of cells that did express MYHC remained morphologically defective (Fig. 9A and 9B). They were at most dinucleated, and were much smaller than the WT myotubes. Compared to the *Rb1*$^{-/-}$ MEFs, the DKOs showed a greater percentage of cells expressing MYHC, and a greater percentage of cells with the morphological character of myotubes: a high degree of multinucleation and an elongated tube-like shape (Fig. 9A and 9B).

Figure 9. Loss of *Kdm5a* in the *Rb1*$^{-/-}$ background rescues features of differentiation while increasing cell cycle entry of differentiated myotubes.

(A) MEFs were induced to differentiate for 3 days. Re-stimulated in DMEM / 20% FBS for 24 hours. EdU was added to the media for 12 hours. Edu incorporation (pink) indicates S-phase entry; MyHC (yellow) is a late marker of myogenic differentiation, and DAPI (blue) stains the nuclei. Left Panel: WT, *Kdm5a*$^{-/-}$, *Rb1*$^{-/-}$, and *Kdm5a*$^{-/-}$*; Rb1*$^{-/-}$. Right Panel: *Kdm5a*$^{-/-}$*; Rb1*$^{-/-}$ MEFs transduced to express WT KDM5A, KDM5AHE demethylase mutant, or KDM5AFS frameshift mutant. **(B)** Quantitation of differentiation. Data is presented as percentage of cells that are differentiated from the total population. Cells were considered to be differentiated if they were MYHC-positive and contained more than two nuclei. Error bars for both charts represent the standard error of the mean of three replicates. **(C)** Quantitation of differentiated cells, marked by MYHC, that were positive for cell cycle reentry, marked by EdU, for each of the indicated genotypes. In the case of multinucleated cells, if multiple nuclei in the same cell were positive for EdU the cell was counted only once. Data is shown as percentage of EdU-positive myotubes, out of the total cell number.

Figure 9

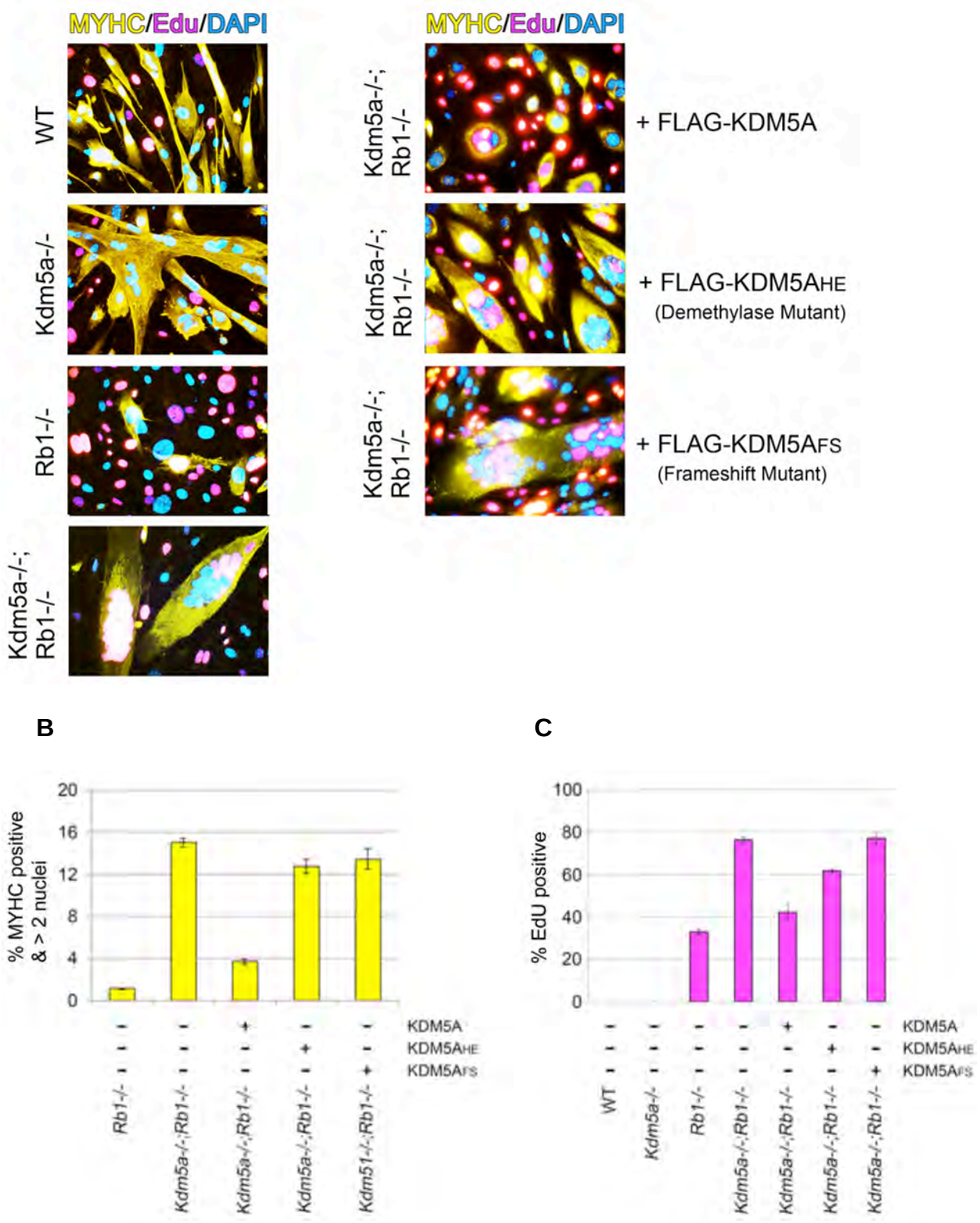
A
MYHC/Edu/DAPI
WT
Kdm5a-/-
Rb1-/-
Kdm5a-/-; Rb1-/-
MYHC/Edu/DAPI
Kdm5a-/-; Rb1-/-
+ FLAG-KDM5A
Kdm5a-/-; Rb1-/-
+ FLAG-KDM5AHE
(Demethylase Mutant)
Kdm5a-/-; Rb1-/-
+ FLAG-KDM5AFS
(Frameshift Mutant)
B
% MYHC positive & > 2 nuclei
20
16
12
8
4
0
KDM5A
KDM5AHE
KDM5AFS
Rb1-/-
Kdm5a-/-;Rb1-/-
Kdm5a-/-;Rb1-/-
Kdm5a-/-;Rb1-/-
Kdm51-/-;Rb1-/-
C
% EdU positive
100
80
60
40
20
0
KDM5A
KDM5AHE
KDM5AFS
WT
Kdm5a-/-
Rb1-/-
Kdm5a-/-;Rb1-/-
Kdm5a-/-;Rb1-/-
Kdm5a-/-;Rb1-/-
Kdm5a-/-;Rb1-/-

We have previously observed that KDM5A cooperates with the pocket family and E2F4 to repress cell cycle genes during differentiation in the lymphoma-derived cell line, U937, which can be induced to differentiate into monocytes and macrophages [15, 16]. We observed that KDM5A, E2F4 and p130 co-localize to cell cycle genes after induction of differentiation [15, 16]. These genes were repressed in a manner that was temporally coordinated with the binding of these factors [15, 16]. Knockdown of *KDM5A* or *E2F4* resulted in derepression of the genes and knockdown of both *KDM5A* and *E2F4* had an additive effect [15, 16]. Given this observation, a logical question that I wanted to address in the myogenic model was: how does the loss of *Kdm5a* affect mitotic re-entry of terminally differentiated cells lacking pRB? It has been shown that pRB is required for cell cycle withdrawal during differentiation, and for maintenance of the post-mitotic state [23, 24, 127]. I induced differentiation in WT, *Kdm5a*$^{-/-}$, *Rb1*$^{-/-}$ and DKO MEFs for 72 hours followed by stimulation in media with 20% FBS for 24 hours, and incorporation of 5-ethynyl-2'-deoxyuridine (EdU) for 12 hours. EdU is a modified thymidine analog that is incorporated into DNA during S phase [147]. EdU incorporation is then detected with a fluorescently labeled probe that identifies cells that are mitotically active [147].

Although the majority of *Rb1*$^{-/-}$ MEFs do not differentiate, a fraction of them do express the late marker MyHC. Among these cells, a significant portion of them had re-entered the cell cycle (Fig. 9A and 9C). This was not surprising, given the previous reports showing the requirement of pRB in cell cycle exit during and after differentiation [126, 127]. Also as expected, none of the WT myotubes were positive for EdU. Like the WT cells, the *Kdm5a*$^{-/-}$ myotubes were negative for incorporation of EdU (Fig. 9A and 9C). This was the case despite our prior observations that knockdown of *KDM5A*

resulted in a derepression of cell cycle genes in a manner that was independent of E2F4 [16]. Interestingly, the loss of *Kdm5a* in addition to *Rb1* in the double knockouts had an exacerbating effect on cell cycle re-entry (Fig. 9A and 9C). There was a more than two fold greater incidence of EdU incorporation in the DKOs compared to the *Rb1*$^{-/-}$ cells.

As we had previously seen in the knockdown model, I have shown here that genetic ablation of *Kdm5a* is also able to rescue defects of differentiation caused by loss of *Rb1*. This model is superior to the knockdown model in that it does not carry the same potential for off-target effects as does RNAi. Also because KDM5A is fully removed in this system, there is no potential for altered function caused by reduced levels of the protein.

Additionally, I have studied here the effect of *Kdm5a* and *Rb1* deletion on the cell cycle during differentiation. Cell cycle withdrawal is a component of normal, terminal differentiation [142]. Cell cycle regulators are upregulated as part of the differentiation program by tissue-specific transcription factors in order to drive cell cycle exit [140, 143]. Although the two processes are tightly linked, they are not mutually inclusive [49]. It has been shown that differentiation can be uncoupled from cell cycle exit [49]. Additionally, it has also been shown that in cells defective for differentiation, rescue of the cell cycle defect does not restore differentiation [17, 49]. The fact that loss of *KDM5A* rescues features of differentiation, like expression of tissue-specific markers and morphological changes, but not cell cycle withdrawal is in agreement with the separation of these two processes, and consistent with our earlier observations that

there are two separate pathways by which KDM5A regulates these two processes [15-17, 49].

B. KDM5A regulation of differentiation requires a functional JmjC catalytic domain.

KDM5A was first identified in 1991, but was largely overlooked for several years (84). The burgeoning interest in this protein began when it was determined to be a histone demethylase in 2007 [63, 64]. Due to this relatively short time frame for study, there is still much to be learned about how KDM5A functions in the cell. We know it is involved in several diverse cellular processes [14-17, 63, 64, 116-119, 121]. We know it can remove all three states of H3K4 methylation, but KDM5A is interesting in that it often localizes to genes that are highly expressed and highly enriched for H3K4me3 [15]. This is a phenomenon that would suggest that KDM5A does not have to act as a transcriptional repressor and demethylate histones when bound to the chromatin. This is not to say that it does not demethylate these target genes under the right circumstances, but it is clear that it does not always act as a demethylase. Further, we know that KDM5A and its homologs in yeast and flies can act as transcriptional activators in a manner that does not involve demethylation [121-125]. So considering this, it is important to ask when studying KDM5A, is histone demethylase activity required for the cellular function(s) in question?

KDM5A is able to cause a global reduction of H3K4me3 when transfected into MEFs (Fig. 10). KDM5AHE mutants have a point mutation at H483 and E485 in the iron-binding site of the JmjC domain. This is a naturally occurring variation that is found in certain JmjC domain proteins [110]. These proteins specifically lack demethylase

activity but the structure and the other functions of these proteins are not affected [110, 148]. They are able to interact with the chromatin and other binding partners and they are able to regulate transcription [110, 148]. This mutation when introduced to the JmjC domain of KDM5A has been shown to eliminate the demethylase capacity of the enzyme in the human cell lines U2OS and 293 [64]. Here, when transfected into MEFs the HE mutation does not affect the localization of the protein to the nucleus, but does eliminate demethylase activity (Fig 10). Although the transfection efficiency of KDM5A into MEFs is low (< 5%), all cells that were positive for KDM5A overexpression had visible global reductions of H3K4me3, while all cells that were positive for KDM5AHE mutants did not.

The HE mutation should not affect the ability KDM5A to interact with pRB as JmjC is not the domain through which KDM5A interacts with pRB [115]. Instead KDM5A has two known RB-interacting domains [115]. Mutation of the canonical pRB interacting domain LXCXE to LXCXA (KDM5A-LXCXA) does not affect demethylation by KMD5A (Fig 10). This is not unexpected, as KDM5A is known to have functions independent of pRB, and KDM5A is able to bind to the chromatin and demethylate independently of pRB [117, 118]. Therefore, specific defects due to a loss of interaction with pRB may be masked by the overall global changes of H3K4me3. Additionally KDM5A has a second non-canonical pRB-interacting domain in the C-terminus [115]. The exact location of this domain has not been determined so that specific mutation of it is not possible. Deletion of the entire C-terminus (KDM5A-ΔC), alone or in combination with the LXCXA mutation (KDM5A-LXCXA-ΔC), prevented global reduction of H3K4me3 (Fig. 10). This is most likely due to the fact that the nuclear localization signal of KDM5A is in the C-terminus

and so this deletion causes a loss of nuclear localization, restricting KDM5A to the cytoplasm [17].

Figure 10. Overexpression of KDM5A in MEFs causes a global reduction of H3K4me3.

Kdm5a$^{-/-}$*; Rb1*$^{-/-}$ MEFs were transfected with pcDNA3-HA-KDM5A, pcDNA3-HA-KDM5AHE, pcDNA3-HA-KDM5A-ΔC, pcDNA3-HA-KDM5A-ΔC-LXCXA, or pcDNA3-HA-KDM5A-LXCXA. Cells were stained for H3K4me3 (green) and KDM5A (red). H3K4me3 was visualized using anti-H3K4me3 primary antibody and anti-rabbit Alexafluor 488 secondary antibody. KDM5A was visualized using an anti-KDM5A antibody (2469) conjugated to a Cy3 fluorophore. Nuclei were stained with DAPI (blue). Images are representative of observations made in greater than 20 fields for each condition and in duplicate wells. Arrows point to cells positively transfected for KDM5A.

Figure 10

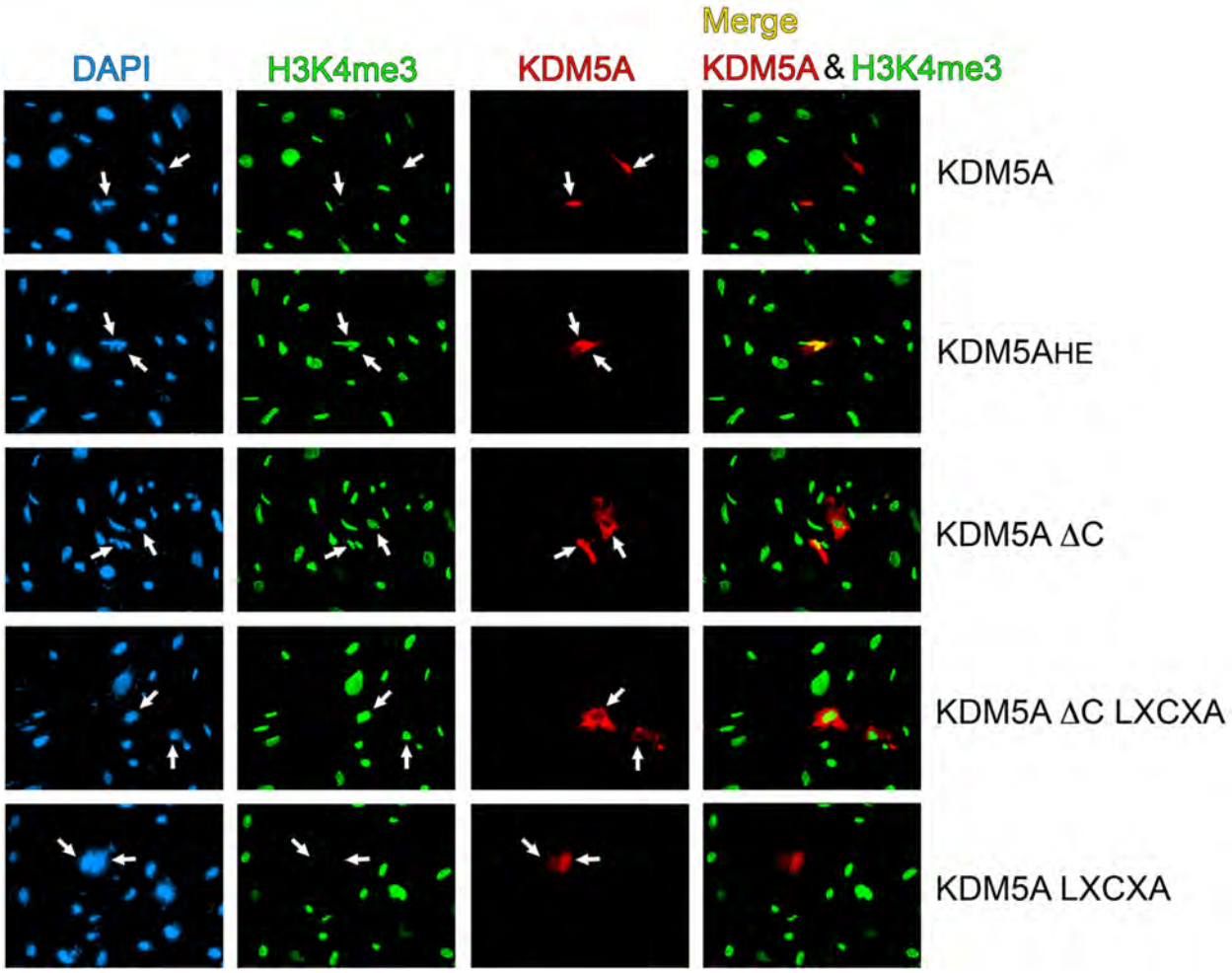
DAPI
H3K4me3
KDM5A
Merge
KDM5A & H3K4me3
KDM5A
KDM5AHE
KDM5A ΔC
KDM5A ΔC LXCXA
KDM5A LXCXA

To further expand upon the requirement for KDM5A to maintain the global state of H3K4 methylation, I looked for changes in the levels of all states of H3K4 methylation in knockout MEFs compared to WT (Fig. 11A). Loss of *Kdm5a* resulted in a roughly 2 – 2.5-fold increase in the global level of trimethylated H3K4, with little if any effect on the di- and mono-methylated states (Fig. 11A and 11B). Deletion of *Rb1* does not cause any change on its own (Fig. 11A and 11B). Loss of one copy of *Kdm5a* results in a minor increase of H3K4me3 that appears to be augmented by the additional loss of *Rb1* (Fig. 11A and 11B).

Figure 11. Loss of KDM5A results in a global increase of trimethylated H3K4.

(A) Western Blot: lysates from WT, *Kdm5a*$^{-/-}$, *Rb1*$^{-/-}$, *Kdm5a*$^{-/-}$*;Rb1*$^{-/-}$, *Kdm5a*$^{+/-}$, and *Kdm5a*$^{+/-}$*;Rb1*$^{-/-}$ MEFs examined for changes in the state of H3K4 methylation caused by the loss of *Kdm5a* and/or *Rb1*. A weak non-specific background band from the anti-KDM5A antibody is visible in the *Kdm5a*$^{-/-}$ lanes. Blots were probed for KDM5A, mon-, di-, and trimethylated H3K4, total H3, and α-tubulin. α-tubulin was used as a loading control here instead of total H3, to control for the possibility that incorporation of H3 may change due to changes in its state of methylation. **(B)** Global H3K4me3 levels were quantified using NIH ImageJ software, and represented as the average fold difference relative to WT. See Material and Methods section (Y) for details. Error bars represent the standard error of the mean of two blots run with lysates from distinct biological replicates.

Figure 11

A

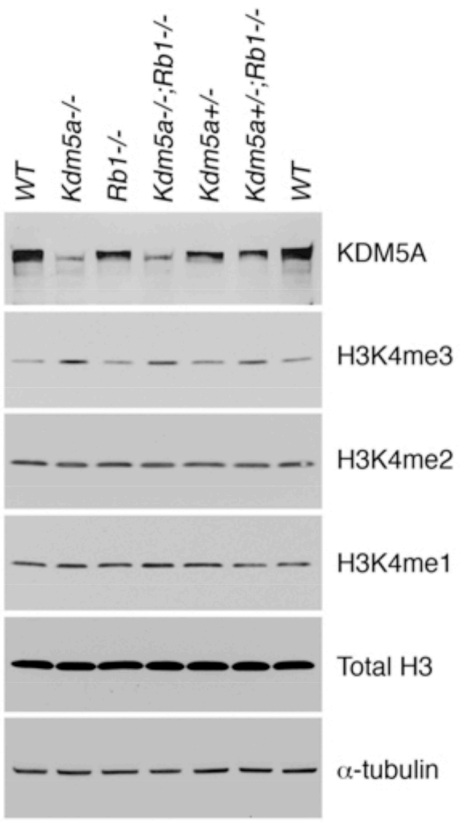
WT
Kdm5a-/-
Rb1-/-
Kdm5a-/-;Rb1-/-
Kdm5a+/-
Kdm5a+/-;Rb1-/-
WT
KDM5A
H3K4me3
H3K4me2
H3K4me1
Total H3
α-tubulin

B

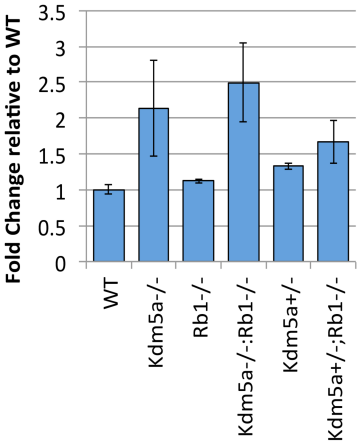
Fold Change relative to WT
3.5
3
2.5
2
1.5
1
0.5
0
WT
Kdm5a-/-
Rb1-/-
Kdm5a-/-;Rb1-/-
Kdm5a+/-
Kdm5a+/-;Rb1-/-

In order to study the requirements for demethylation by KDM5A during differentiation, I subcloned *KDM5A* and *KDM5AHE* into lentiviral vectors with a CMV promoter, an N-terminal FLAG tag, and hygromycin resistance (Fig 7). I was able to transduce MEFs with high efficiency and the expressed proteins displayed correct localization, determined by immunofluorescence staining (Fig. 12A). Western blotting showed that the size of the protein product is also as expected (Fig. 12B). The expression level for both WT and mutant *KDM5A* is below that of the endogenous protein in MEFs. The mutant protein showed higher levels than the WT protein. Cells transduced to express higher levels of the exogenous protein died.

Using these constructs, I evaluated the requirement for KDM5A demethylase activity in the regulation of differentiation. *Kdm5a*$^{-/-}$*; Rb1*$^{-/-}$ MEFs transduced to express either KDM5A, KDM5AHE, or a frameshift mutant (KDM5AFS) used as a negative control were induced to differentiate in parallel with WT, *Kdm5a*$^{-/-}$, and *Rb1*$^{-/-}$ MEFs. If the demethylase activity of KDM5A is required for its role in blocking differentiation, then the reintroduction of WT KDM5A but not the KDM5AHE mutant, should revert the differentiation phenotype back towards that of the *Rb1*$^{-/-}$ MEFs. Cells were stained for MyHC, EdU and DAPI. Differentiation was quantified based on expression of MyHC and the degree of multinucleation. Reintroduction of WT KDM5A restored the *Rb1*$^{-/-}$ phenotype while the cells expressing the KDM5AHE mutant exhibited a phenotype similar to the DKOs (Fig. 9A and 9B). The effect on cell cycle regulation during differentiation was evaluated by quantitatively comparing EdU incorporation. Again, the WT KDM5A restored the *Rb1*$^{-/-}$ phenotype while the KDM5AHE mutant had a much weaker effect (Fig. 9A and 9C).

Figure 12. Validation of lentiviral constructs made to express KDM5A and KDM5AHE

(A) Immunofluorescent staining. MEFs: WT, *Kdm5a*$^{-/-}$*;Rb1*$^{-/-}$, and *Kdm5a*$^{-/-}$*;Rb1*$^{-/-}$ transduced with lenti-CMV-FLAG-KDM5A or lenti-CMV-FLAG-KDM5AHE. Stained with anti-FLAG (red) or anti-KDM5A 2469 (green) antibodies and DAPI. **(B)** Western blots. MEFs: WT, *Kdm5a*$^{-/-}$*;Rb1*$^{-/-}$, and *Kdm5a*$^{-/-}$*;Rb1*$^{-/-}$ transduced with lenti-CMV-FLAG-KDM5A or lenti-CMV-FLAG-KDM5AHE. The blots were probed with anti-FLAG antibody (left panel) and anti-KDM5A antibody 2469 (right panel). α-tubulin was run as a loading control.

Figure 12

A

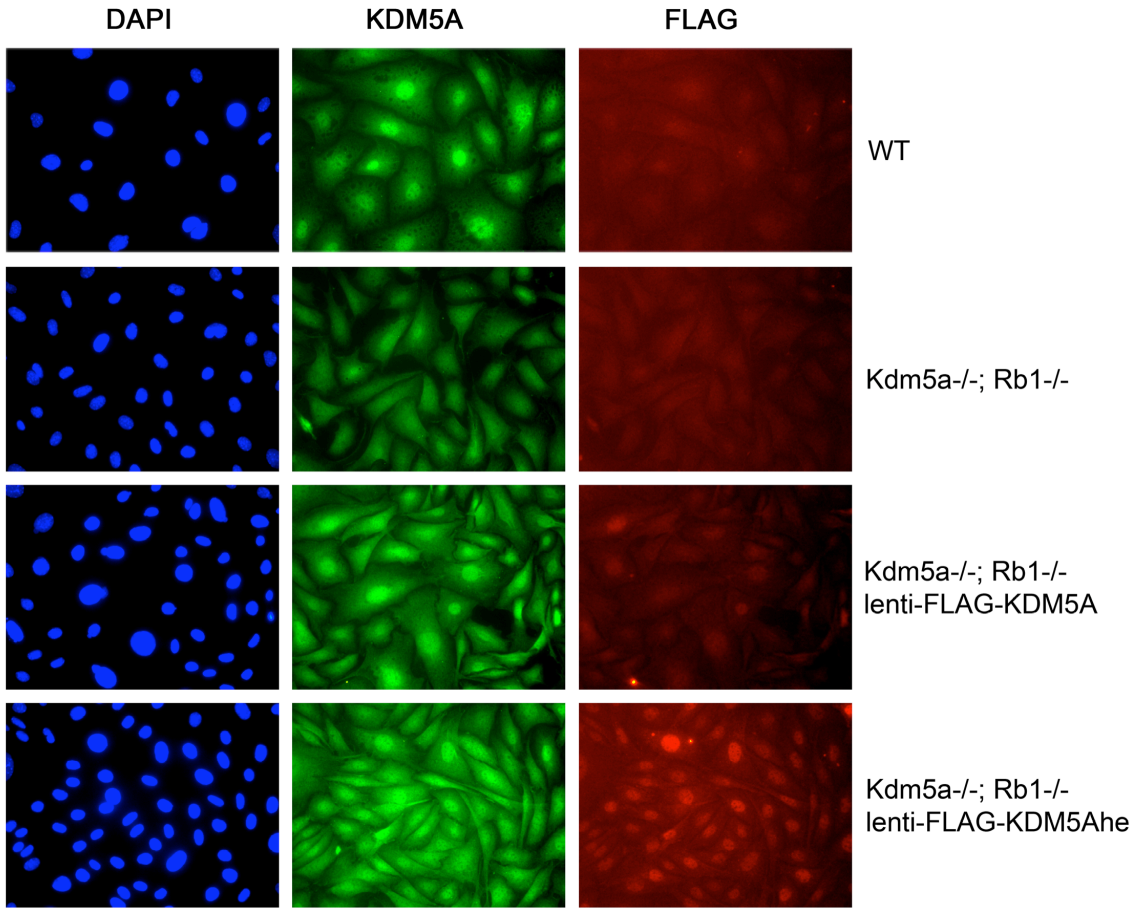
DAPI
KDM5A
FLAG
WT
Kdm5a-/-; Rb1-/-
Kdm5a-/-; Rb1-/-
lenti-FLAG-KDM5A
Kdm5a-/-; Rb1-/-
lenti-FLAG-KDM5Ahe

B.

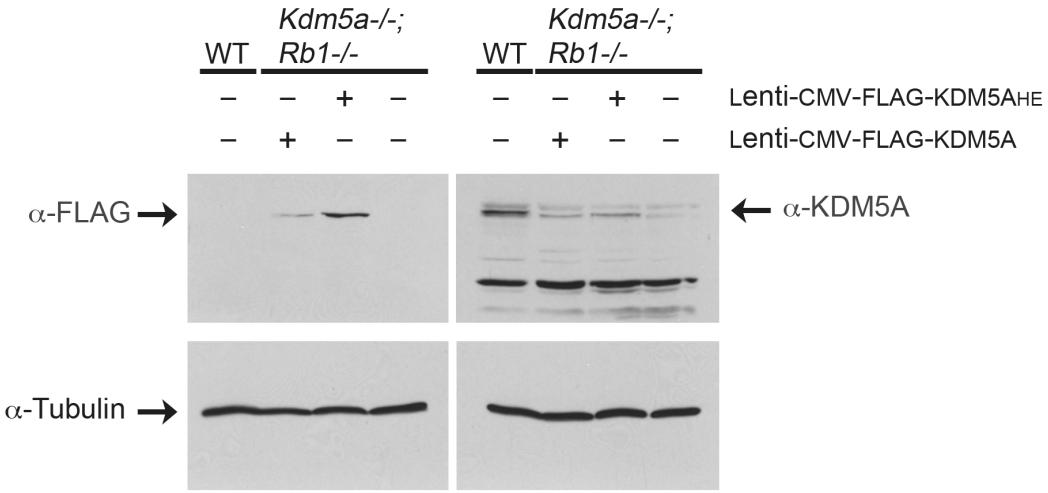
WT
Kdm5a-/-; Rb1-/-
WT
Kdm5a-/-; Rb1-/-
– – + – – – + – Lenti-CMV-FLAG-KDM5AHE
– + – – – + – – Lenti-CMV-FLAG-KDM5A
α-FLAG
α-KDM5A
α-Tubulin

KDM5A is a known histone demethylase. Here I have reconfirmed its capacity for this by overexpression in MEFs. I observed that overexpressed KDM5A but not KDM5AHE that contains a point mutation in the enzymatic domain, causes a global reduction of H3K4me3. Importantly, I was able to demonstrate that the reverse is also true. That loss of KDM5A causes a global increase in H3K4me3 but not in the other states of H3K4 methylation. This result indicates specific and necessary role for KDM5A in the regulation of H3K4me3 in the cell.

Additionally I have shown that this ability to regulate H3K4me3 by KDM5A is necessary for its role as a negative regulator of differentiation. Reintroduction of WT KDM5A but not KDM5AHE, caused a differentiation defect in DKOs that was similar to that in *Rb1*$^{-/-}$ cells. This is an important point to establish because KDM5A has a dichotomous role in transcriptional regulation, where the requirement of histone demethylation appears to be context dependent [13-17, 63, 64, 116-125].

C. KDM5A and pRB share a common set of genes involved in metabolism.

The data thus far supports the proposed model where KDM5A negatively regulates differentiation, while pRB promotes differentiation by relieving this repressive effect. The salient question that remains is: what is the mechanism of this action? Both pRB and KDM5A are transcriptional regulators, and so it is likely that clues into the nature of their relationship during differentiation lie at the level of gene expression [17]. To investigate the transcriptional program(s) controlled by these two factors during differentiation, I performed RNA-sequencing analysis in collaboration with the Lopez-Bigas group at the Universitat Pompeu Fabra in Barcelona, Spain. The purpose was

twofold: (1) to determine what genes are deregulated in *Rb1*$^{-/-}$ cells during differentiation as an indication of the genetic events that are responsible for defective differentiation in these cells. (2) To determine how the additional loss of *Kdm5a* affects expression of these genes in the double knockouts. We can predict if our model is correct, that loss of Kdm5a in the DKOs will restore expression of the genes necessary for differentiation back towards WT levels.

Differential expression from four genotypes, WT, *Kdm5a*$^{-/-}$, *Rb1*$^{-/-}$, and *Kdm5a*$^{-/-}$*; Rb1*$^{-/-}$ performed in biological replicates, was determined relative to the WT cells. In addition to these four conditions, I also ran a second set of WT and *Kdm5a*$^{-/-}$*; Rb1*$^{-/-}$ cells that were processed to isolate myotubes from undifferentiated cells. Even among the WT MEFs a percentage of cells remain undifferentiated. Because of this I developed a technique to purify differentiated myotubes from the heterogeneous population (Fig. 13). This data was also used to verify the results obtained from the non-purified populations.

Figure 13. Purification of myotubes from undifferentiated MEFs.

(A) For both WT and *Kdm5a*$^{-/-}$*; Rb1*$^{-/-}$ cells, 72 hours after induction of differentiation, myotubes were purified from a mixed population that contained undifferentiated and differentiated cells. The media was removed from the well and saved as conditioned media. Cells were rinsed with PBS then trypsinized and resuspended in growth media. When in suspension myotubes lose their tube-shape morphology and adopt a more spherical shape. Multinucleated myotubes are larger than undifferentiated MEFs. This property was used to distinguish them from the undifferentiated cells. Myotubes sank to the bottom of the tissue culture dish faster than the undifferentiated cells. The top ¾ of media was slowly removed by pipette taking with it mostly undifferentiated cells leaving the differentiated cells at the bottom of the dish. See materials and methods section (H), for details of procedure. **(B)** *Kdm5a*$^{-/-}$*; Rb1*$^{-/-}$ cells induced to differentiate. Images taken of cells in culture before purification on the left, after purification center, and after purification and nuclei were stained with DAPI on the right.

Figure 13

A

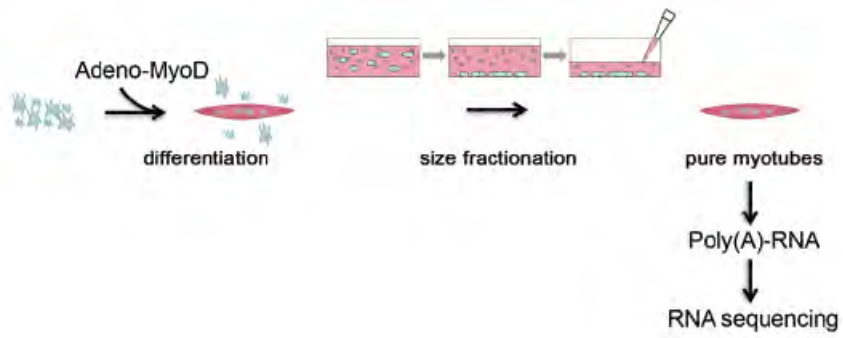
Adeno-MyoD
differentiation
size fractionation
pure myotubes
Poly(A)-RNA
RNA sequencing

B

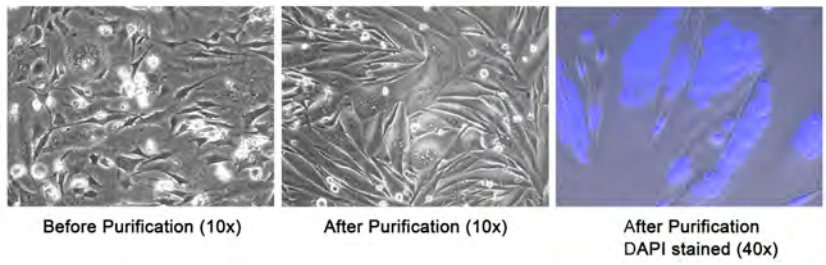
Before Purification (10x)
After Purification (10x)
After Purification
DAPI stained (40x)

I created several gene lists based on a defined set of criteria. First I selected only the protein-coding genes. Second I excluded genes for which there were fewer than 20 copies of the transcript in both pairwise conditions. For example, when comparing differential expression between WT and *Rb1*$^{-/-}$ cells, there had to be at least 20 copies of transcript for a given gene in either the WT or *Rb1*$^{-/-}$. If both the WT and *Rb1*$^{-/-}$ had fewer than 20 transcripts the gene was excluded from the list. Third, I did not include differentially expressed genes where the adjusted p-value for the differential expression was greater than 0.05. All lists met this minimum standard. From this point I created a number of different lists with specific thresholds related to differential expression (Table II). These lists were then used for gene ontology (GO) enrichment analysis for Biological Process (GOBP), and Cellular Component (GOCC). For example enrichment analysis for Biological Process can tells us which ontological terms related to biological processes appear among a given list of genes, at a rate that is higher than expected by chance [149]. Hypothetically if we perform this analysis on a list of genes that show higher expression in *Rb1*$^{-/-}$ cells compared to WT, we would expect to see terms associated with the cell cycle, based on the well-established role of pRB as a potent cell cycle repressor [9]. The advantage of this type of analysis is that it is an unbiased method to analyze thousands of genes and identify what are likely to be important categories. Thus allowing us to simplify what began as an overwhelming list of genes into a manageable set of ontologies and the associated genes [149]. The significantly enriched ontology terms can help to steer us towards the most important genes.

Table II. Gene lists generated from RNA-seq data of differentially expressed genes and used for enrichment analysis shown in figure 14.

A master list was created that included only the protein-coding genes. Included only genes with at least 20 copies of the transcript in at least one of genotypes being compared. Included only genes where the adjusted p-value for differential expression was less than 0.05. From the master list, several lists were created in order to address particular questions. Question 1: What are the genes that are defective in expression in *Rb1*$^{-/-}$ cells compared to WT after induction of differentiation? Defective expression meaning either higher than WT (“UP”) or lower than WT (“Down”), [Lists 1 and 2] . Question 2: What genes that have decreased expression in *Rb1*$^{-/-}$ compared to WT are also target genes of KDM5A? [List 3]. Question 3: What genes that show decreased expression in *Rb1*$^{-/-}$ cells are restored back toward WT levels (“rescued”) due to the additional loss of KDM5A? [List 4]. Question 4: What genes that are “rescued” in the DKOs compared to *Rb1*$^{-/-}$ are also KDM5A targets? [List 5].

Enrichment analysis compared each gene list to a list of background genes. The background gene list included all mouse genes from the Ensemble database version 59, excluding non-protein-coding genes and genes on the X and Y chromosomes. The Gene Ontology terms associated with each gene were downloaded from the gene ontology database at www.geneontology.org and used as a reference list to identify terms that are significantly enriched in each of the lists of genes analyzed.

Table II

List #	Genotypes compared	DE thresholds	Gene criteria and number	Label
1	$Rb1^{-/-}$ vs WT	>1.7 fold increase	All genes (3,432)	Up
2	$Rb1^{-/-}$ vs WT	>1.7 fold decrease	All genes (2,766)	Down
3	$Rb1^{-/-}$ vs WT	>1.2 fold decrease	Only Kdm5a targets genes (734)	Down-targets
4	DKO vs $Rb1^{-/-}$	>1.3 fold rescue	All genes (2,426)	Rescue
5	DKO vs $Rb1^{-/-}$	>1.3 fold rescue	Only Kdm5a target genes (330)	Rescue-targets

Enrichment analysis for GOBP of differentially expressed genes in the *Rb1*$^{-/-}$ condition compared to WT revealed that the genes with higher expression in the *Rb1*$^{-/-}$ cells are in fact enriched in GO terms that one might predict based on what we know about pRB function. We see processes associated with cell cycle, proliferation, cell division, DNA damage, and apoptosis (Fig 14A). Also as expected and consistent with the results of the differentiation assays, there is a decrease in expression of genes involved in muscle systems (Fig. 14A). On the other hand, what was quite interesting to see, was that the most significantly enriched terms identified in the list of genes with decreased expression in the *Rb1* knockouts had to do with metabolism and mitochondrial function (Fig. 14A). New evidence is revealing pRB to be a major regulator of metabolic pathways with an impact on several downstream cellular processes [40, 44, 45, 150, 151]. Mitochondrial biogenesis and mitochondrial function have been shown to be required for myogenic differentiation as well as differentiation of other tissue types, and so this may be a critical gene set affected by loss of *Rb1*$^{-/-}$ [151-154].

Considering the connection between mitochondrial function and differentiation, the defective expression of the metabolic gene set in the *Rb1*$^{-/-}$ cells may be an important causative factor in the defect in differentiation. If this is true, then we could predict that in the DKO cells where the differentiation phenotype is largely rescued, we should also see a rescue at the level of gene expression for the metabolic genes. Indeed, analysis of the list of genes that are restored back towards WT levels in the *Kdm5a*$^{-/-}$*; Rb1*$^{-/-}$ cells when compared to the *Rb1*$^{-/-}$ cells shows a high degree of

enrichment for genes involved in metabolism and mitochondrial function along with the muscle related genes (Fig. 14B).

Consistent with the above results that identified metabolic processes, enrichment analysis for GOCC revealed that genes with decreased expression in the *Rb1* knockouts coded for components of muscle cells and for mitochondrial components (Fig. 14D). Interestingly the mitochondrial terms were the most significantly enriched, even more so than the muscle terms. All mitochondrial terms had an adjusted p-value of less than 7×10^{-13} compared to 2×10^{-4} for muscle-related terms. Other cellular components were also enriched to a lesser extent in the down-regulated list, but the majority of these were not rescued by the additional loss of *Kdm5a* in the DKOs (Fig. 14D), while the mitochondrial components and muscle related components showed highly significant enrichment in the rescued list of genes (Fig. 14D).

Figure 14. Loss of *Kdm5a* in a *Rb1*$^{-/-}$ background rescues expression of metabolic genes in cells induced to differentiate.

RNA-seq followed by gene ontology enrichment analysis for Biological Process (GOBP) or Cellular Component (GOCC) was performed on differentially expressed genes for *Rb1*$^{-/-}$ vs. WT, and *Kdm5a*$^{-/-}$*;Rb1*$^{-/-}$ vs. *Rb1*$^{-/-}$. Data is presented as heatmaps. Each column represents a list of genes that was analyzed. Each cell represents by color, the statistical significance of enrichment. Grey is no significance. Significance increases from yellow to red. **(A)** Enriched terms (GOBP) from the list of genes that have higher expression in *Rb*$^{-/-}$ compared to WT (Table II list 1) labeled "UP" at the top of the column and enriched terms from the list of genes that have lower expression in *Rb*$^{-/-}$ compared to WT (Table II list 2) labeled "DOWN" at the top of the column. The adjusted p-value is $< 8 \times 10^{-4}$ for all enriched terms shown. **(B)** Enrichment of terms (GOBP) from the gene list where expression is rescued "Resc" in DKOs compared to *Rb1*$^{-/-}$, back towards WT levels (Table II list 4). The adjusted p-value is $< 3 \times 10^{-4}$ for all enriched terms shown. **(C)** Left column: enrichment of terms (GOBP) from the list of genes that have lower expression in *Rb*$^{-/-}$ compared to WT and are also KDM5A target genes, labeled "DOWN" at the top of the column (Table II list 3). Right column: Enrichment of terms from genes that are KDM5A targets and whose expression is rescued "Resc" back towards WT levels in the DKOs compared to *Rb1*$^{-/-}$ (Table II list 5). The adjusted p-value is $< 3 \times 10^{-4}$ for all enriched terms shown. **(D)** Left column: enrichment of terms (GOCC) from the list of genes that have lower expression in Rb$^{-/-}$ compared to WT (Table II list 2) labeled "DOWN" at the top of the column. Middle column: enrichment of terms from the gene list where expression is rescued "Resc" in DKOs compared to *Rb1*$^{-/-}$, back towards WT

levels (Table II list 4). Right column: enrichment of terms from genes that are KDM5A targets and whose expression is rescued “Resc” back towards WT levels in the DKOs compared to *Rb1*$^{-/-}$ (Table II list 5). The adjusted p-value is < 0.04 for all enriched terms shown.

Figure 14

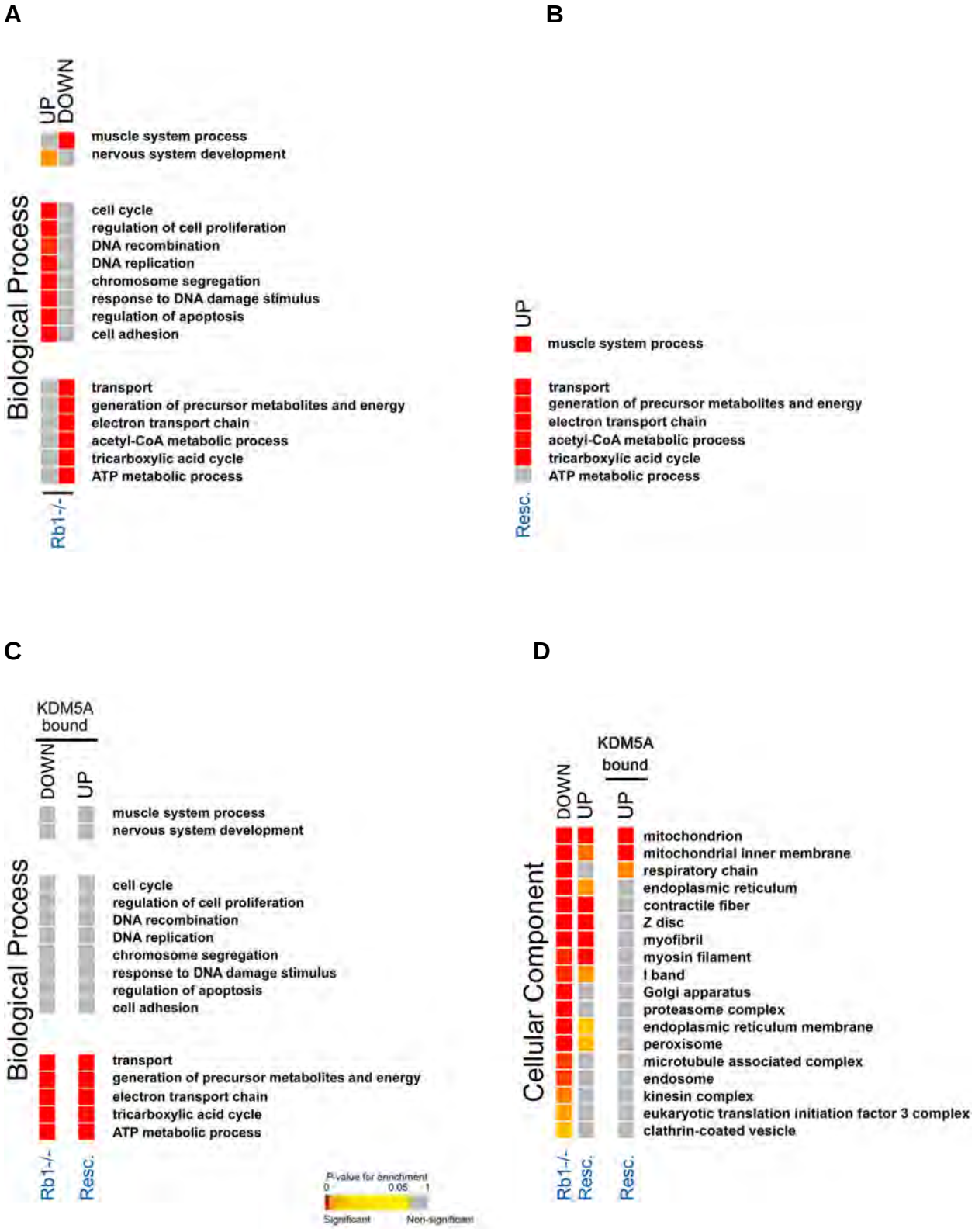
A
UP
DOWN
muscle system process
nervous system development
Biological Process
cell cycle
regulation of cell proliferation
DNA recombination
DNA replication
chromosome segregation
response to DNA damage stimulus
regulation of apoptosis
cell adhesion
transport
generation of precursor metabolites and energy
electron transport chain
acetyl-CoA metabolic process
tricarboxylic acid cycle
ATP metabolic process
Rb1-/-
B
UP
muscle system process
transport
generation of precursor metabolites and energy
electron transport chain
acetyl-CoA metabolic process
tricarboxylic acid cycle
ATP metabolic process
Resc.
C
KDM5A bound
DOWN
UP
muscle system process
nervous system development
Biological Process
cell cycle
regulation of cell proliferation
DNA recombination
DNA replication
chromosome segregation
response to DNA damage stimulus
regulation of apoptosis
cell adhesion
transport
generation of precursor metabolites and energy
electron transport chain
tricarboxylic acid cycle
ATP metabolic process
Rb1-/-
Resc.
P-value for enrichment
0
0.05
1
Significant
Non-significant
D
KDM5A bound
DOWN
UP
UP
Cellular Component
mitochondrion
mitochondrial inner membrane
respiratory chain
endoplasmic reticulum
contractile fiber
Z disc
myofibril
myosin filament
I band
Golgi apparatus
proteasome complex
endoplasmic reticulum membrane
peroxisome
microtubule associated complex
endosome
kinesin complex
eukaryotic translation initiation factor 3 complex
clathrin-coated vesicle
Rb1-/-
Resc.
Resc.

The next important question to be asked here is whether pRB and KDM5A are direct or indirect regulators of the gene sets that are rescued in the DKO condition. We know from earlier work that KDM5A is a direct regulator of metabolic genes in human and mice cells [15, 16]. Additionally, publicly available ChIP-seq data for pRB in human fibroblast cells has shown that pRB directly binds to genes coding for mitochondrial components [155].

I used genome-wide Chromatin Immuno-precipitation Sequencing (ChIP-seq) data for KDM5A binding, in mES cells that was performed in our lab, compared to the RNA-seq data, to identify the differentially expressed genes that are also direct targets. KDM5A-bound target regions were determined by comparing in duplicate ChIP-seq peak data in mES cells where KDM5A is floxed to mES cells where KDM5A is deleted [16]. Enrichment analysis for GOBP on the list of genes that were rescued in the DKOs compared to *Rb1*$^{-/-}$ and were also KDM5A targets, showed again that a highly significant portion of these genes are involved in metabolic processes, but not cell cycle or developmental processes (Fig 14C). Analysis for GOCC on the same list showed the highly significant enrichment for mitochondrial terms only (Fig. 14D). No enrichment was observed for muscle related terms or any other cellular components that are defective in the *Rb1*$^{-/-}$ cells (Fig. 14D).

So the sum of all of the above results indicates that pRB and KDM5A are both direct regulators of a set of genes that code for metabolic pathway and mitochondrial components. Expression of these genes is decreased due to the loss of *Rb1*, but the additional loss of *Kdm5a* in the DKOs shifts their expression back towards WT levels. This implicates pRB as a positive regulator and KDM5A a negative regulator of this

gene set and suggests that these genes are likely to be important for how pRB and KDM5A regulate differentiation.

The genome wide analysis performed here was of great use as a first step in narrowing the focus from all possible genes in the genome down to a most likely group of genes. However, the data is limited in its utility to definitively assess in detail the gene expression and chromatin binding dynamics of this myogenic system. Some of the reasons for this are as follows: the ChIP-seq data was derived from proliferating and non-muscle cell types. For the RNA-seq data, the minimal threshold for fold increase of target gene expression in the DKOs compared to *Rb1*$^{-/-}$ was set as low as 1.3. Because of these reasons, I did more detailed and in depth experiments on a smaller scale.

I performed qPCR and ChIP-qPCR on a representative set of genes in cells induced to differentiate down the myogenic lineage. These methods allow me to look closely at gene expression of relevant genes, as well as the binding dynamics of both KDM5A and pRB at the same target genes during myogenic differentiation. I chose genes associated with mitochondrial metabolic processes that were identified to be KDM5A target genes that had decreased expression in the *Rb1*$^{-/-}$ cells and at least partially rescued expression in the DKOs. They are representative of several different mitochondrial complexes and are involved in different mitochondrial functions such as oxidative metabolism and mitochondrial dynamics (Table III).

Gene	Mitochondrial Role	Location
MFN2	Fusion of mitochondria	Outer mitochondrial membrane
NDUFS4	ETC complex I (NADH dehydrogenase) subunit	Inner mitochondrial membrane
SDHD	ETC complex 2 (succinate dehydrogenase) subunit	Inner mitochondrial membrane
UQCRC1	ETC complex 3 (Ubiquinol-cytochrome-c reductase) subunit	Inner mitochondrial membrane
COX6B1	ETC complex 4 (cytochrome c oxidase) subunit	Mitochondrion intermembrane space
ATP5A1	ETC complex 5 (ATP synthase) subunit	Inner mitochondrial membrane

Table III. Mitochondrial components and their role in the mitochondrion.

The table lists the mitochondrial component genes whose expression dynamics are studied in figure 15. Left column s the gene symbol. Center column is the role within the mitochondrion. Right column is the location in the mitochondrion.

By qPCR I compared gene expression in WT, *Rb1*$^{-/-}$, *Kdm5a*$^{-/-}$, and DKOs at three time-points after induction of differentiation: 0hr(undifferentiated), 24hr(early time-point), and 96hr(late time-point). In the WT cells, expression of all these genes increased as differentiation progressed with time (Fig. 15). This observation is in accordance with the increase in mitochondrial biogenesis that is known to occur during myogenic differentiation [156, 157]. In the *Kdm5a*$^{-/-}$ cells, expression of these genes also increased as differentiation progressed, to levels equal to or in many cases greater than that of the WT cells (Fig. 15). *Rb*$^{-/-}$ cells were unable to increase expression of these genes during differentiation, however; the additional loss of *Kdm5a* in the DKO condition fully restored the expression dynamics similar to WT in most cases: *Ndufs4*, *Sdhd*, *Uqcrc1*, *Cox6b1* (Fig. 15). At two genes, *Mfn2* and *Atp5a1*, expression levels were partially restored to WT levels, but still significantly increased compared to expression in the *Rb1*$^{-/-}$ cells (Fig. 15).

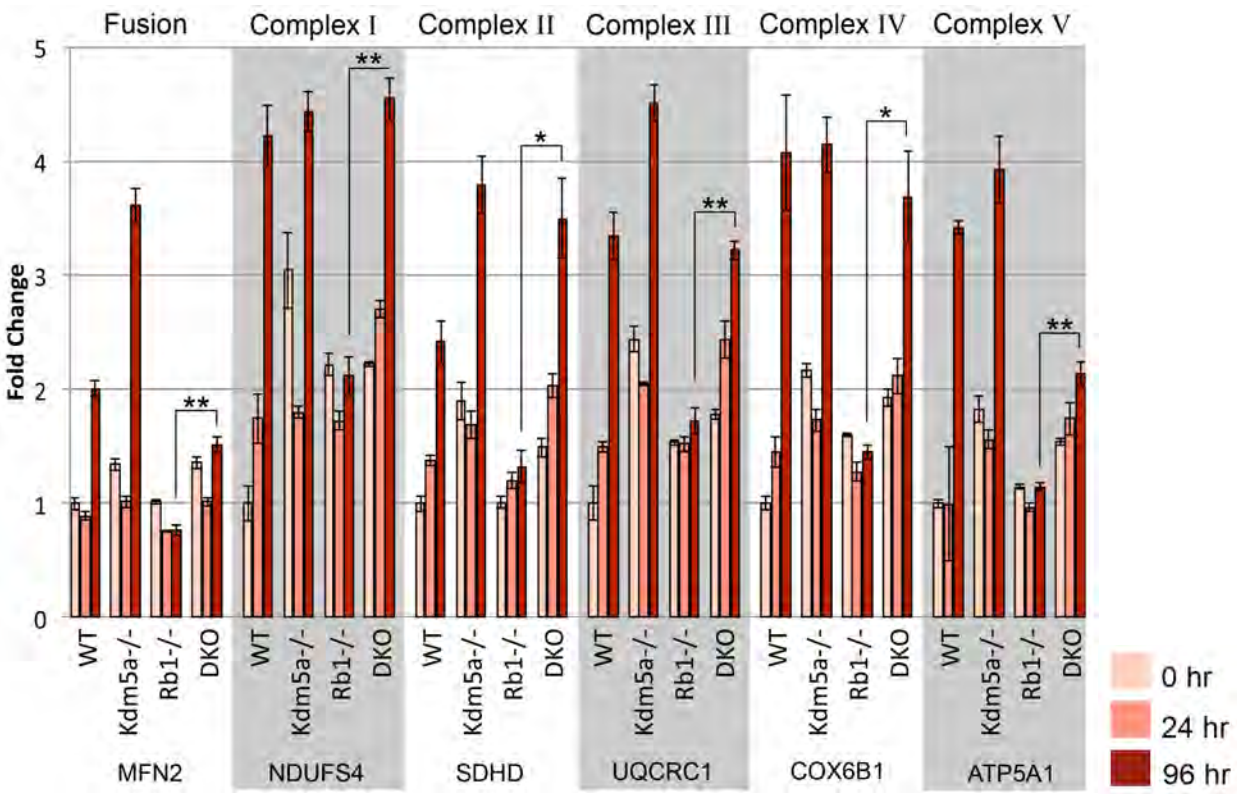

Figure 15. *Rb1*$^{-/-}$ MEFs do not properly upregulate genes encoding mitochondrial components when induced to differentiate, while the additional loss of *Kdm5a* restores expression back towards WT levels.

MEFs were induced to differentiate for 0, 24 and 96 hours. qPCR was performed for the indicated genes at each time-point in each genotype, and shown as fold change relative to WT at 0hr for each gene. Error bars represent the standard error of the mean of 3 replicates. The statistical significance for the condition DKO compared to *Rb1*$^{-/-}$ at 96 hours was determined by the Student's t-test and shown as p-values above the bars. * p-value ≤ 0.005. ** p-value ≤ 0.001.

Following the gene expression studies, I looked more closely at the binding of pRB and KDM5A to common metabolic target genes during differentiation using ChIP-qPCR. Traditionally pRB has proven itself to be quite intractable with respect to chromatin IPs. Because of this, I decided to use an epitope-tagged exogenous pRB for the ChIP experiment. As with *KDM5A*, I subcloned *RB1* into a CMV-FLAG-lentivector (Fig. 7). Validation experiments with this construct showed high transduction efficiency into *Rb1*$^{-/-}$ MEFs (Fig. 16A). The expressed protein was the expected size as determined by Western Blot (Fig. 16B), and localized appropriately in the nucleus (Fig. 16A). Functionally the exogenous pRB was able to rescue differentiation when introduced into the *Rb1*$^{-/-}$ MEFs (Fig. 17A and 17B). I did ChIP-qPCR for KDM5A and FLAG-RB using these cells under proliferating conditions and at 0hr and 24hr after induction of differentiation. Both KDM5A and FLAG-RB bound to the promoter region in proliferating cells (Fig. 18A and 18B). As differentiation progressed, binding of FLAG-RB increased while binding of KDM5A decreased (Fig. 18A and 18B). The decrease in KDM5A binding appears to be dependent on the presence of pRB, at least at some genes, as the level of KDM5A bound to the MFN2 promoter in *Rb1*$^{-/-}$ cells did not change after induction of differentiation (Fig. 18C).

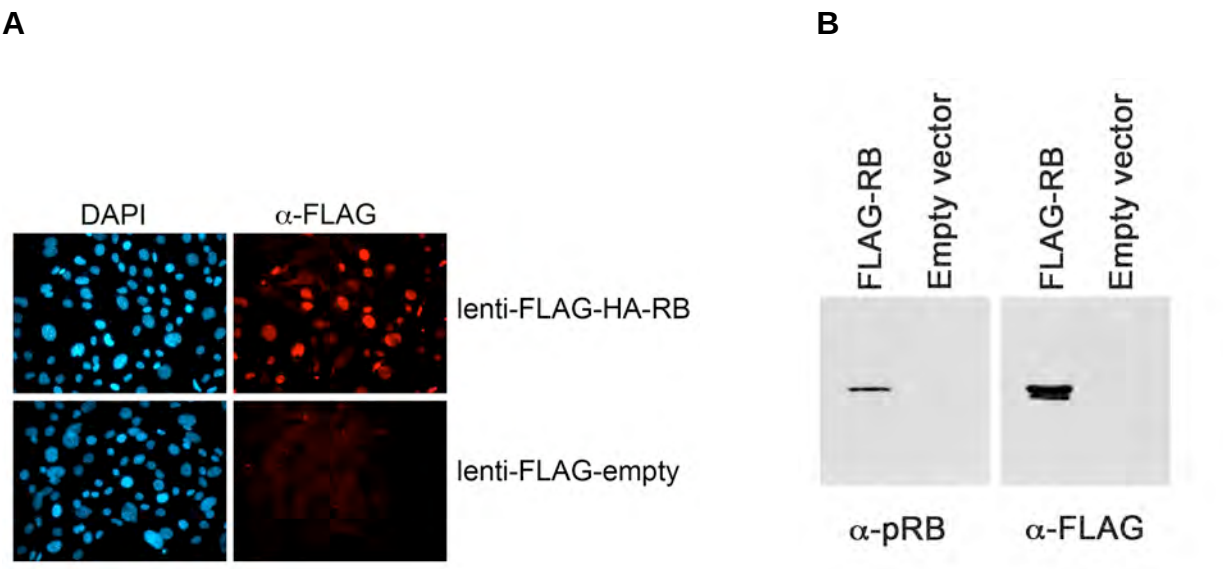

Figure 16. Validation of lentiviral constructs made to express *RB1*.

(A) Immunofluorescent staining. *Rb1*$^{-/-}$ MEFs transduced with lenti-CMV-FLAG-HA-RB. Stained with anti-FLAG (red) and DAPI (blue). **(B)** Western blot. *Rb1*$^{-/-}$ MEFs transduced with lenti-CMV-FLAG-HA-RB or lenti-CMV-FLAG-empty. Probed with anti-RB antibody (left panel) and anti-FLAG antibody (right panel).

A

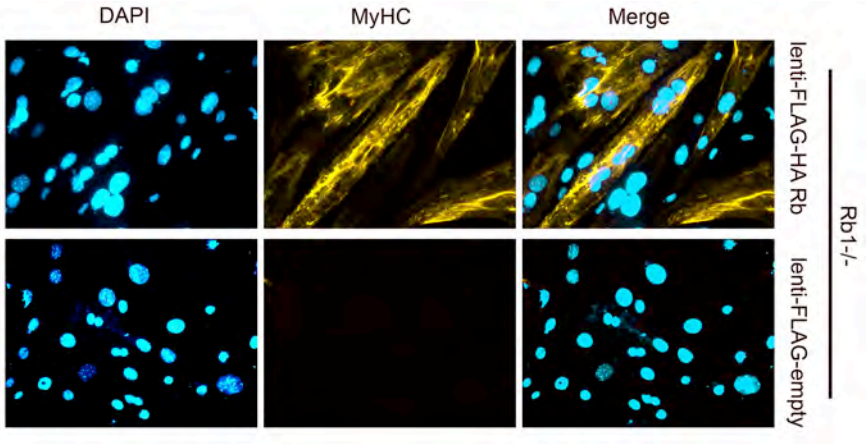

B

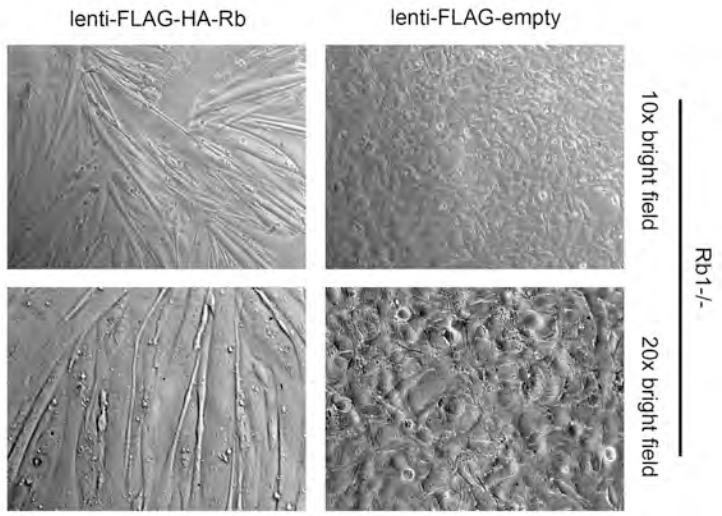

Figure 17. Functional validation of pRB expressed from lentiviral constructs.

(A) *Rb1*$^{-/-}$ MEFs transduced with lenti-CMV-MyoDER[T] and lenti-CMV-FLAG-HA-RB or lenti-CMV-FLAG-empty. Induced to differentiate for 72hr. Cells were stained with anti-MyHC and DAPI. **(B)** Bright field images 10x and 20x magnification.

Figure 18. Chromatin binding dynamics of pRB and KDM5A at the promoter of several genes associated with different aspects of mitochondrial function.

Rb1$^{-/-}$ MEFs were transduced with Lenti-CMV-FLAG-HA-RB and Lenti-CMV-MyoDER[T]. Proliferating cells were subconfluent in growth media. 0hr cells were confluent in differentiation media but MyoDER[T] was not induced. 24hr cells were confluent in differentiation media and induced to differentiate for 24hr. **(A)** ChIP-qPCR was performed for FLAG-RB. **(B)** ChIP-qPCR was performed for KDM5A. Binding at target genes is shown compared to a negative control region (Igr2). Error bars for A and B represent the standard error of the mean for 3 replicate PCR reactions. **(C)** *Rb1*$^{-/-}$ MEFs were transduced with Lenti-CMV-MyoDER[T] and induced to differentiate. ChIP-qPCR was performed for KDM5A at the *Mfn2* promoter compared to a negative control region, Igr2. Error bars represent the standard error of the mean from two replicate chromatin IPs.

Figure 18

A

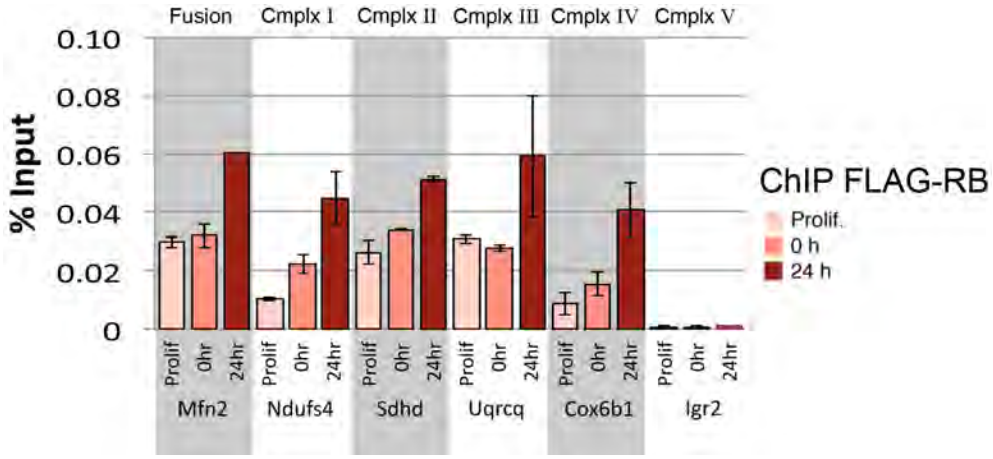

B

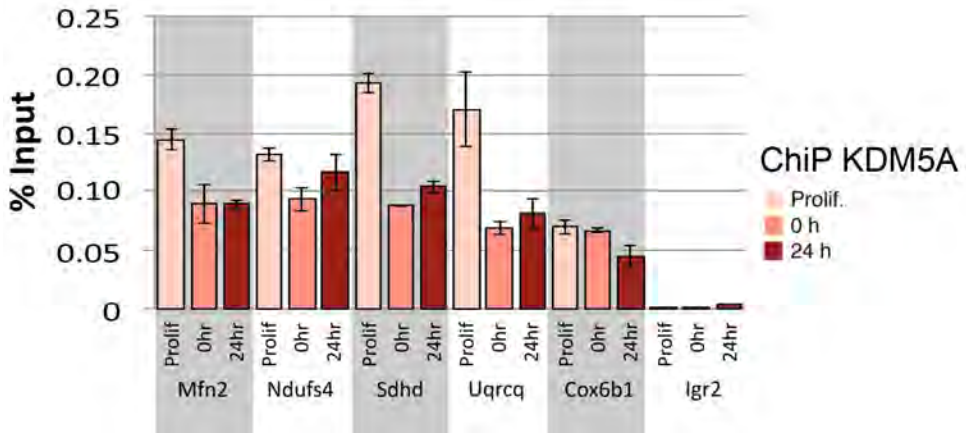

C

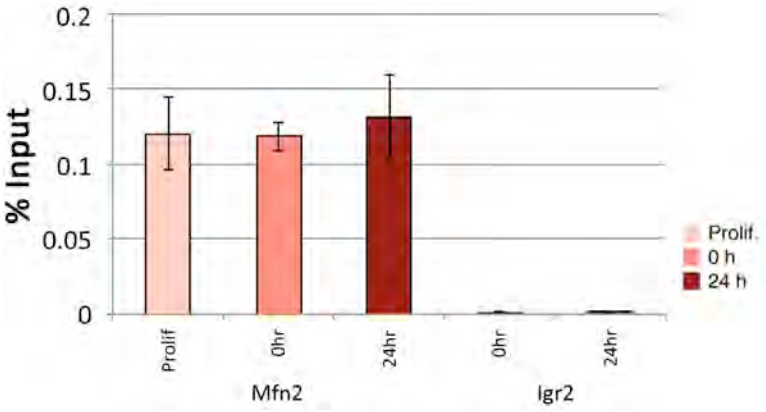

The sum of these results indicates that both KDM5A and pRB are direct regulators of mitochondrial component genes. The evidence for this lies in the observation that both of these factors bind to the promoters of multiple mitochondrial component genes and that the loss of either *Kdm5a* or *Rb1*$^{-/-}$ has a direct effect on gene expression. The binding dynamics of each protein show that they can both bind to the same target genes but in an opposing manner. KDM5A has a higher degree of enrichment in the undifferentiated state, that is reduced as differentiation proceeds, while; pRB starts out at a lower level and increases binding as differentiation progresses. Additionally, KDM5A does not come off the promoter in cells that lack pRB. These events occur at the earliest stages of differentiation suggesting a causative role in the regulation of the process. This is in agreement with the hypothesis that KDM5A acts as a negative regulator of gene expression and pRB promotes expression at least in part by causing the removal of KDM5A from the promoter.

D. *Rb1*$^{-/-}$ MEFs are defective in mitochondrial biogenesis when induced to differentiate. Additional loss of *Kdm5a* rescues the defect.

The gene expression and ChIP data show KDM5A and pRB to be direct regulators of genes coding for mitochondrial components. pRB appears to be a positive regulator required for proper gene expression during differentiation. Conversely, KDM5A seems to have a negative regulatory role at these genes in opposition to pRB, and fitting with the working model. Based on this genetic evidence, it is reasonable to expect that the mitochondria in *Rb*$^{-/-}$ MEFs may have measurable defects in cells induced to differentiate and additional loss of *Kdm5a* may rescue any such defects.

Mitochondria are highly dynamic organelles. They can exist in many shapes and sizes at any given moment in a cell, depending on the cell type, energy demands, stress, and environmental factors [156]. In MEFs they exist primarily in tubular networks and as well as in small rod and spherical shapes [158]. Normally during myogenesis, mitochondria undergo drastic morphological changes [156, 157, 159, 160]. These changes involve fusion events, where the mitochondria fuse together forming mitochondrial structures that can be recognized by the large round morphology [157, 158]. Evidence suggests that this increased mitochondrial biogenesis as it is called, is not simply a downstream effect of myogenesis meant to fulfill the increased energy demands of muscle cells, but it may actually be a prerequisite for differentiation [151-154, 161].

In order to evaluate the potential effects on mitochondrial morphology due to the loss of *Rb1* or *Kdm5a*, I induced WT, *Kdm5a*$^{-/-}$, *Rb1*$^{-/-}$, and DKO MEFs to differentiate for 72 hours. I then stained for the mitochondrial marker cytochrome c oxidase (CoxIV) and imaged by confocal microscopy using a 100x objective. Mitochondria in the WT cells formed large, round, densely packed structures that extending throughout the length of the myotube (Fig. 19A and 19B). The mitochondria in *Rb1*$^{-/-}$ cells displayed obvious defects. They appeared to be much smaller and highly fragmented (Fig. 19A and 19B). The mitochondria in the *Kdm5a*$^{-/-}$ cells appeared to be normal. Importantly, the defective morphology observed in the *Rb1*$^{-/-}$ cells was rescued by the additional loss of *Kdm5a* in the DKOs (Fig. 19A and 19B).

Mitochondria in general are relatively small subcellular organelles [162]. The resolution achieved by immunofluorescence and confocal microscopy was effective in

its use to identify the larger morphological differences among the four genotypes being studied. However, this method is not sufficient if one wishes to see details of mitochondrial structure. Because of these limitations, I used electron microscopy to obtain high-resolution images of the mitochondria. There did not appear to be any defects in the inner cristae structure of the mitochondria in the *Rb1*$^{-/-}$ cells (Fig. 19C). However, quantification of both the number and size of the mitochondria showed that the *Rb1*$^{-/-}$ cells contained more mitochondria than WT cells and they were smaller in size (Fig. 19D and 19E). These results are consistent with what could be expected in cells with a decrease in mitochondrial fusion during differentiation. The additional loss of *Kdm5a* in the DKOs rescued the defects in both size and number of mitochondria (Fig. 19D and 19E).

Figure 19. *Rb1*$^{-/-}$ MEFs are defective in mitochondrial biogenesis upon induction of differentiation. The additional loss of *Kdm5a* in double knockouts rescues this defect.

(A) MEFs were induced to differentiate for 72 hours, fixed and stained for expression of the mitochondrial membrane protein CoxIV (green) and DAPI (blue). Confocal images were taken with a 100x objective. Left panel are representative images of each genotype. Right: digitally zoomed to areas indicated in the red box. One representative mitochondrial structure for each genotype is circled in the zoomed in panel. **(B)** Mitochondrial morphology was segregated into four descriptive groups: Spheres & Rods; Tubules; Dense Tubules; Large Spheres & Dense Tubules. Morphology was quantified as the percentage cells containing mitochondria that fit each group. Error bars represent the standard error of the mean of at least 3 replicates. Below the chart are examples of the various indicated mitochondrial morphologies. Mitochondria were stained for CoxIV in green. DAPI stained nuclei in blue. **(C)** MEFs were induced to differentiate for 72 hours. Images of mitochondria from each genotype were taken by scanning electron microscope. **(D)** Mitochondrial size was quantified by area, using ImageJ software and shown relative to WT. At least 86 mitochondria from at least 5 microscopic fields were quantified for each genotype. Each field was from a different cell. The size of all mitochondria in a given field was averaged. The average sizes from all fields ($n \geq 5$) were then used to determine the standard error of the mean. **(E)** Mitochondrial number was quantified as number of mitochondria per field in at least 5 fields for each genotype. Each field was in a different cell. Greater than 100 total mitochondria for each genotype were counted. The average number of mitochondria

was determined for each field. The average numbers from all fields ($n \geq 5$) were then used to determine the standard error of the mean.

Figure 19

A

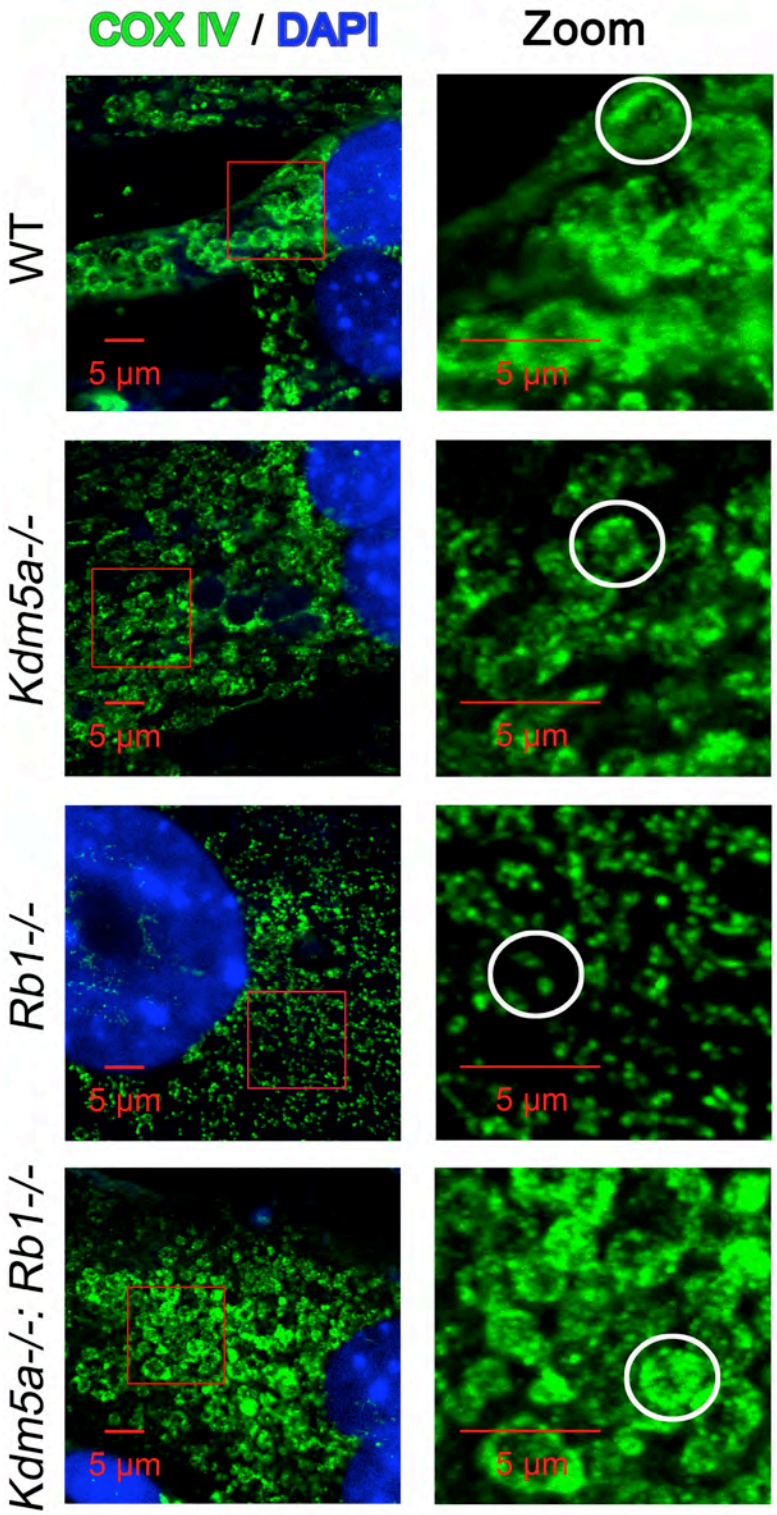
COX IV / DAPI
Zoom
WT
Kdm5a-/-
Rb1-/-
Kdm5a-/-: Rb1-/-
5 µm
5 µm
5 µm
5 µm
5 µm
5 µm
5 µm
5 µm

Figure 19

B

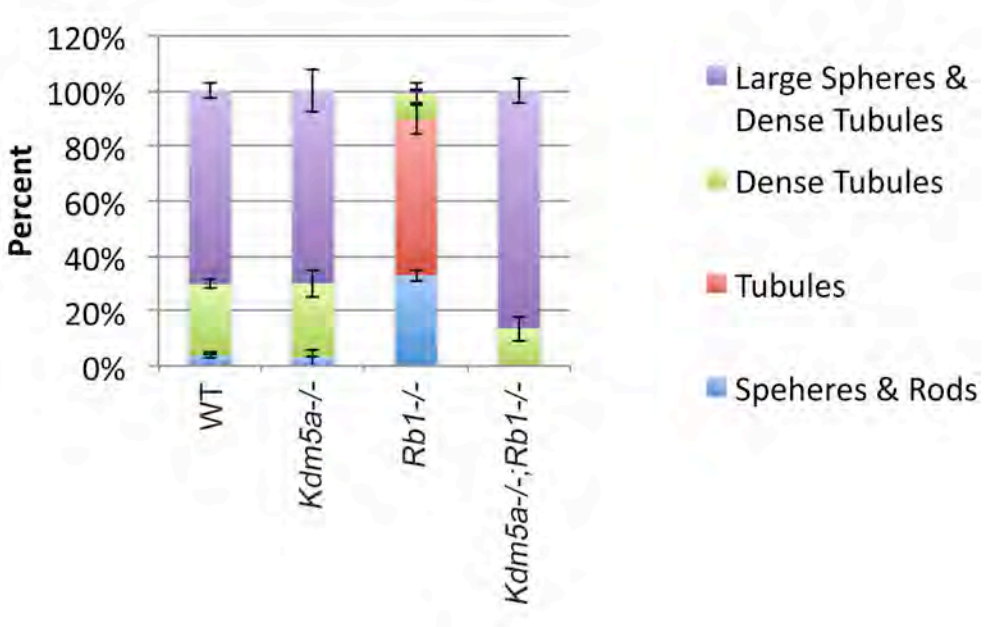
120%
100%
80%
60%
40%
20%
0%
Percent
WT
Kdm5a-/-
Rb1-/-
Kdm5a-/-;Rb1-/-
Large Spheres & Dense Tubules
Dense Tubules
Tubules
Speheres & Rods

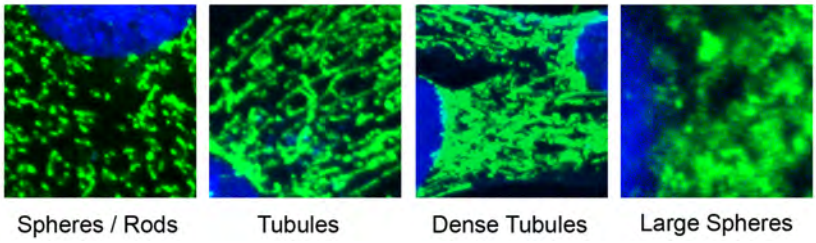
Spheres / Rods
Tubules
Dense Tubules
Large Spheres

Figure 19

C

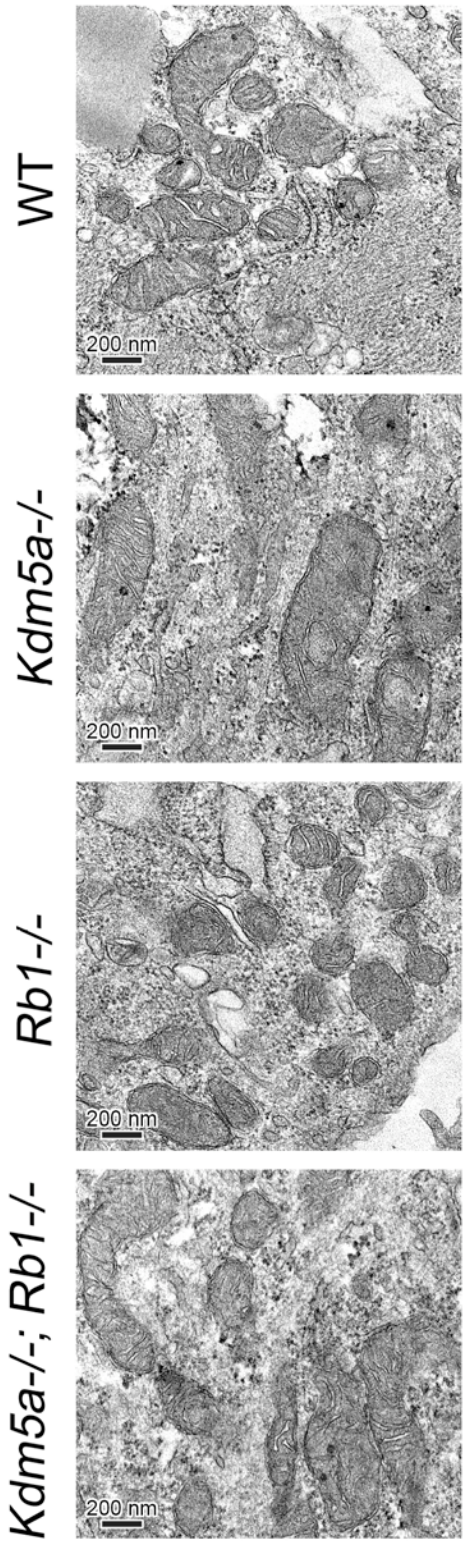

Figure 19

D

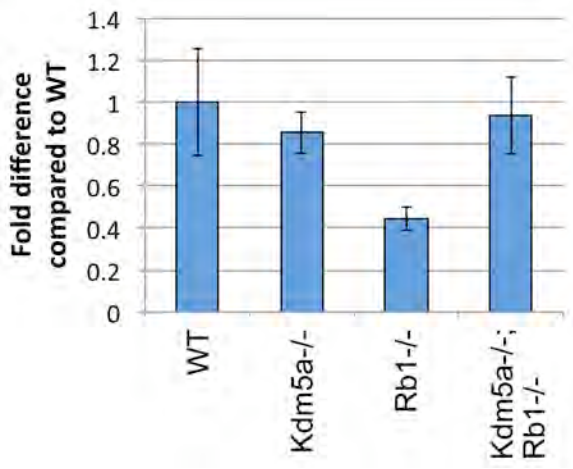
Fold difference compared to WT
1.4
1.2
1
0.8
0.6
0.4
0.2
0
WT
Kdm5a-/-
Rb1-/-
Kdm5a-/-; Rb1-/-

E

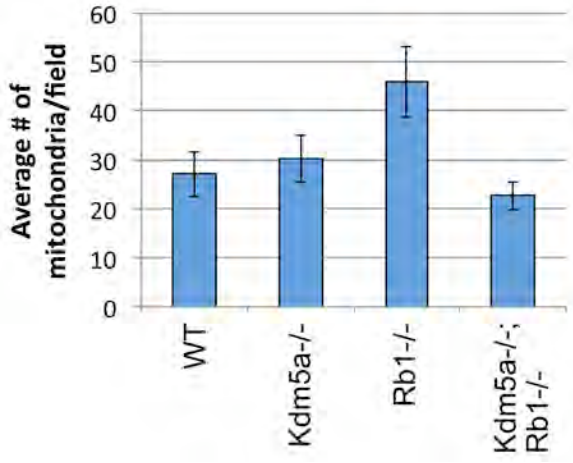
Average # of mitochondria/field
60
50
40
30
20
10
0
WT
Kdm5a-/-
Rb1-/-
Kdm5a-/-; Rb1-/-

E. *Rb1*$^{-/-}$ MEFs are defective in mitochondrial function when induced to differentiate. Additional loss of *Kdm5a* rescues the defects.

The abnormal mitochondrial biogenesis observed in the *Rb1*$^{-/-}$ MEFs during differentiation may be indicative of a defect in function. To evaluate mitochondrial function during differentiation, I measured the rate of oxygen consumption in MEFs during a time-course of differentiation using a Seahorse XF24 Extracellular Flux Analyzer [163]. Oxygen consumption is a standard measure of mitochondrial function as it is directly linked to the electron transport chain (ETC) and ATP production [163]. It is particularly relevant for this study, as I have shown that genes encoding several components of the ETC are directly regulated by pRB and KDM5A.

I analyzed the basal and maximal rates of oxygen consumption for WT, *Rb1*$^{-/-}$, *Kdm5a*$^{-/-}$, and DKO MEFs in multiple conditions: proliferating, 0hr, and 24hr differentiated. WT cells had an additional 12hr differentiated time-point. The basal rate represents the normal rate of oxygen consumption for a given cell type in a given condition. The maximal rate reflects the highest possible rate of consumption for a given cell type in a given condition [163]. This was achieved by treating the cells with an ionophore (FCCP) that uncouples ATP production from oxygen consumption essentially "removing the brakes" from mitochondrial oxygen consumption [163].

We see an increase in both the basal and maximal rates of consumption in the WT cells as differentiation progresses (Fig. 20). It is significant that the maximal rate of consumption is increasing during differentiation. Because the maximal rate is the highest potential for oxygen consumption in a cell, the increased maximal rate of consumption must be due to an increase in mitochondrial biogenesis. These results are consistent with the microscopy studies that show such an increase. Like the WT cells,

the *Kdm5a*$^{-/-}$ cells increase their oxygen consumption during differentiation (Fig. 20). *Rb1*$^{-/-}$ cells do not show an increase in either the basal or maximal levels of oxygen consumption, but the additional loss of *Kdm5a* in the DKOs rescues this defect (Fig. 20).

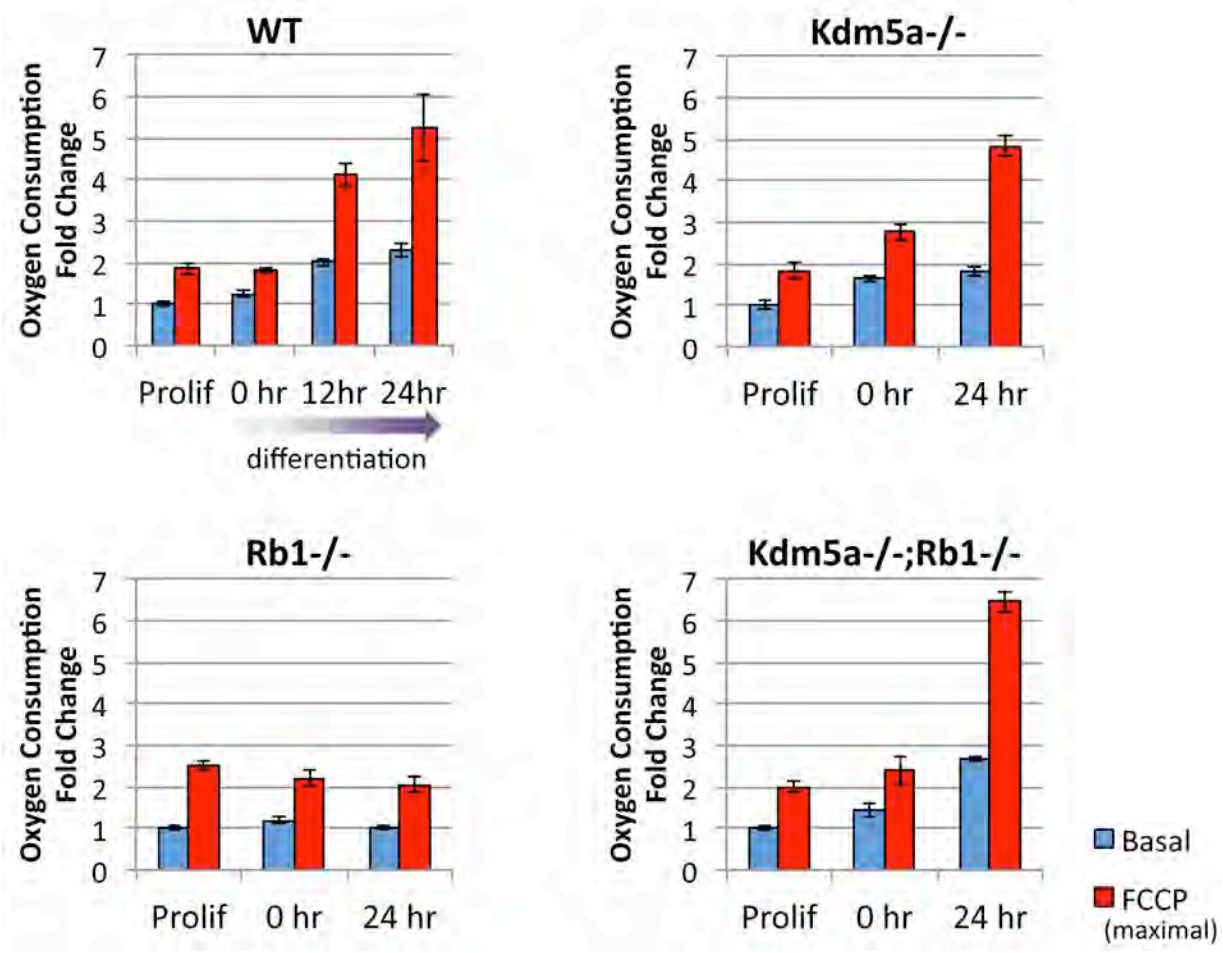

Figure 20. Fold change in the rate of oxygen consumption after induction of differentiation.

The rate of oxygen consumption both basal (blue) and maximal (red) was measured in MEFs (WT, *Kdm5a*$^{-/-}$, *Rb1*$^{-/-}$, and *Kdm5a*$^{-/-}$*;Rb1*$^{-/-}$). Three conditions: Proliferating cells in normal growth media; 0hr cells expressing empty lentiviral vector in differentiation media for 24 hours; Differentiated cells expressing lenti-CMV-MYOD in differentiation media for 24hr (WT cells also have a12hr differentiation time-point). Shown as fold change relative to the basal level in proliferating cells for each genotype. Error bars represent the standard error of the mean of at least 4 replicates.

Besides oxidative phosphorylation via the electron transport chain, cells produce ATP by glycolysis [164]. Glycolysis was evaluated simultaneously with the rate of oxygen consumption in these cells. The purpose was to determine if metabolic differences between the genotypes were specific to the mitochondrial compartment, and if glycolysis was altered to compensate for any defects in oxidative metabolism. The rate of glycolysis can be inferred by measuring the rate of acidification of the cell culture media [163]. Acidification is caused by the release of lactic acid - a product of glycolytic metabolism. In WT cells, the rate of glycolysis increased as differentiation progressed (Fig. 21). Glycolysis in all other genotypes including the *Rb1*$^{-/-}$ cells, increased during differentiation (Fig. 21).

We see that both oxidative phosphorylation and glycolysis are upregulated early during differentiation, but only oxidative phosphorylation fails to increase in the *Rb1*$^{-/-}$ cells by 24hrs after induction. The glycolytic rate increase may be delayed at the 0hr time-point, but by 24hrs, glycolysis does increase 2 fold, which is roughly the same fold increase seen in WT cells. These data suggest that the metabolic defects in *Rb1*$^{-/-}$ cells are limited to mitochondrial metabolism during differentiation.

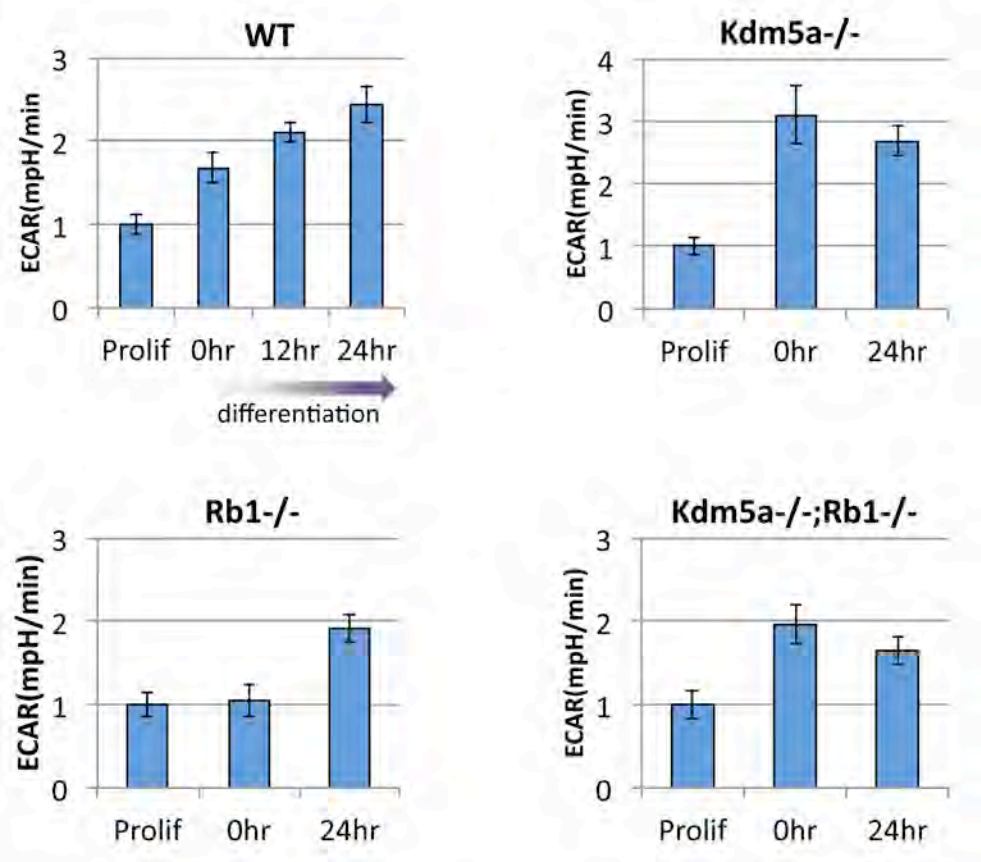

Figure 21. Fold change in the rate of extra cellular acidification (ECAR) after induction of differentiation.

ECAR indicates the rate of glycolysis by measuring the change in milli-pH units per minute (mpH/min) due to lactic acid released into the media as a byproduct of glycolytic metabolism. It was measured in MEFs (WT, *Kdm5a*$^{-/-}$, *Rb1*$^{-/-}$, and *Kdm5a*$^{-/-}$;*Rb1*$^{-/-}$). Three conditions: Proliferating cells in normal growth media; 0hr cells expressing empty lentiviral vector in differentiation media for 24 hours; Differentiated cells expressing lenti-CMV-MYOD in differentiation media for 24hr (WT cells also have a12hr differentiation time-point). Shown as fold change relative to the proliferating condition for each genotype. Error bars represent the standard error of the mean of at least 4 replicates.

Another indication of mitochondrial function is membrane potential [165]. Mitochondria maintain an electrochemical gradient across the inner mitochondrial membrane [165]. They harness the free energy of this gradient for use in ATP production, and so any perturbations in the electron transport chain may be detected as changes in the membrane potential [165]. To evaluate differences in membrane potential during differentiation, I stained cells that were induced to differentiate for 72 hours, with Mitotracker Red CMX ROS. Mitotracker is a fluorescent dye that localizes to the mitochondria in a manner that is dependent upon the mitochondrial inner membrane potential. Higher potential results in higher retention of the dye, and therefore greater fluorescence intensity [165]. *Rb1*$^{-/-}$ cells showed a lower potential relative to WT, consistent with the decrease in biogenesis and the decrease in oxygen consumption (Fig. 22). *Kdm5a*$^{-/-}$ showed a higher potential. The defective membrane potential seen in the *Rb1*$^{-/-}$ cells was restored in the *Kdm5a*$^{-/-}$*;Rb1*$^{-/-}$ DKOs (Fig. 22).

The results of this section link the defects of mitochondrial component gene expression in *Rb1*$^{-/-}$ cells to defects in mitochondrial biogenesis and mitochondrial function. Likewise the rescue effect on gene expression caused by the additional loss of *Kdm5a* leads to a rescue of mitochondrial biogenesis and function. This significance of this finding lies in the requirement of mitochondrial biogenesis and function for differentiation [151-154, 161, 166-170]. It offers a potential mechanism to explain why *Rb1*$^{-/-}$ cells fail to differentiate and how the additional loss of *Kdm5a* can rescue the defect.

Figure 22. Decreased mitochondrial membrane potential in *Rb1*$^{-/-}$ is rescued in the *Kdm5a*$^{-/-}$;*Rb1*$^{-/-}$ cells.

WT, *Kdm5a*$^{-/-}$, *Rb1*$^{-/-}$, and *Kdm5a*$^{-/-}$;*Rb1*$^{-/-}$ were induced to differentiate for 72 hours. Cells were incubated with Mitotracker Red, fixed and then stained with DAPI. Confocal images were taken with a 40x objective. Exposure time was set in the WT condition. Fluorescence intensity of Mitotracker is used to gauge mitochondrial membrane potential. Differences in intensity represent differences in mitochondrial inner membrane potential.

Figure 22

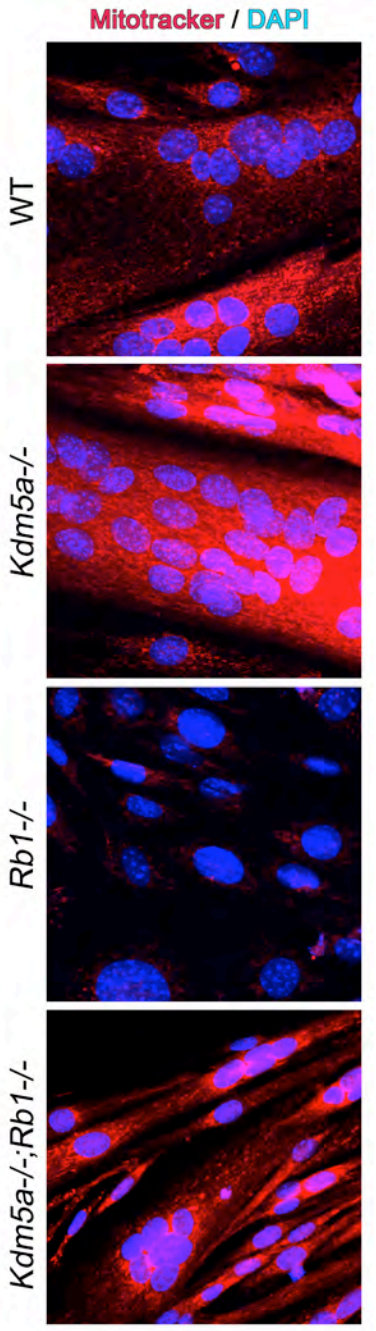

F. Myogenic differentiation of MEFs requires mitochondrial function.

If myogenic differentiation requires normal mitochondrial function, then a disruption of normal function should prevent differentiation. Other groups have reported that differentiation in myoblast cell lines can be blocked, by treating the cells with inhibitors of the electron transport chain [152, 154]. I performed similar experiments using MEFs.

I used two different inhibitors of the ETC that target two different ETC complexes: rotenone and sodium azide (NaN_3). Rotenone is a specific inhibitor of the mitochondrial ETC complex I [171]. It works by binding to and blocking the ubiquinone-binding pocket of complex I, and disrupting the ubiquinone reductase reaction - the first step in the electron transport chain reaction [172]. Sodium azide inhibits ETC complex IV [173]. It works by binding to the heme cofactor of cytochrome c [173]. I induced WT MEFs to differentiate in the presence of these compounds. I used two concentrations for each: 10 nM and 50 nM of rotenone ; 10 mM and 20 mM of sodium azide. As an additional control for the disruption of mitochondrial function, I induced cells to differentiate in media without glutamine supplementation and a low concentration of glucose.

Differentiation was blocked by both concentrations of rotenone (Fig. 23). The low concentration of sodium azide did not noticeably affect differentiation but the 20 mM treatment effectively blocked differentiation (Fig. 23). To address the possibility that rotenone and sodium azide treatment prevent differentiation by inducing apoptosis, I first transduced the cells with an adeno-vector to express BCL2, a potent anti-apoptotic factor. This resulted in a decrease in cell death determined by comparing cell numbers

in plus-BCL2 condition to the minus-BCL2 condition, but did not overcome the differentiation block (Fig. 23).

Consistent with this result, there is actually an increase in apoptosis in DKOs compared to *Rb1*$^{-/-}$ during differentiation, even though the DKOs differentiate better (Fig. 24A and 24B).

The block of differentiation by rotenone and sodium azide in this system is consistent with the previously identified requirement for mitochondrial function as a prerequisite for proper differentiation [152, 154]. It is possible that off target effects of the drug treatments may be responsible for inhibition of differentiation however there are several points that favor mitochondrial inhibition as the likely cause. (1) Rotenone is highly specific for ETC complex I [171]. Sodium azide which targets complex IV has a lower specificity but the primary target is the ETC complex [173]. (2) Other reagents such as thenoyltrifluoroacetone and antimycin A that target complex II and III, respectively, have been shown to block differentiation in other systems [152]. Additionally, chloramphenicol that specifically blocks mitochondrial protein synthesis, and Carbonyl cyanide-*4*-(trifluoromethoxy)phenylhydrazone that disrupts the mitochondrial innermembrane potential, also inhibit differentiation [154]. All of these drugs are commonly used to study mitochondrial function and affect mitochondria at different levels [174]. (3) While it is possible that all of these reagents have off target effects, it is unlikely that the secondary targets of all of these drugs, that act through multiple different mechanisms, would be responsible for inhibition of differentiation as opposed to the primary targets that affect mitochondria. (4) Additionally I have

eliminated the potential secondary effect of apoptosis as the cause of the loss of differentiation, as the block of apoptosis with BCL2 did not rescue differentiation.

Figure 23. Mitochondrial function is necessary for differentiation.

WT MEFs were induced to differentiate in the presence of two different inhibitors of mitochondrial function. Rotenone inhibits ETC complex I, and sodium azide (NaN_3) inhibits ETC complex IV. Two concentrations for each inhibitor were used either alone or in combination with adeno-CMV-BCL2, which was used to block apoptosis. Untreated cells were used as a positive control. Cells not induced to differentiate were used as a negative control. Cells treated with reduced glucose and without glutamine were also used as an additional control for defective mitochondrial function.

Figure 23

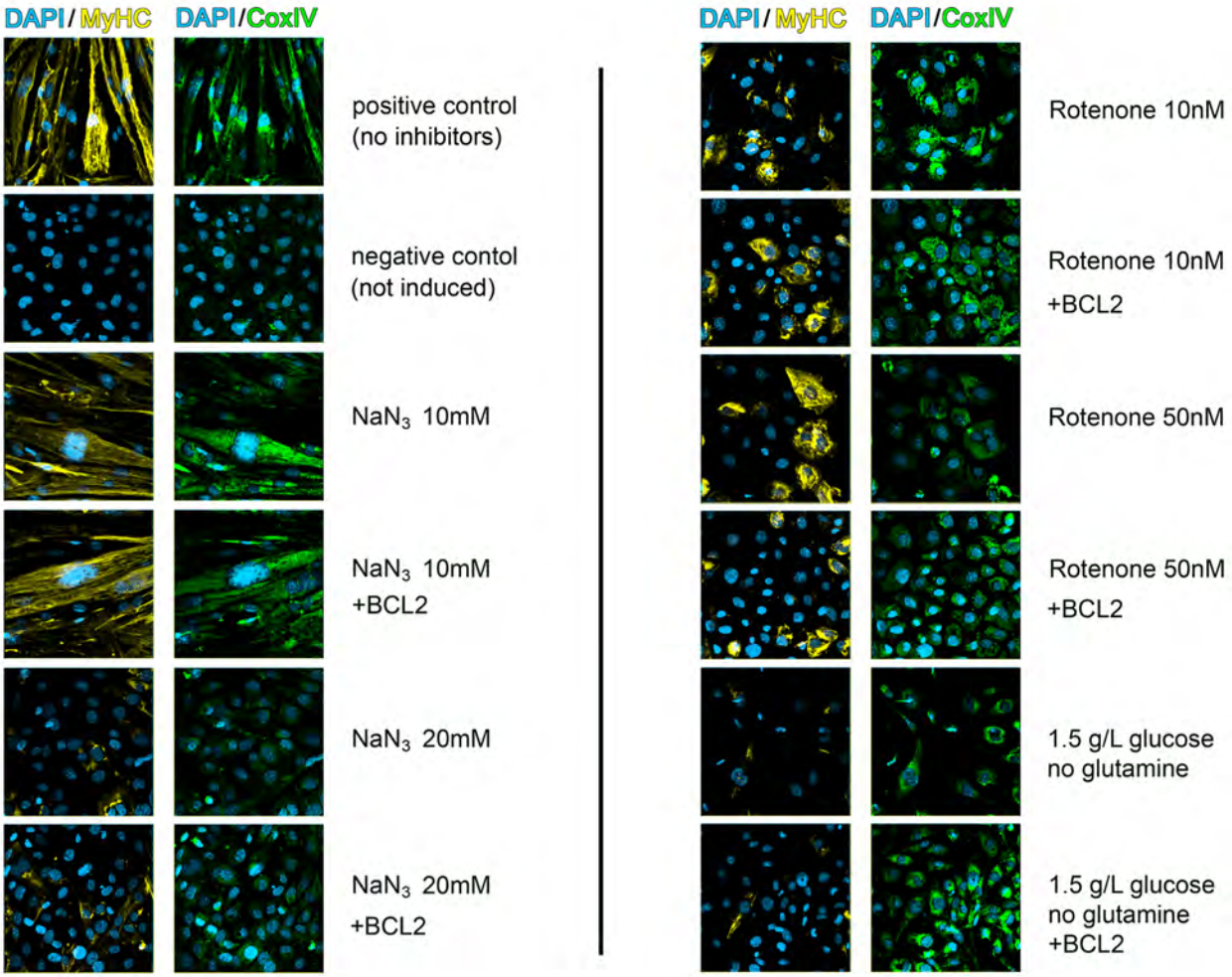
DAPI / MyHC
DAPI / CoxIV
positive control (no inhibitors)
negative contol (not induced)
NaN3 10mM
NaN3 10mM +BCL2
NaN3 20mM
NaN3 20mM +BCL2
DAPI / MyHC
DAPI / CoxIV
Rotenone 10nM
Rotenone 10nM +BCL2
Rotenone 50nM
Rotenone 50nM +BCL2
1.5 g/L glucose no glutamine
1.5 g/L glucose no glutamine +BCL2

Figure 24. *Kdm5a*$^{-/-}$*; Rb1*$^{-/-}$ MEFs induced to differentiate have higher rates of cell death than WT and *Rb1*$^{-/-}$ cells.

WT, *Rb1*$^{-/-}$, and *Kdm5a*$^{-/-}$*; Rb1*$^{-/-}$ MEFs were induced to differentiate for 0, 2, 4, and 6 days. TUNEL assays were performed for each time point along with immunofluorescent staining for MYHC, and DAPI staining for nuclei. **(A)** Representative image of the D6 time point. **(B)** Quantification of TUNEL positive cells for each genotype at each time point. Data is shown as percent TUNEL-positive cells out of total cell number. In the case of multinucleated cells, if multiple nuclei in the same cell were positive for TUNEL, the cell was counted only once. Error bars represent the standard error of the mean of three replicates.

Figure 24

A

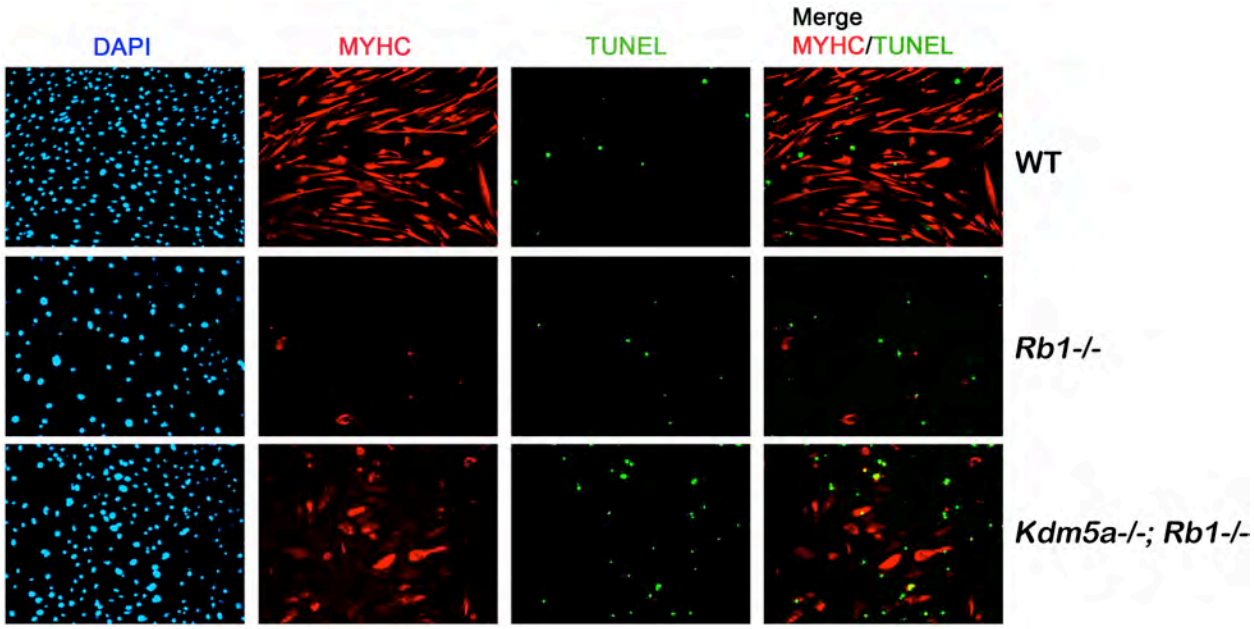
DAPI
MYHC
TUNEL
Merge
MYHC/TUNEL
WT
Rb1-/-
Kdm5a-/-; Rb1-/-

B

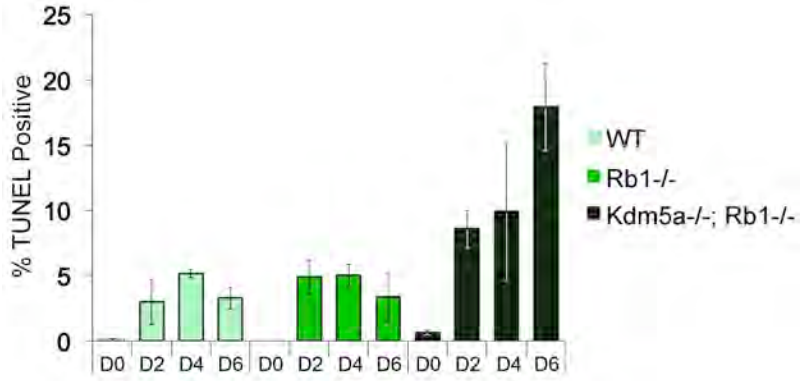
% TUNEL Positive
25
20
15
10
5
0
D0 D2 D4 D6 D0 D2 D4 D6 D0 D2 D4 D6
WT
Rb1-/-
Kdm5a-/-; Rb1-/-

G. Higher levels of ROS in *Rb1*$^{-/-}$ when induced to differentiate.

Reactive oxygen species have long been considered to be simply the harmful byproducts of oxidative metabolism [175]. However, emerging evidence points to a more complex picture than initially thought [176]. ROS have been shown to be important signaling molecules in the cell with roles in multiple cellular processes including proliferation and differentiation [176]. With respect to differentiation, it is interesting that ROS signaling can be a positive or negative regulator depending on the tissue type [177, 178]. In the case of myogenic differentiation, it has been shown that ROS has an inhibitory effect on differentiation [178]. With this in mind I decided to measure the relative levels of ROS in my system in proliferating cells and cells induced to differentiate. I treated cells with a reduced fluorescein, 2'-7'-dichlorodiydrofluorescein diacetate (H_2DCFDA) a non-fluorescent compound that enters mitochondria and is converted to the fluorescent 2',7'-dichlorofluorescein (DCF) when oxidized by ROS. I then measured the fluorescence by FACS as an indication of levels of ROS in each genotype.

By this method I observed that when proliferating, the *Rb1*$^{-/-}$ cells showed levels of ROS similar to WT (Fig. 25A). The DKOs however showed a two-fold increase in ROS compared to WT (Fig. 25A). These differences observed in ROS levels of the DKOs relative to WT were somewhat surprising. Interestingly, ROS signaling has been shown to be involved in regulating cell cycle progression from G1 to S phase [179]. Higher levels of ROS promoted entry into S phase [179]. From observations made during this study we know that the DKO MEFs proliferate at a higher rate than both WT and *Rb1*$^{-/-}$ and this is consistent with the higher levels of ROS seen in the DKOs in the

proliferative state. *Kdm5a*$^{-/-}$ proliferate the slowest, and also show the lowest levels of ROS in the proliferating condition (Fig. 25A). This link between ROS and cell cycle regulation may help to explain this observation, but will require further study in the future.

In contrast to the proliferating state, when the cells were induced to differentiate I found that the *Rb1*$^{-/-}$ cells had higher levels of ROS compared to WT and that the DKOs had reduced levels (Fig. 25B). The increase of ROS in the *Rb1*$^{-/-}$ cells in the differentiating condition was less than 1.5 fold greater than WT, but was reproducible and statistically significant. Additionally this increase observed in the *Rb1*$^{-/-}$ cells is within a range that has been observed to have physiological implications for differentiation [177, 180].

A higher level of ROS in the *Rb1*$^{-/-}$ cells, after induction of differentiation, is another indication of defective mitochondria and is consistent with my other findings. Increased ROS may simply be a symptom of the mitochondrial defect, but it may also be a contributing factor toward the loss of differentiation. Since ROS has been established as a signal that negatively regulates myogenic differentiation, this observation deserves further attention in the future, to determine with finality if it is a cause or effect event in this particular system [178].

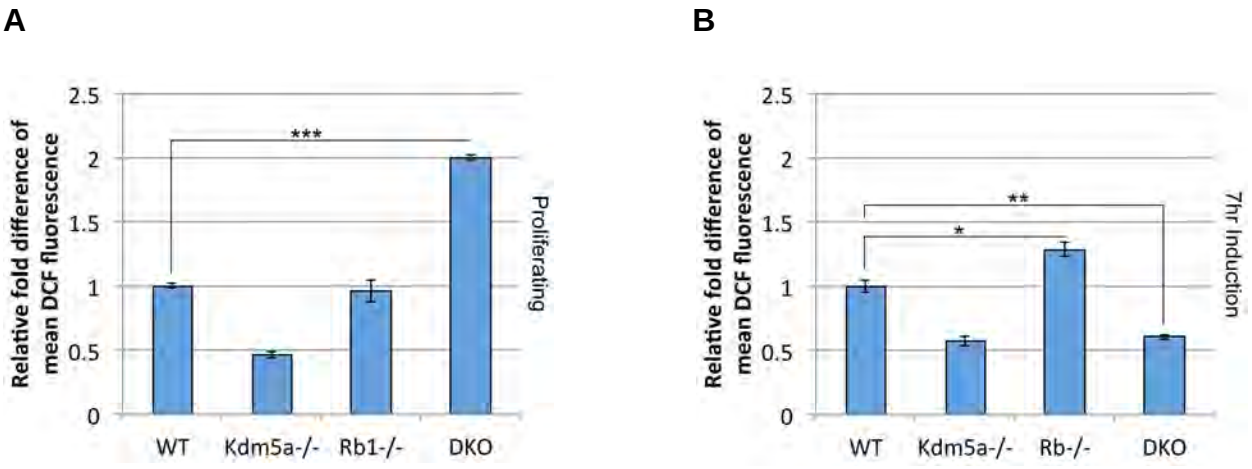

Figure 25. *Rb1*$^{-/-}$ MEFs have higher levels of ROS compared to WT after induction of differentiation, and the additional loss of *Kdm5a* rescues this defect.

MEFs were cultured for two conditions: proliferating and induced to differentiate for 7hrs. The 7hr time-point was chosen so that cells could be analyzed early after induction of differentiation but before cellular fusion events occurred (**A**) In the proliferating condition, levels of ROS in *Rb1*$^{-/-}$ cells are the same as WT but 2 times greater in the DKOs. (**B**) After induction of differentiation for 7 hours, the levels of ROS in the *Rb1*$^{-/-}$ increase significantly while the ROS in DKOs is significantly reduced compared to WT. ROS was measured by DCF fluorescence of 10,000 cells for each genotype by FACS. Results are shown as the relative fold difference of DCF fluorescence for each genotype compared to WT. Error bars represent the standard error of the mean of 3 replicates. P-values were determined by the Student's t-test. *** p-value < 2 x 10^{-6} ; ** p-value 0.002, * p-value 0.03.

H. KDM5A is a phosphoprotein whose phosphorylation state changes during differentiation.

One pressing, yet still unanswered question regarding KDM5A is: how is KDM5A itself regulated? We know that it is involved in many cellular processes [13-17, 63, 64, 116-119, 121]. It interacts with several different binding partners, and binds to a variety of different genes and to different regulatory regions in the genome [14-17, 109, 116, 118, 119, 121]. One common way in which proteins are regulated is through post-translational modification [181]. The most well known modification is phosphorylation of serine, threonine, and tyrosine residues [181]. KDM5A contains several consensus sequences for phosphorylation by numerous different kinases (Table IV) that are involved in cell cycle, differentiation, and metabolic regulation. These were identified using Scansite 2.0, set at the highest stringency for statistical significance [182]. High stringency sequences must score by similarity to the consensus, to within the top 0.2% of sequences matching the consensus, referenced against the Swis-Prot protein database for vertebrates. I determined by Western Blot using C2C12 myoblasts that KDM5A is in fact phosphorylated (Fig 26A). I found that KDM5A becomes less phosphorylated or possibly unphosphorylated as differentiation progresses, and this phenomenon is blocked by the addition of Insulin-like growth factor-1 (IGF1) to the media (Fig 26B). Interestingly, the insulin-like growth factor-1 receptor (IGF-1R) has been shown to be an upstream regulator of KDM5A although the mechanism of this regulation is not known [183]. Besides the two bands representing KDM5A and phospho-KDM5A there is a third band running higher than the others. This is not a phosphorylated form of KDM5A, as it is not affected by phosphatase treatment (Fig 26A). Alternatively, it may represent a different form of post-translational modification of

the KDM5A protein. It appears more abundant in the condition of + phosphatase inhibitors and λphosphatase (Fig 26A right lane). It is not clear why this is the case, but if it is an alternative modification then it may be that the increased modification is a response to the specific treatment of that condition. This band also decreases during differentiation in a manner similar to the phospho-KDM5A band, and it also appears to be stabilized by IGF1 treatment (Fig 26B).

Here we see the dynamic state of phosphorylation of KDM5A during differentiation. There are several kinases that may be responsible for phosphorylating KDM5A based on the *in silico* analysis, but experimental evidence must be acquired in the future to identify the actual kinase(s). It is interesting that consensus target sequences of well-known metabolic regulators such as AKT, Insulin Receptor, and AMP kinase are contained in the KDM5A sequence.

The change in the phosphorylation state of KDM5A during differentiation may have a regulatory function in controlling the dynamic role of KDM5A in the differentiation process. I have shown that KDM5A binds to mitochondrial target genes in undifferentiated cells and comes off as differentiation progresses. Conversely, KDM5A shows reduced binding to cell cycle genes in proliferating cells and increased binding towards the later stages of differentiation [15, 16]. It is possible that the changes in phosphorylation state direct the changes in binding preference of KDM5A during differentiation. It would be interesting to identify the specific residue(s) that is phosphorylated and to determine its requirement for the two different functions of KDM5A during differentiation.

Kinase	Consensus Sequence	Location
Insulin Receptor	ILPEEEE**Y**ALSGWNL	Y438
AKT1	QMRQRKG**T**LSVNFVD	T285
AKT1	SRRPRLE**T**ILSLLVS	T1225
Calmodulin dependent kinase 2	FGEGKQK**S**KELKKMD	S1524
AMP kinase	TFLKKNS**S**HTLLQVL	S1067
DNA PK	YDDEETD**S**DEDIRET	S1345
Casein Kinase 2	MDYDDEE**T**DSDEDIR	T1343
Casein Kinase 2	YDDEETD**S**DEDIRET	S1345
Casein Kinase 2	DWSGAEE**S**DDENAVC	S1603
Cdk5	SCSQGSS**T**PRKQPRK	T1415
Cdc2	SCSQGSS**T**PRKQPRK	T1415
ERK1	AKKQGPV**S**PGPAPPP	S1666

Table IV. Predicted sites of phosphorylation of KDM5A by protein kinases.

Left column indicates the kinase. Center column indicates the consensus sequence identified in KDM5A, for phosphorylation by the indicated kinase. Right column indicates the location and specific residue of the predicted phosphorylation site within the KDM5A sequence.

Figure 26. KDM5A is a phosphoprotein. Phosphorylation decreases during differentiation. Supplementation of IGF1 into the media stabilizes the phosphorylated state of KDM5A during differentiation.

(A) Western blot of C2C12 myoblast cells. Cells were lysed in the presence of either a phosphatase inhibitor cocktail, λphosphatase, or a combination of both. Blots were probed with anti-KDM5A antibodies; or antibodies to detect phospho-IGF-1R were used as a control for the efficacy of the treatments. **(B)** C2C12 cells were induced to differentiate in the presence or absence of supplemental IGF1 added to the media. (-) indicates that no IGF1 was added; (+) indicates that IGF1 was added at the time of induction of differentiation; (-/+) indicates that IGF1 was added 48hrs after induction. Cells were lysed at 24hr, 48hr, 72hr, and 96hr after induction. Blots were probed for KDM5A, phospho-IGF-1R, and total IGF1Rβ, and α–tubulin was used as a loading control. The uppermost band in both (A) and (B) appears not to be a phosphorylated form of KDM5A as it is not affected by phosphatase treatment.

Figure 26

A

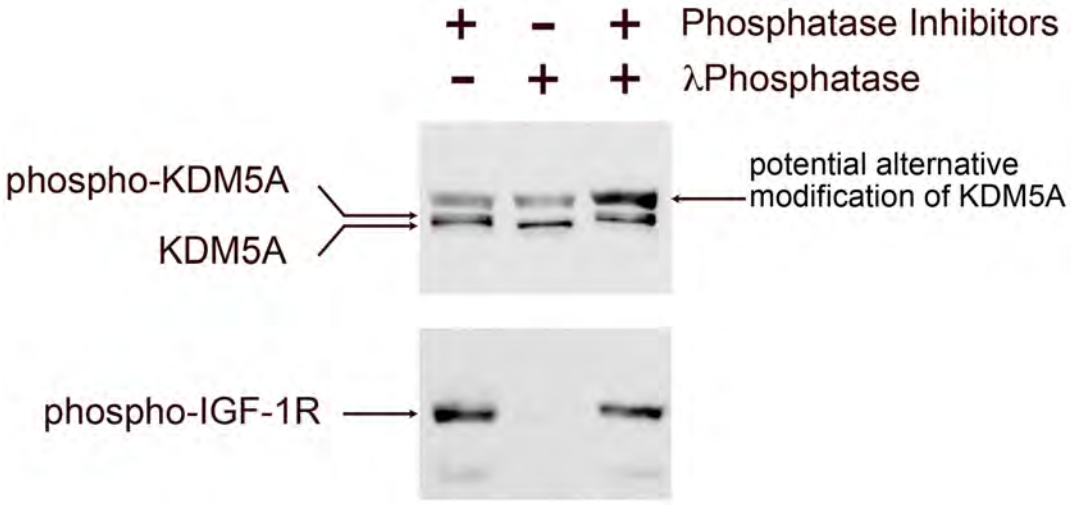
+ - + Phosphatase Inhibitors
- + + λPhosphatase
phospho-KDM5A
KDM5A
potential alternative modification of KDM5A
phospho-IGF-1R

B

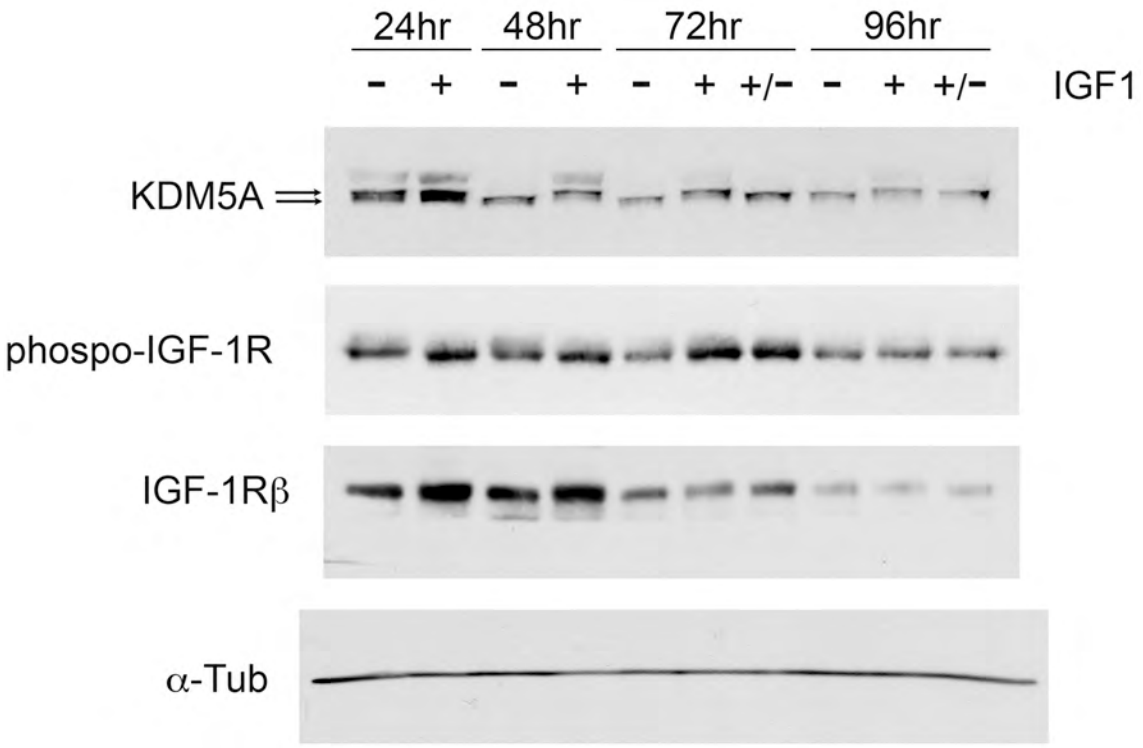
24hr 48hr 72hr 96hr
- + - + - + +/- - + +/- IGF1
KDM5A
phospo-IGF-1R
IGF-1Rβ
α-Tub

IV. DISCUSSION

Cancer is a worldwide disease that affects all ethnicities and ages. The incidence rate of cancer in 2012 was estimated by the World Health Organization to be 14 million new cases [184]. It is the number one killer in developed countries and number two in undeveloped nations. The global rate is predicted to increase to 19 million new yearly cases by 2025 [184]. The importance of the RB pathway to cancer cannot be understated. The fact that it is defective in most cancers means that if successful treatments for this disease are to be developed we must have a thorough understanding of the full scope of it's role in cellular processes [55]. Currently our knowledge includes details of only sections of the larger picture. Much attention has been focused on pRB and the E2F family and how they regulate the cell cycle [29]. This is however is a limited perspective. It is known that pRB is involved in numerous cellular processes including apoptosis, differentiation, senescence, autophagy and metabolism [34, 39-46, 48, 185]. pRB works as an adapter protein, its function is dependent upon interactions with other proteins. To date, it has been linked to at least 110 other proteins [18]. There is no denying the complexity and difficulty of the task.

The results of my work are a positive contribution to this larger goal. The role of pRB as a tumor suppressor is connected to its role as a regulator of differentiation [49]. pRB as regulator of differentiation is linked to the histone demethylase, KDM5A [17]. Here I have shown how the requirement of pRB for differentiation is coupled to its function in metabolic regulation. I have shed more light onto the nature of the

relationship between pRB and KDM5A and clarified the mechanism by which the loss of *KDM5A* can rescue the defects of differentiation in cells lacking a functional pRB.

pRB itself poses significant problems as a target for therapy. First, pRB is a tumor suppressor, it is the loss of function that results in tumorigenesis [25, 41, 51]. It would be a tall task to somehow restore function in cancers where the *RB1* gene is mutated or deleted. In most cancers however, it is not the *RB1* gene itself that is affected, but rather different upstream regulators. Negative regulators like Cyclin D1 and CDK4 are overexpressed or duplicated while positive regulators like $p16^{INK_4A}$ are deleted or epigenetically silenced [28, 186]. Drugs targeting CDKs are currently in development but due the complexity and context dependency of this pathway in cancer, it is unlikely that targeting a single part of the pathway will be sufficient [187]. There is a need for additional approaches. Targeting a downstream component of the RB pathway has the potential to be effective whether it is the *RB1* gene itself or any of the upstream genes that are deregulated. KDM5A is such a downstream component and offers certain advantages as a drug target [13, 17]. First, it has an opposing role to pRB in cancer. Genetic deletion of *Kdm5a* suppressed tumorigenesis in the $Rb1^{+/-}$ cancer model [13]. This suggests that a KDM5A inhibitor may also have similar tumor suppressive effects. Furthermore, KDM5A is an enzyme and enzymes are “druggable” [68]. Inhibitors targeting other epigenetic enzymes such as histone deacetylases are already in use [68]. The cumulative data for KDM5A points to it role as a regulator of differentiation as key to its role in cancer [13, 17, 183, 188, 189]. My data shows that the catalytic domain of KDM5A is required for regulation of differentiation, supporting the notion that an inhibitor could be effective.

To approach KDM5A as a target for therapy in the RB pathway we must understand the complex dynamic between KDM5A and the pocket proteins. The function of KDM5A within the RB pathway is context dependent [13-17]. It can cooperate with, or antagonize RB, depending on the cellular process in question [13-17]. This is important information to consider when designing and implementing strategies to target the RB pathway in cancer. Even within the framework of differentiation, KDM5A can simultaneously work with and against pRB [15-17]. It cooperates to repress cell cycle genes during permanent cell cycle withdrawal and it can positively regulate transcription of developmental genes during differentiation [13, 15-17]. Despite this capacity as an active driver of differentiation, its role as a negative regulator of differentiation seems to be dominant. The evidence for this is the fact that differentiation defects in *Rb1*$^{-/-}$ cells can be rescued, by knocking down or deleting *Kdm5a* [17]. As I showed, *Kdm5a*$^{-/-}$*; Rb1*$^{-/-}$ cells can differentiate, and exhibit both morphological and molecular features of terminally differentiated myotubes. They express both early and late markers of differentiation, and fuse into large multinucleated cells with the tube-like shape of myotubes.

The effects of losing KDM5A as a positive regulator of differentiation are not however completely overcome by the effects of losing KDM5A the negative regulator [13, 15-17, 61]. The double knockouts differentiate as we can see, but not without a price. The most striking example of this is the effect that I observed on cell cycle withdrawal during differentiation. A large percentage of the double knockout myotubes were positive for S phase entry, even though they were highly multinucleated, and expressed the late myogenic marker, myosin heavy chain. In the majority of these

myotubes, it was not just a single nucleus within the multinucleated cells, but rather several if not all of the nuclei in the cell that had reentered the cell cycle.

The antagonistic role of KDM5A towards pRB also seems to be more important than the cooperative role with respect to carcinogenesis. This was nicely demonstrated in *Rb1*$^{+/-}$ mice where loss of *Kdm5a* suppressed tumor formation and greatly extended survival of the mice [13]. This is the case despite my observation of an exacerbation of the cell cycle defect *in vitro*, and despite work by others that showed a role for KDM5A in cooperation with pRB to promote senescence [14]. The tumor suppressive effect must then be due to the loss of KDM5A as a pRB-antagonist. What then is the mechanism of this tumor suppressive effect? The accumulated evidence thus far suggests that restoration of differentiation potential is the critical process [13, 17, 183, 188, 189].

I have shown that the loss of *Rb1* causes a decrease in the expression of several genes coding for mitochondrial components during myogenesis and that pRB directly binds to the promoters of these genes. This defective expression correlates with a failure of *Rb1*$^{-/-}$ cells to undergo proper mitochondrial biogenesis during differentiation and a failure of mitochondrial function during differentiation. It is a significant observation that the *Rb1*$^{-/-}$ cells have decreased expression of these genes coding for mitochondrial components. One of the goals of my work has been to identify the mechanism by which *Rb1*$^{-/-}$ cells fail to differentiate. The observation that *Rb1*$^{-/-}$ cells have decreased expression of these genes does not prove that the loss of pRB is the cause of defective expression or that defective expression of these genes is the cause of defective differentiation. That being said, a link between pRB and mitochondrial

metabolism has been established. Several others have also connected pRB to defective gene expression of mitochondrial components in other cell types and model systems [20, 34, 44, 45, 151]. Additionally a link between mitochondria and differentiation has been identified if not yet fully elucidated. It has been shown by several groups using multiple different models, that mitochondrial biogenesis and mitochondrial function are required for differentiation [151-154, 161, 166-170].

For example, Myelodsyplastic Syndrome (MDS) is a heterogeneous group of blood disorders caused by defective hematopoiesis and characterized by dysplasia and anemia that often leads to leukemia [190]. In the zebrafish model, a screen for genes that can recapitulate human MDS identified a point mutation in the *Hsp9ab* gene that was sufficient to cause the phenotype in fish embryos [170]. The embryos had defects in erythrocyte differentiation and died at 72 hours post fertilization [170]. HSP9AB is a highly conserved chaperone protein that primarily localizes to the mitochondrial matrix and is involved in the folding of mitochondrial proteins [191]. Mutations in this gene are known to cause mitochondrial-specific defects and are associated with numerous human diseases [191]. This was true in this zebrafish model as well, where they detected elevated ROS levels specifically in the blood cells [170]. Importantly, reintroduction of WT HSP9AB by injecting the embryos with *Hsp9ab* RNA was able to rescue the phenotype [170]. The key point of this data as it pertains to my work is that they showed that a mutation in a gene that regulates mitochondrial function leading to defective mitochondria was sufficient to inhibit differentiation.

Another group has shown in the hematopoietic model, that defects of differentiation in *Rb1* null cells may be linked to defects in the mitochondria [151]. This

group used a conditional tissue-specific *Rb1* knockout mouse model to delete *Rb1* in the erythroid compartment of mice [151]. With this system they identified a block in the development of early erythroblasts into late erythroblasts and anemia resembling the kind found in patients with MDS [151]. By gene set enrichment analysis, they saw that the most significantly downregulated sets of genes were those that coded for components of the mitochondrial oxidative phosphorylation and electron transport chain pathways [151]. In order to examine the potential connection between the decreased expression of the mitochondrial components and the defects in differentiation, they used siRNA against the *Ppargc1b* gene that codes for PGC-1β [151]. PGC-1β is a transcriptional coactivator that is involved in regulating mitochondrial biogenesis and function by coactivating expression of nuclear genes coding for mitochondrial components [192]. Knockdown of this factor resulted in defects of erythropoietic differentiation and demonstrated the requirement for proper expression of the mitochondria-related genes to allow differentiation [151]. Likewise, treatment of the cells with chloramphenicol, a specific inhibitor of mitochondrial ribosomes that does not affect cytoplasmic ribosomes, resulted in defective mitochondrial function that was determined by evaluating mitochondrial membrane potential [151]. Importantly, treatment of the cells with chloramphenicol also caused an inhibition of differentiation [151].

Mitochondrial biogenesis has been shown to be required for differentiation in the myogenic model, including skeletal muscle and cardiac muscle [152-154, 161, 193]. In one study, treatment of myoblasts with chloramphenicol inhibited myogenic differentiation, while overexpression of the mitochondrial T3 receptor that promotes mitochondrial biogenesis, enhanced myogenic differentiation [154].

In my system I have shown that inhibition of mitochondrial function with two different ETC complex inhibitors results in defective differentiation. The phenotype of the cells treated with these inhibitors was similar to that of the *Rb1*$^{-/-}$ cells when induced to differentiate: small, mostly containing single nuclei, and a low capacity to express the myogenic marker MYHC.

Besides the use of mitochondrial inhibitors, knockout mouse models have also been used to demonstrate the requirement of mitochondria for myogenesis [193]. *MFN1*, *MFN2* and *OPA1* are nuclear encoded genes that regulate mitochondrial fusion – a key process in mitochondrial homeostasis and critical to mitochondrial biogenesis [158]. *MFN1* and *MFN2* regulate outer mitochondrial membrane fusion while *OPA1* regulates fusion of the inner mitochondrial membrane [158]. Genetic ablation of these genes is embryonic lethal in mice and zebrafish [194, 195]. Conditional KO in cardiomyocytes causes cardiomyopathy characterized by underdeveloped cardiac structures [193]. Recently it was shown that deletion of *Mfn1* and *Mfn2* in the cardiomyocytes of mouse embryos causes defective expression of key cardiac developmental transcription factors, such as GATA4, SRF, NKX2.5, MYOCD [193]. This led to hypoplastic hearts featuring underdeveloped cardiac structures such as ventricular walls and trabeculae [193]. In agreement with the *in vivo* studies, differentiation of mouse ES cells into cardiomyocytes was defective when levels of MFN2 and OPA1 were decreased by gene trapping [193]. This defect was rescued by the re-expression of these two factors using retroviral expression vectors [193]. The mechanism of inhibition was linked at least in part to increased Ca^{+2} released from the defective mitochondria that increased the activity of the calcium-dependent protein

phosphatase calcineurin [193]. Calcineurin is known to be involved in developmental regulation, it indirectly affects gene transcription by directly regulating transcription factors [196].

The above studies demonstrate the requirement of mitochondrial biogenesis and function for differentiation. However, it must be considered that the defects of gene expression that I observed during differentiation could be indirectly due to defective differentiation through some other mechanism caused by loss of *Rb1* in these cells. This is conceivable if the differentiation process is the driver of the changes in metabolic gene expression. Currently, it is not entirely clear if differentiation precedes changes in mitochondrial biogenesis or if mitochondrial biogenesis precedes differentiation. Some emerging evidence so far is coming out in favor of the latter [154, 193, 197].

For example, it has been shown that requisite changes to the mitochondria are not limited to the “forward” direction of differentiation, but are also necessary for the reprogramming that occurs in induced pluripotent stem (iPS) cells [198]. The mitochondria and metabolic signature of ES and iPS cells are markedly different from that of differentiated cells [198, 199]. The pluripotent cells contain mitochondria that are less well developed and less active compared to the mitochondria of differentiated cells [198]. Consistent with this, pluripotent cells rely more on glycolytic metabolism and less on oxidative phosphorylation [198]. Just as mitochondria undergo an increase in biogenesis when myoblast differentiate into myotubes, mitochondria during iPS reprogramming undergo a reversal of sorts into the less mature state found in pluripotent cells [161, 198]. Concurrent with the switch from oxidative to glycolytic metabolism, expression of genes coding for mitochondrial oxidative phosphorylation

decreases while expression of glycolytic genes increases during reprogramming [197]. Significantly, the changes in expression of the metabolic genes, precedes the changes in expression of the pluripotency genes by several days [197]. This is an important point, because it demonstrates that metabolic gene expression is not only a requirement of this type of differentiation, but is actually a pre-requirement for expression of the developmental regulators themselves [197].

In the myogenic model a key myogenic transcription factor was found to be downstream of mitochondrial function [154]. Myogenin along with MYOD and MYF5, and MRF4 is a member of the MRF family of transcription factors, and it is required for terminal differentiation [135]. It has been shown that inhibition of mitochondrial protein synthesis with chloramphenicol, at the induction of differentiation, was sufficient to prevent the normal upregulation of myogenin but did not affect *Myod* or *Myf5* [154]. The same result was achieved using two different inhibitors of mitochondria, fccp that eliminates mitochondrial inner membrane potential, and with oligomycin, an inhibitor of ETC complex V [154]. Conversely, the overexpression of the mitochondrial T3 receptor, that stimulates mitochondrial biogenesis, enhanced expression of the myogenin gene, but not *Myod* or *Myf5* [154].

In my system I found a similar effect on myogenin expression (Fig. 8). It was not properly upregulated in the *Rb1*$^{-/-}$ cells compared to WT, but was restored in the DKOs. The results of the study discussed in the previous paragraph would suggest that this defect in myogenin expression could be due to a defect in mitochondria.

I found that the upregulation of myogenin and mitochondrial biogenesis are early events in the myogenic system that I used. I detected expression of the myogenin

protein by 12 hours after induction in WT cells (Fig. 8). Similarly, I measured increased oxygen consumption at 12 hours in WT cells (Fig. 20). I do not have data at earlier time points for oxygen consumption, nor do I have gene expression data at earlier differentiating time-points. A more thorough investigation into the temporal dynamics of the mitochondrial genes and early development regulators like myogenin should be done in order to fully clarify the epistatic relationship between these two gene sets. A comparison of gene expression between 0 and 12 hours post-induction of differentiation would determine if upregulation of the mitochondrial components comes before or after the myogenic regulators.

Importantly, I have demonstrated that the decrease in metabolic gene expression and the mitochondrial defects of the *Rb1*$^{-/-}$ cells during differentiation are reversed by the additional loss of *Kdm5a*. Using both genome-wide and gene-specific techniques, I showed that pRB and KDM5A bind directly to genes coding for a broad array of mitochondrial components involved in different aspects of mitochondrial function. For example, they both bind to genes that regulate mitochondrial fusion and all of the ETC complexes (Table III). They exhibit inverse temporal binding dynamics at the promoter region during differentiation. pRB binding increases while KDM5A binding decreases from the proliferating condition to the early stages of differentiation. The loss of KDM5A from the promoter of *Mfn2*, a gene necessary mitochondrial biogenesis, required pRB, as there was no change in binding during differentiation in the *Rb1*$^{-/-}$ cells. It is not certain if these observations of deregulated chromatin-binding reflect a cause or a consequence of defective differentiation. In support of causation, is my observation that changes in binding of KDM5A and pRB occur, at the 0hr time-point (Fig. 18A and 18B).

This is an important point. Myogenic differentiation in cell culture requires three conditions: (1) Expression of the myogenic regulatory factor MYOD [200, 201]. MYOD is expressed endogenously in myoblast cell lines. In MEFs exogenous MYOD is supplied via viral vectors prior to induction. (2) The cells must reach a state of confluence before they are induced [202, 203]. (3) Removal of mitogenic stimuli in the media [202].

The purpose of confluence is not simply a convenience of proximity to allow cellular fusion, but is a necessary step in the induction process [202, 203]. Cells that are not allowed to reach confluence will not differentiate properly [203]. Conversely, cells that have reached confluence can then be dispersed and successfully induced to differentiate as determined by biochemical markers, even though fusion cannot occur because the cells are not longer in contact [203]. Additionally it has been shown using mutant cell lines that are able to differentiate as characterized by expression of muscle-specific markers, but unable to fuse into multinucleated myotubes, still require cell-cell contact by confluent conditions [202].

In my experiments, the point of confluence is the 0hr time-point. This is also the time-point where KDM5A was lost from the promoter of mitochondrial target genes, as determined by ChIP assay (Fig. 18B). Binding of pRB at the same promoters begins to increase at this time point in some but not all of the same genes (Fig. 18A). This observation is significant because it places KDM5A and pRB regulation of mitochondrial component genes at the earliest stages of differentiation before defects of differentiation are detectable.

The opposing binding dynamics of KDM5A and pRB at common target genes and the requirement of pRB for KDM5A to come off the promoter deserves further

study. This data in combination with previous publications suggests that a likely mechanism for pRB regulation of KDM5A during differentiation is by direct interaction [12, 17]. Mutations that specifically eliminate KDM5A-binding to pRB could be used to evaluate in greater detail the nature of the relationship between pRB and KDM5A at their gene targets. We know that pRB and KDM5A interact during differentiation [17]. I have demonstrated that KDM5A remains bound to the promoter of *Mfn2* in the absence of pRB, but I don't know if this is because pRB is actively removing it, or if it is a secondary consequence of the loss of pRB. This type of KDM5A mutant could be used to address two fundamental questions regarding the nature of the relationship between pRB and KDM5A: (1) is the direct interaction between pRB and KDM5A necessary for pRB to promote differentiation? (2) Does pRB binding to KDM5A cause it to leave the chromatin? KDM5A has two pRB-interacting domains (Fig. 4) [12, 115, 204]. One is the well-known, canonical LXCXE domain. Mutation of this domain in KDM5A (KDM5A-LXCXA) eliminates binding through this domain [17, 115]. However, the second non-canonical domain is also sufficient for binding [17, 115]. The precise location and sequence of this domain is not yet known [115]. It would have to be identified in order to make KDM5A mutants that are unable to interact with pRB.

I found that the ability of KDM5A to block differentiation requires the enzymatic JmjC domain. Iron is a cofactor for KDM5A [110]. Point mutations in two amino acids required for coordinating the Fe(2+) atom resulted in the inability of KDM5A to block differentiation when reintroduced into *Kdm5a*$^{-/-}$;*Rb1*$^{-/-}$ cells. This is a key point with respect to the potential for developing strategies to target this pathway as a therapy.

An interesting question that remains, is how do mitochondrial defects block differentiation? Mitochondria are responsible for an array of important cellular functions including generation of ATP and ROS; generating anabolic precursors, and cofactors for enzymes; calcium signaling, and apoptosis [205]. One or all of these processes may contribute to myogenic regulation. Additionally they have the capacity for retrograde signaling, where they can signal to the nucleus in a manner that affects gene expression [156, 205]. For example changes in the release of Ca^{2+} to the cytoplasm by unhealthy mitochondria can directly affect the activity of the Ca^{2+} dependent phosphatase, calcineurin. Downstream of calcineurin are several factors that can directly affect transcription [205]. Recently it was shown that genetic ablation of genes required for mitochondrial fusion caused an increase in Ca^{2+} release leading to higher calcineurin activity that was linked to an increase in Notch signaling activity that ultimately resulted in an inhibition of cardiomyocyte differentiation [193]. The inhibition of differentiation was partially rescued by treatment of the cells with an inhibitor of Notch signaling [193]. These results indicate a potential mechanism for regulation of differentiation by mitochondria.

Another signaling molecule associated with mitochondria is ROS [205]. High levels of ROS have been shown to inhibit myogenic differentiation in the C2C12 myoblast cell line [178]. Conversely, treatment of these cells with antioxidants enhances differentiation. I observed increased levels of ROS in *Rb1*$^{-/-}$ MEFs induced to differentiate compared to WT, and these levels were reduced in the DKOs. This data offers a potential mechanism to explain defective differentiation in *Rb1*$^{-/-}$ cells and rescue in DKO cells through mitochondria.

It may depend on which particular aspect of mitochondrial function is affected that determines how differentiation is blocked (e.g. membrane fusion vs. ETC activity). There may be multiple possible mechanisms [205]. In the case of widespread dysfunction as I observed in the *Rb*$^{-/-}$ cells, there may be several layers of inhibition. I have made attempts to rescue mitochondrial biogenesis using compounds such as bezafibrate that are agonists of PPARα, a transcriptional activator of mitochondrial component genes that promotes mitochondrial biogenesis [206, 207]. The utility of this method is that it attempts to broadly rescue defective mitochondrial, to overcome all potential layers of dysfunction that might individually inhibit differentiation and occlude any positive rescue effect of a more particular restoration of mitochondria function. These attempts however, did not work. A possible explanation here is that the drugs may augment PPARα activity, but this may not be sufficient to overcome the transcriptional defects caused by loss of pRB. Further tests could be done here such as qPCR to see if in fact transcription of the mitochondrial component genes is upregulated by this treatment.

Currently the working model for KDM5A and pRB regulation of differentiation places pRB and KDM5A as both cooperating and opposing regulators of common gene sets (Fig. 27). Previous work has shown that KDM5A can repress cell cycle genes by demethylation of H3K4me3 during differentiation [15, 16]. The same genes are corepressed by a separate complex containing E2F4 and the RB-family protein, p130 [15, 16]. This complex is required for histone deacetylation, likely by recruitment of an HDAC enzyme [16]. Cell cycle withdrawal occurs after cells reach the stage of committed myoblasts [142].

Here I have shown that KDM5A and pRB are opposing coregulators of nuclear genes coding for mitochondrial components during myogenic differentiation (Fig. 27). The mitochondria are unique cellular organelles in that they posses their own genome [208]. However transcriptional regulation of mitochondrial biogenesis and function occurs primarily in the nucleus [209]. There are at least 1098 nuclear genes coding for proteins with mitochondrial function compared to 37 genes coded by mtDNA [208, 209]. KDM5A and pRB target several of these nuclear genes that are involved in multiple aspects of mitochondrial function, some of which I studied in detail. For example, *Mfn2* is required for mitochondrial membrane fusion during mitochondrial biogenesis [158]. *Ndufs4*, *Sdhd*, *Uqcrc1*, *Cox6b1* all code for components of different ETC complexes. These complexes are required to generate the membrane potential across the inner mitochondrial membrane and are the foundation of aerobic respiration [165]. *Atp5a1* codes for a subunit of ATP synthase which uses the free energy of the membrane potential to generate ATP [165]. All of the above genes were found to be deregulated in *Rb1*$^{-/-}$ cells by qPCR and either fully or at least partially rescued by the additional loss of *Kdm5a* in the DKOs.

Figure 27. Working model.

KDM5A binds to and maintains the basal expression level of nuclear genes that code for mitochondrial components in undifferentiated cells. Upon induction of differentiation pRB causes the displacement of KDM5A from these genes resulting in upregulation that is necessary for differentiation. In the absence of pRB, cells are defective in differentiation because pRB is not available to relieve the repressive effect of KDM5A. Defective gene expression of mitochondrial components leads to defective mitochondrial biogenesis and mitochondrial function. Defects in the mitochondria result in an early failure of differentiation. Also during differentiation, KDM5A is recruited to E2F- target cell cycle genes as differentiation progresses. KDM5A is recruited independently of E2F4 and the pocket proteins. KDM5A contributes to permanent repression of these genes by demethylation of H3K4me3.

Figure 27

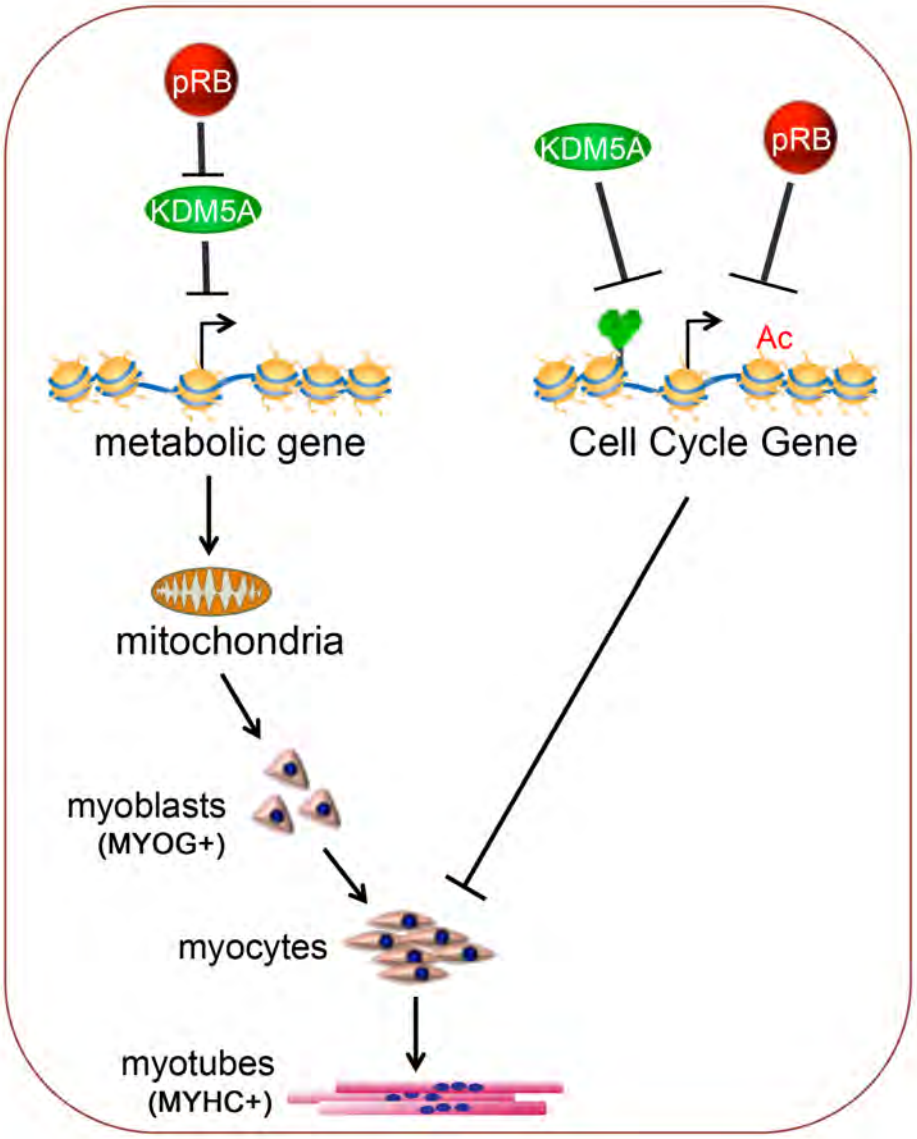
pRB
KDM5A
metabolic gene
mitochondria
myoblasts
(MYOG+)
myocytes
myotubes
(MYHC+)
KDM5A
pRB
Ac
Cell Cycle Gene

In my working model, deregulated expression of mitochondrial component genes in *Rb1*$^{-/-}$ cells results in defects in the mitochondria themselves (Fig. 27). The requirement of mitochondria for differentiation and the early timing of the molecular and genetic events, suggest that it is this defect that ultimately leads to the failure of differentiation [151-154, 161, 167-170, 197-199]. That being said, additional studies directed at the cause and effect nature of this finding should be done in the future. Studies aimed at determining in detail, the timing of expression of the mitochondrial components compared to the myogenic factors, and studies to identify the requirements of the KDM5A-pRB interaction for differentiation could provide important data to support my claims.

CITED LITERATURE

1. Tzen, C.Y., et al., Differentiation, cancer, and anticancer activity. Biochem Cell Biol., 1988. **66**(6): p. 478-489.

2. Filipak, M., et al., Integrated control of proliferation and differentiation of mesenchymal stem cells. Environ Health Perspect. **80**: p. 117-125.

3. Scott Re, M.P.B., An initiator of carcinogenesis selectively and stably inhibits stem cell differentiation: a concept that initiation of carcinogenesis involves multiple phases. Proc Natl Acad Sci U S A, 1985. **82**(9): p. 2995-9.

4. Scott, R.E., et al., Regulation of differentiation, proliferation and cancer suppressor activity. Int J Dev Biol., 1993. **37**(1): p. 67 - 74.

5. Romero O. A. and Sanchez-CespedesM., The SWI/SNF genetic blockade: effects in cell differentiation, cancer and developmental diseases. . Oncogene, 2013: p. 1-9.

6. Golebiewska A., L.M. Atkinson Sp, and L. Armstrong, Epigenetic landscaping during hESC differentiation to neural cells. Stem Cells, 2009. **27**(6): p. 1298 - 308.

7. Gan Q. and M. Yoshida T, OG., Owens G.K., Concise review: epigenetic mechanisms contribute to pluripotency and cell lineage determination of embryonic stem cells. Stem Cells, 2006. **25**(1): p. 2-9.

8. Asp P, B.R., Vethantham V, Parisi F, Micsinai M, Cheng J, Bowman C, Kluger Y, Dynlacht BD, Genome-wide remodeling of the epigenetic landscape during myogenic differentiation. Proc Natl Acad Sci U S A, 2011. **108**(22): p. 149-58.

9. De Falco, G. and S. Comes F, C., pRb: master of differentiation. Coupling irreversible cell cycle withdrawal with induction of muscle-specific transcription. Oncogene, 2006. **25**(38): p. 5244-9.

10. Wang, G.G., et al., Haematopoietic malignancies caused by dysregulation of a chromatin-binding PHD finger. Nature, 2009. **459**(7248): p. 847-5.

11. Friedmann-Morvinski D. and V.I. M., Dedifferentiation and reprogramming: origins of cancer stem cells. EMBO Rep., 2014. **15**(3): p. 244-53.

12. Deborah Defeo-Jones, P.S.H., Raymond E. Jones, Kathleen M. Haskell, Gerald A. Vuocolo, Michelle G. Hanobik, Hans E. Huber, Alien Oliff, Cloning of cDNAs for cellular proteins that bind to the retinoblastoma gene product. Nature, 1991. **352**(6332): p. 251-254.

13. Lin, W., et al., Loss of the retinoblastoma binding protein 2 (RBP2) histone demethylase suppresses tumorigenesis in mice lacking Rb1 or Men1. Proc Natl Acad Sci U S A, 2011. **108**(33): p. 13379-86.

14. Chicas, A., et al., H3K4 demethylation by Jarid1a and Jarid1b contributes to retinoblastoma-mediated gene silencing during cellular senescence. Proc Natl Acad Sci U S A, 2012. **109**(23): p. 8971-6.

15. Lopez-Bigas, N., et al., Genome-wide analysis of the H3K4 histone demethylase RBP2 reveals a transcriptional program controlling differentiation. Mol Cell, 2008. **31**(4): p. 520-30.

16. Beshiri, M.L., et al., Coordinated repression of cell cycle genes by KDM5A and E2F4 during differentiation. Proc Natl Acad Sci U S A, 2012. **109**(45): p. 18499-504.

17. Benevolenskaya, E.V., et al., Binding of pRB to the PHD protein RBP2 promotes cellular differentiation. Mol Cell, 2005. **18**(6): p. 623-35.

18. Morris, E.J. and N.J. Dyson, Retinoblastoma protein partners. Adv Cancer Res, 2001. **82**: p. 1-54.

19. Khidr, L. and P.L. Chen, RB, the conductor that orchestrates life, death and differentiation. Oncogene, 2006. **25**(38): p. 5210-9.

20. Nicolay, B.N. and N.J. Dyson, The multiple connections between pRB and cell metabolism. Curr Opin Cell Biol, 2013. **25**(6): p. 735-40.

21. Hansen K, L.J., Holm K, Kjerulff AA, Bartek J., Dissecting functions of the retinoblastoma tumor suppressor and the related pocket proteins by integrating

genetic, cell biology, and electrophoretic techniques. Electrophoresis, 1999. **20**(2): p. 372-81.

22. Classon, M. and N. Dyson, p107 and p130: versatile proteins with interesting pockets. Exp Cell Res, 2001. **264**(1): p. 135-47.

23. Lipinski, M.M. and T. Jacks, The retinoblastoma gene family in differentiation and development. Oncogene, 1999. **18**(55): p. 7873-82.

24. Huh, M.S., et al., Rb is required for progression through myogenic differentiation but not maintenance of terminal differentiation. J Cell Biol, 2004. **166**(6): p. 865-76.

25. Friend, S.H., et al., A human DNA segment with properties of the gene that predisposes to retinoblastoma and osteosarcoma. Nature, 1986. **323**(6089): p. 643-6.

26. Ortega, S., M. Malumbres, and M. Barbacid, Cyclin D-dependent kinases, INK4 inhibitors and cancer. Biochim Biophys Acta, 2002. **1602**(1): p. 73-87.

27. Harbour, J.W. and D.C. Dean, The Rb/E2F pathway: expanding roles and emerging paradigms. Genes Dev, 2000. **14**(19): p. 2393-409.

28. Knudsen, E.S. and K.E. Knudsen, Tailoring to RB: tumour suppressor status and therapeutic response. Nat Rev Cancer, 2008. **8**(9): p. 714-24.

29. Burkhart, D.L. and J. Sage, Cellular mechanisms of tumour suppression by the retinoblastoma gene. Nat Rev Cancer, 2008. **8**(9): p. 671-82.

30. Thomas, D.M., et al., The Retinoblastoma Protein Acts as a Transcriptional Coactivator Required for Osteogenic Differentiation. Molecular cell, 2001. **8**(2): p. 303-316.

31. Frolov, M.V. and N.J. Dyson, Molecular mechanisms of E2F-dependent activation and pRB-mediated repression. J Cell Sci, 2004. **117**(Pt 11): p. 2173-81.

32. Goodrich, D.W., The retinoblastoma tumor-suppressor gene, the exception that proves the rule. Oncogene, 2006. **25**(38): p. 5233-43.

33. Sherr, C.J. and J.M. Roberts, CDK inhibitors: positive and negative regulators of G1-phase progression. Genes Dev, 1999. **13**(12): p. 1501-12.

34. Ambrus, A.M., et al., Loss of dE2F compromises mitochondrial function. Dev Cell, 2013. **27**(4): p. 438-51.

35. Barriere, C., et al., Mice thrive without Cdk4 and Cdk2. Mol Oncol, 2007. **1**(1): p. 72-83.

36. Kozar, K., et al., Mouse development and cell proliferation in the absence of D-cyclins. Cell, 2004. **118**(4): p. 477-91.

37. Malumbres, M., et al., Mammalian cells cycle without the D-type cyclin-dependent kinases Cdk4 and Cdk6. Cell, 2004. **118**(4): p. 493-504.

38. Sherr, C.J. and J.M. Roberts, Living with or without cyclins and cyclin-dependent kinases. Genes Dev, 2004. **18**(22): p. 2699-711.

39. Ianari, A., et al., Proapoptotic function of the retinoblastoma tumor suppressor protein. Cancer Cell, 2009. **15**(3): p. 184-94.

40. Hilgendorf, K.I., et al., The retinoblastoma protein induces apoptosis directly at the mitochondria. Genes Dev, 2013. **27**(9): p. 1003-15.

41. Weinberg, R.A., The Rb gene and the negative regulation of cell growth. Blood, 1989. **74**(2): p. 529-32.

42. Cobrinik, D., et al., The retinoblastoma protein and the regulation of cell cycling. Trends Biochem Sci, 1992. **17**(8): p. 312-5.

43. Calo, E., et al., Rb regulates fate choice and lineage commitment in vivo. Nature, 2010. **466**(7310): p. 1110-4.

44. Reynolds, M.R., et al., Control of glutamine metabolism by the tumor suppressor Rb. Oncogene, 2014. **33**(5): p. 556-66.

45. Nicolay, B.N., et al., Loss of RBF1 changes glutamine catabolism. Genes Dev, 2013. **27**(2): p. 182-96.

46. Jiang, H., et al., RB-E2F1: molecular rheostat for autophagy and apoptosis. Autophagy, 2010. **6**(8): p. 1216-7.

47. Medema, R.H., et al., Growth suppression by p16ink4 requires functional retinoblastoma protein. Proceedings of the National Academy of Sciences, 1995. **92**(14): p. 6289-6293.

48. Chellappan, S.P., et al., The E2F transcription factor is a cellular target for the RB protein. Cell, 1991. **65**(6): p. 1053-1061.

49. Sellers, W.R., et al., Stable binding to E2F is not required for the retinoblastoma protein to activate transcription, promote differentiation, and suppress tumor cell growth. Genes & Development, 1998. **12**(1): p. 95-106.

50. Wu, L., et al., Extra-embryonic function of Rb is essential for embryonic development and viability. Nature, 2003. **421**(6926): p. 942-947.

51. Jacks, T., et al., Effects of an Rb mutation in the mouse. Nature, 1992. **359**(6393): p. 295-300.

52. Clarke, A.R., et al., Requirement for a functional Rb-1 gene in murine development. Nature, 1992. **359**(6393): p. 328-30.

53. Lee, E.Y.H.P., et al., Mice deficient for Rb are nonviable and show defects in neurogenesis and haematopoiesis. Nature, 1992. **359**(6393): p. 288-294.

54. Harbour, J.W., Molecular basis of low-penetrance retinoblastoma. Arch Ophthalmol, 2001. **119**(11): p. 1699-704.

55. Nevins, J.R., The Rb/E2F pathway and cancer. Hum. Mol. Genet., 2001. **10**(7): p. 699-703.

56. Dick, F.A., Structure-function analysis of the retinoblastoma tumor suppressor protein - is the whole a sum of its parts? Cell Div., 2007. **2**(26).

57. Novitch, B.G., et al., Skeletal muscle cells lacking the retinoblastoma protein display defects in muscle gene expression and accumulate in S and G2 phases of the cell cycle. J Cell Biol, 1996. **135**(2): p. 441-56.

58. De Luca, A., et al., The retinoblastoma gene family and its role in proliferation, differentiation and development. Histol Histopathol, 1996. **11**(4): p. 1029-34.

59. Chen, P.L., et al., Retinoblastoma protein positively regulates terminal adipocyte differentiation through direct interaction with C/EBPs. Genes & Development, 1996. **10**(21): p. 2794-2804.

60. Gutierrez, G.M., E. Kong, and P.W. Hinds, Master or slave: The complex relationship of RBP2 and pRb. Cancer Cell. **7**(6): p. 501-502.

61. van Oevelen, C., et al., A role for mammalian Sin3 in permanent gene silencing. Mol Cell, 2008. **32**(3): p. 359-70.

62. Rayman JB, T.Y., Indjeian VB, Dannenberg JH, Catchpole S, Watson RJ, te Riele H, Dynlacht BD, E2F mediates cell cycle-dependent transcriptional repression in vivo by recruitment of an HDAC1/mSin3B corepressor complex. Genes Dev, 2002. **16**(8): p. 933-47.

63. Klose, R.J., et al., The retinoblastoma binding protein RBP2 is an H3K4 demethylase. Cell, 2007. **128**(5): p. 889-900.

64. Christensen, J., et al., RBP2 belongs to a family of demethylases, specific for tri- and dimethylated lysine 4 on histone 3. Cell, 2007. **128**(6): p. 1063-76.

65. Eissenberg, J.C. and A. Shilatifard, Histone H3 lysine 4 (H3K4) methylation in development and differentiation. Dev Biol, 2010. **339**(2): p. 240-9.

66. Schwartz, Y.B. and V. Pirrotta, Polycomb silencing mechanisms and the management of genomic programmes. Nat Rev Genet, 2007. **8**(1): p. 9-22.

67. Tollervey, J.R. and V.V. Lunyak, Epigenetics: judge, jury and executioner of stem cell fate. Epigenetics, 2012. **7**(8): p. 823-40.

68. Campbell RM, T.P., Cancer epigenetics drug discovery and development: the challenge of hitting the mark. J Clin Invest, 2014. **124**(1): p. 64-9.

69. Chen, Q.W., et al., Epigenetic regulation and cancer (review). Oncol Rep, 2014. **31**(2): p. 523-32.

70. Boumber, Y. and J.P. Issa, Epigenetics in cancer: what's the future? Oncology, 2011. **25**(3): p. 220 -226.

71. Feinberg, A.P. and B. Tycko, The history of cancer epigenetics. Nat Rev Cancer, 2004. **4**(2): p. 143-53.

72. Storb, U., Why does somatic hypermutation by AID require transcription of its target genes? Adv Immunol, 2014. **122**: p. 253-77.

73. Goldberg, A.D., C.D. Allis, and E. Bernstein, Epigenetics: a landscape takes shape. Cell, 2007. **128**(4): p. 635-8.

74. Holliday, R., Epigenetics: a historical overview. Epigenetics, 2006. **1**(2): p. 76-80.

75. Wallace, D.C. and W. Fan, Energetics, epigenetics, mitochondrial genetics. Mitochondrion, 2010. **10**(1): p. 12-31.

76. Zentner, G.E. and S. Henikoff, Regulation of nucleosome dynamics by histone modifications. Nat Struct Mol Biol, 2013. **20**(3): p. 259-66.

77. Noma, K., C.D. Allis, and S.I. Grewal, Transitions in distinct histone H3 methylation patterns at the heterochromatin domain boundaries. Science, 2001. **293**(5532): p. 1150-5.

78. Litt, M.D., et al., Correlation between Histone Lysine Methylation and Developmental Changes at the Chicken β-Globin Locus. Science, 2001. **293**(5539): p. 2453-2455.

79. Schneider, R. and R. Grosschedl, Dynamics and interplay of nuclear architecture, genome organization, and gene expression. Genes Dev, 2007. **21**(23): p. 3027-43.

80. Mekhail, K. and D. Moazed, The nuclear envelope in genome organization, expression and stability. Nat Rev Mol Cell Biol, 2010. **11**(5): p. 317-28.

81. Hemberger, M., W. Dean, and W. Reik, Epigenetic dynamics of stem cells and cell lineage commitment: digging Waddington's canal. Nat Rev Mol Cell Biol, 2009. **10**(8): p. 526-37.

82. Kouzarides, T., Chromatin modifications and their function. Cell, 2007. **128**(4): p. 693-705.

83. Sims, R.J., 3rd and D. Reinberg, Histone H3 Lys 4 methylation: caught in a bind? Genes Dev, 2006. **20**(20): p. 2779-86.

84. Ruthenburg, A.J., C.D. Allis, and J. Wysocka, Methylation of lysine 4 on histone H3: intricacy of writing and reading a single epigenetic mark. Mol Cell, 2007. **25**(1): p. 15-30.

85. Binda, O., On your histone mark, SET, methylate! Epigenetics, 2013. **8**(5): p. 457-63.

86. Yun, M., et al., Readers of histone modifications. Cell Res, 2011. **21**(4): p. 564-78.

87. Bernstein, B.E., et al., Methylation of histone H3 Lys 4 in coding regions of active genes. Proc Natl Acad Sci U S A, 2002. **99**(13): p. 8695-700.

88. Islam, A.B., et al., Selective targeting of histone methylation. Cell Cycle, 2011. **10**(3): p. 413-424.

89. Kouzarides, T., Histone methylation in transcriptional control. Curr Opin Genet Dev, 2002. **12**(2): p. 198-209.

90. Martin, C. and Y. Zhang, The diverse functions of histone lysine methylation. Nat Rev Mol Cell Biol, 2005. **6**(11): p. 838-49.

91. Min, J., et al., Structure of the catalytic domain of human DOT1L, a non-SET domain nucleosomal histone methyltransferase. Cell, 2003. **112**(5): p. 711-23.

92. Xiao, B., J.R. Wilson, and S.J. Gamblin, SET domains and histone methylation. Current Opinion in Structural Biology, 2003. **13**(6): p. 699-705.

93. Feng, Q., et al., Methylation of H3-Lysine 79 Is Mediated by a New Family of HMTases without a SET Domain. Current biology : CB, 2002. **12**(12): p. 1052-1058.

94. Marmorstein, R., Structure of SET domain proteins: a new twist on histone methylation. Trends Biochem Sci, 2003. **28**(2): p. 59-62.

95. Litt, M., Y. Qiu, and S. Huang, Histone arginine methylations: their roles in chromatin dynamics and transcriptional regulation. Biosci Rep, 2009. **29**(2): p. 131-41.

96. Wang, Y., et al., Human PAD4 regulates histone arginine methylation levels via demethylimination. Science, 2004. **306**(5694): p. 279-83.

97. Cuthbert, G.L., et al., Histone deimination antagonizes arginine methylation. Cell, 2004. **118**(5): p. 545-53.

98. Shi, Y., et al., Histone demethylation mediated by the nuclear amine oxidase homolog LSD1. Cell, 2004. **119**(7): p. 941-53.

99. Tsukada, Y., et al., Histone demethylation by a family of JmjC domain-containing proteins. Nature, 2006. **439**(7078): p. 811-6.

100. Cloos, P.A., et al., Erasing the methyl mark: histone demethylases at the center of cellular differentiation and disease. Genes Dev, 2008. **22**(9): p. 1115-40.

101. Metzger, E., et al., LSD1 demethylates repressive histone marks to promote androgen-receptor-dependent transcription. Nature, 2005. **437**(7057): p. 436-9.

102. Cloos, P.A., et al., The putative oncogene GASC1 demethylates tri- and dimethylated lysine 9 on histone H3. Nature, 2006. **442**(7100): p. 307-11.

103. Fodor, B.D., et al., Jmjd2b antagonizes H3K9 trimethylation at pericentric heterochromatin in mammalian cells. Genes Dev, 2006. **20**(12): p. 1557-62.

104. Klose, R.J., et al., The transcriptional repressor JHDM3A demethylates trimethyl histone H3 lysine 9 and lysine 36. Nature, 2006. **442**(7100): p. 312-6.

105. Whetstine, J.R., et al., Reversal of histone lysine trimethylation by the JMJD2 family of histone demethylases. Cell, 2006. **125**(3): p. 467-81.

106. Gumiero A, M.C., Pearson AR, Raven EL, Moody PC., Nature of the ferryl heme in compounds I and II. J Biol Chem, 2011. **286**(2): p. 1260-8.

107. Tu, S., et al., The ARID domain of the H3K4 demethylase RBP2 binds to a DNA CCGCCC motif. Nat Struct Mol Biol, 2008. **15**(4): p. 419-21.

108. Capili, A.D., et al., Solution structure of the PHD domain from the KAP-1 corepressor: structural determinants for PHD, RING and LIM zinc-binding domains. EMBO J, 2001. **20**(1-2): p. 165-77.

109. Beshiri, M.L., et al., Genome-wide analysis using ChIP to identify isoform-specific gene targets. J Vis Exp, 2010(41).

110. Klose, R.J., E.M. Kallin, and Y. Zhang, JmjC-domain-containing proteins and histone demethylation. Nat Rev Genet, 2006. **7**(9): p. 715-27.

111. Huang, F., et al., The JmjN domain of Jhd2 is important for its protein stability, and the plant homeodomain (PHD) finger mediates its chromatin association independent of H3K4 methylation. J Biol Chem, 2010. **285**(32): p. 24548-61.

112. Chen, Z., et al., Structural insights into histone demethylation by JMJD2 family members. Cell, 2006. **125**(4): p. 691-702.

113. Clissold, P.M. and C.P. Ponting, JmjC: cupin metalloenzyme-like domains in jumonji, hairless and phospholipase A2beta. Trends Biochem Sci, 2001. **26**(1): p. 7-9.

114. Wagner, E.J. and P.B. Carpenter, Understanding the language of Lys36 methylation at histone H3. Nat Rev Mol Cell Biol, 2012. **13**(2): p. 115-26.

115. Kim, Y.W., et al., Differential specificity for binding of retinoblastoma binding protein 2 to RB, p107, and TATA-binding protein. Mol Cell Biol, 1994. **14**(11): p. 7256-64.

116. Pasini, D., et al., Coordinated regulation of transcriptional repression by the RBP2 H3K4 demethylase and Polycomb-Repressive Complex 2. Genes Dev, 2008. **22**(10): p. 1345-55.

117. Ge, Z., et al., Chromatin remodeling: recruitment of histone demethylase RBP2 by Mad1 for transcriptional repression of a Myc target gene, telomerase reverse transcriptase. FASEB J, 2010. **24**(2): p. 579-86.

118. Liefke, R., et al., Histone demethylase KDM5A is an integral part of the core Notch-RBP-J repressor complex. Genes Dev, 2010. **24**(6): p. 590-601.

119. Hayakawa, T., et al., RBP2 is an MRG15 complex component and down-regulates intragenic histone H3 lysine 4 methylation. Genes to Cells, 2007. **12**(6): p. 811-826.

120. Christensen, J., et al., RBP2 Belongs to a Family of Demethylases, Specific for Tri-and Dimethylated Lysine 4 on Histone 3. Cell, 2007. **128**(6): p. 1063-1076.

121. DiTacchio, L., et al., Histone lysine demethylase JARID1a activates CLOCK-BMAL1 and influences the circadian clock. Science, 2011. **333**(6051): p. 1881-5.

122. Roguev, A., et al., The Saccharomyces cerevisiae Set1 complex includes an Ash2 homologue and methylates histone 3 lysine 4. EMBO J, 2001. **20**(24): p. 7137-48.

123. Li, F., et al., Lid2 is required for coordinating H3K4 and H3K9 methylation of heterochromatin and euchromatin. Cell, 2008. **135**(2): p. 272-83.

124. Gildea, J.J., R. Lopez, and A. Shearn, A screen for new trithorax group genes identified little imaginal discs, the Drosophila melanogaster homologue of human retinoblastoma binding protein 2. Genetics, 2000. **156**(2): p. 645-63.

125. Secombe, J., et al., The Trithorax group protein Lid is a trimethyl histone H3K4 demethylase required for dMyc-induced cell growth. Genes Dev, 2007. **21**(5): p. 537-51.

126. Blais, A., et al., An initial blueprint for myogenic differentiation. Genes Dev, 2005. **19**(5): p. 553-69.

127. Blais, A., et al., Retinoblastoma tumor suppressor protein-dependent methylation of histone H3 lysine 27 is associated with irreversible cell cycle exit. J Cell Biol, 2007. **179**(7): p. 1399-412.

128. Cao Y, Y.Z., Sarkar D, Lawrence M, Sanchez GJ, Parker MH, MacQuarrie KL, Davison J, Morgan MT, Ruzzo WL, Gentleman RC, Tapscott SJ., Genome-wide MyoD binding in skeletal muscle cells: a potential for broad cellular reprogramming. Dev Cell, 2010. **18**(4): p. 662-74.

129. Davis, R.L. and L. Weintraub H., A. B., Expression of a single transfected cDNA converts fibroblasts to myoblasts. Cell, 1987. **51**(6): p. 987-1000.

130. Peckham, M., Engineering a multi-nucleated myotube, the role of the actin cytoskeleton. J Microsc, 2008. **231**(3): p. 486-93.

131. Boudriau, S., et al., Cytoskeletal structure of skeletal muscle: identification of an intricate exosarcomeric microtubule lattice in slow- and fast-twitch muscle fibers. Journal of Histochemistry & Cytochemistry, 1993. **41**(7): p. 1013-1021.

132. Molkentin, J.D. and E.N. Olson, Combinatorial control of muscle development by basic helix-loop-helix and MADS-box transcription factors. Proc Natl Acad Sci U S A, 1996. **93**(18): p. 9366-73.

133. Buckingham, M., Skeletal muscle formation in vertebrates. Curr Opin Genet Dev, 2001. **11**(4): p. 440-8.

134. Mok, G.F. and D. Sweetman, Many routes to the same destination: lessons from skeletal muscle development. Reproduction, 2011. **141**(3): p. 301-12.

135. Pownall, M.E., M.K. Gustafsson, and C.P. Emerson, Jr., Myogenic regulatory factors and the specification of muscle progenitors in vertebrate embryos. Annu Rev Cell Dev Biol, 2002. **18**: p. 747-83.

136. Jeffery D Molkentin, E.N.O., Defining the regulatory networks for muscle development. Current Opinion in Genetics & Development, 1996. **6**(4): p. 445-453.

137. Cheng, C.S., et al., Conditions that promote primary human skeletal myoblast culture and muscle differentiation in vitro. Am J Physiol Cell Physiol., 2014. **306**(4): p. C385-95.

138. Velica, P. and C.M. Bunce, A quick, simple and unbiased method to quantify C2C12 myogenic differentiation. Muscle Nerve, 2011. **44**(3): p. 366-70.

139. Abmayr, S.M. and G.K. Pavlath, Myoblast fusion: lessons from flies and mice. Development, 2012. **139**(4): p. 641-56.

140. Halevy O, N.B., Spicer DB, Skapek SX, Rhee J, Hannon GJ, Beach D, Lassar AB, Correlation of terminal cell cycle arrest of skeletal muscle with induction of p21 by MyoD. Science, 1995. **267**(5200): p. 1018-21.

141. Kenneth Walsh, H.P., Cell cycle exit upon myogenic differentiation. Current Opinion in Genetics & Development, 1997. **7**(5): p. 597-602.

142. Walsh, K. and H. Perlman, Cell cycle exit upon myogenic differentiation. Curr Opin Genet Dev, 1997. **7**(5): p. 597-602.

143. Martelli F, C.C., Santarelli G, Polikar B, Felsani A, Caruso M, MyoD induces retinoblastoma gene expression during myogenic differentiation. Oncogene, 1994. **9**(12): p. 3579-90.

144. Zhang, H.S., et al., Exit from G1 and S Phase of the Cell Cycle Is Regulated by Repressor Complexes Containing HDAC-Rb-hSWI/SNF and Rb-hSWI/SNF. Cell, 2000. **101**(1): p. 79-89.

145. Campeau E, R.V., Rodier F, Smith CL, Rahmberg BL, Fuss JO, Campisi J, Yaswen P, Cooper PK, Kaufman PD, A versatile viral system for expression and depletion of proteins in mammalian cells. PLoS One, 2009. **4**(8): p. 1-18.

146. Livak, K.J. and T.D. Schmittgen, Analysis of relative gene expression data using real-time quantitative PCR and the 2(-Delta Delta C(T)) Method. Methods, 2001. **25**(4): p. 402-8.

147. Salic, A. and T.J. Mitchison, A chemical method for fast and sensitive detection of DNA synthesis in vivo. Proc Natl Acad Sci U S A, 2008. **105**(7): p. 2415-20.

148. Son, J., et al., Nucleosome-binding activities within JARID2 and EZH1 regulate the function of PRC2 on chromatin. Genes & Development, 2013. **27**(24): p. 2663-2677.

149. Perez-Llamas, C. and N. Lopez-Bigas, Gitools: analysis and visualisation of genomic data using interactive heat-maps. PLoS One, 2011. **6**(5): p. 1-6.

150. Ciavarra, G. and E. Zacksenhaus, Rescue of myogenic defects in Rb-deficient cells by inhibition of autophagy or by hypoxia-induced glycolytic shift. J Cell Biol, 2010. **191**(2): p. 291-301.

151. Sankaran, V.G., S.H. Orkin, and C.R. Walkley, Rb intrinsically promotes erythropoiesis by coupling cell cycle exit with mitochondrial biogenesis. Genes Dev, 2008. **22**(4): p. 463-75.

152. Spitkovsky, D., et al., Activity of complex III of the mitochondrial electron transport chain is essential for early heart muscle cell differentiation. FASEB J, 2004. **18**(11): p. 1300-2.

153. Pawlikowska, P., et al., Not only insulin stimulates mitochondriogenesis in muscle cells, but mitochondria are also essential for insulin-mediated myogenesis. Cell Proliferation, 2006. **39**(2): p. 127-145.

154. Rochard, P., et al., Mitochondrial Activity Is Involved in the Regulation of Myoblast Differentiation through Myogenin Expression and Activity of Myogenic Factors. Journal of Biological Chemistry, 2000. **275**(4): p. 2733-2744.

155. Chicas, A., et al., Dissecting the unique role of the retinoblastoma tumor suppressor during cellular senescence. Cancer Cell, 2010. **17**(4): p. 376-87.

156. Picard, M., et al., Mitochondrial morphology transitions and functions: implications for retrograde signaling? Am J Physiol Regul Integr Comp Physiol, 2013. **304**(6): p. R393-406.

157. Sogl, B., G. Gellissen, and R.J. Wiesner, Biogenesis of giant mitochondria during insect flight muscle development in the locust, Locusta migratoria (L.). Transcription, translation and copy number of mitochondrial DNA. Eur J Biochem, 2000. **267**(1): p. 11-7.

158. Chan, D.C., Fusion and fission: interlinked processes critical for mitochondrial health. Annu Rev Genet, 2012. **46**: p. 265-87.

159. Hood, D.A. and S. Iqbal, Muscle mitochondrial ultrastructure: new insights into morphological divergences. J Appl Physiol (1985), 2013. **114**(2): p. 159-60.

160. Rai, M. and U. Nongthomba, Effect of myonuclear number and mitochondrial fusion on Drosophila indirect flight muscle organization and size. Exp Cell Res, 2013. **319**(17): p. 2566-77.

161. Wagatsuma, A. and K. Sakuma, Mitochondria as a potential regulator of myogenesis. Scientific World Journal, 2013. **2013**: p. 1-10.

162. Kennady, P.K., et al., Variation of mitochondrial size during the cell cycle: A multiparameter flow cytometric and microscopic study. Cytometry Part A, 2004. **62A**(2): p. 97-108.

163. Wu, M., et al., Multiparameter metabolic analysis reveals a close link between attenuated mitochondrial bioenergetic function and enhanced glycolysis dependency in human tumor cells. American Journal of Physiology - Cell Physiology, 2007. **292**(1): p. C125-C136.

164. H. Wackerhage, K.M., U. Hoffmann, D. Leyk, D. Essfeld, J. Zange, Glycolytic atp production estimated from31p magnetic resonance spectroscopy measurements during ischemic exercisein vivo. Magnetic Resonance Materials in Physics, Biology and Medicine, 1996. **4**(3-4): p. 151 - 155.

165. Perry, S.W., et al., Mitochondrial membrane potential probes and the proton gradient: a practical usage guide. Biotechniques, 2011. **50**(2): p. 98-115.

166. Herzberg NH, Z.R., Wolterman RA, Ruiter JP, Wanders RJ, Bolhuis PA, van den Bogert C, Differentiation and proliferation of respiration-deficient human myoblasts. Biochim Biophys Acta, 1993. **1181**(1): p. 63-7.

167. A Rötig, V.C., S Blanche, J P Bonnefont, F Ledeist, N Romero, J Schmitz, P Rustin, A Fischer and J M Saudubray, Pearson's marrow-pancreas syndrome. A multisystem mitochondrial disorder in infancy. The Journal of Clinical Investigation, 1990. **86**(5): p. 1601 - 1608.

168. Inoue, S., et al., Pathogenic mitochondrial DNA-induced respiration defects in hematopoietic cells result in anemia by suppressing erythroid differentiation. FEBS Lett, 2007. **581**(9): p. 1910-6.

169. Firkin, F.C., Mitochondrial Lesions in Reversible Erythropoietic Depression Due to Chloramphenicol. The Journal of Clinical Investigation, 1972. **51**: p. 2085 - 2092.

170. Craven, S.E., et al., Loss of Hspa9b in zebrafish recapitulates the ineffective hematopoiesis of the myelodysplastic syndrome. Blood, 2005. **105**(9): p. 3528-34.

171. Todd B. Sherer, R.B., Claudia M. Testa, Byoung Boo Seo, Jason R. Richardson, Jin Ho Kim, Gary W. Miller, Takao Yagi, AkemiMatsuno-Yagi, and J. Timothy Greenamyre, Mechanism of Toxicity in Rotenone Models of Parkinson's Disease. The Journal of Neuroscience, 2003. **23**(34): p. 10756-64.

172. Fendel, U., et al., Exploring the inhibitor binding pocket of respiratory complex I. Biochim Biophys Acta, 2008. **1777**(7-8): p. 660-5.

173. M. Catherine Bennett, G.W.M., Young-Hwa Kwon and Gregory M. Rose, Chronic In Vivo Sodium Azide Infusion Induces Selective and Stable Inhibition of Cytochrome c Oxidase. Journal of Neurochemistry, 1996. **66**(6): p. 2606 - 2611.

174. Y., H., The mitochondrial electron transport and oxidative phosphorylation system. Annu Rev Biochem., 1985. **54**: p. 1015-69.

175. Rodney E. Shackelford, W.K.K., and Richard S. Paules, Oxidative Stress and Cell Cycle Checkpoint Function. Free Radical Biology & Medicine, 2000. **28**(9): p. 1387-1404.

176. Glasauer, A. and N.S. Chandel, Ros. Curr Biol, 2013. **23**(3): p. R100-2.

177. Tormos, K.V., et al., Mitochondrial complex III ROS regulate adipocyte differentiation. Cell Metab, 2011. **14**(4): p. 537-44.

178. Hansen, J.M., et al., A reducing redox environment promotes C2C12 myogenesis: implications for regeneration in aged muscle. Cell Biol Int, 2007. **31**(6): p. 546-53.

179. Menon SG, S.E., Spitz DR, Higashikubo R, Sturm M, Zhang H, Goswami PC., Redox regulation of the G1 to S phase transition in the mouse embryo fibroblast cell cycle. Cancer Res, 2003. **63**(1): p. 2109-17.

180. Carriere, A., et al., Mitochondrial reactive oxygen species control the transcription factor CHOP-10/GADD153 and adipocyte differentiation: a mechanism for hypoxia-dependent effect. J Biol Chem, 2004. **279**(39): p. 40462-9.

181. Prabakaran, S., et al., Post-translational modification: nature's escape from genetic imprisonment and the basis for dynamic information encoding. Wiley Interdiscip Rev Syst Biol Med, 2012. **4**(6): p. 565-83.

182. Obenauer, J.C., Scansite 2.0: Proteome-wide prediction of cell signaling interactions using short sequence motifs. Nucleic Acids Research, 2003. **31**(13): p. 3635-3641.

183. Sharma, S.V., et al., A chromatin-mediated reversible drug-tolerant state in cancer cell subpopulations. Cell, 2010. **141**(1): p. 69-80.

184. Gulland, A., Global cancer prevalence is growing at "alarming pace," says WHO. BMJ., 2014. **348**(g1338).

185. Medema RH1, H.R., Lam F, Weinberg RA, Growth suppression by p16ink requires functional retinoblastoma protein. Proc Natl Acad Sci USA, 1995. **92**(14): p. 6289-6293.

186. Malumbres, M. and M. Barbacid, To cycle or not to cycle: a critical decision in cancer. Nat Rev Cancer, 2001. **1**(3): p. 222-31.

187. Cen, L., et al., p16-Cdk4-Rb axis controls sensitivity to a cyclin-dependent kinase inhibitor PD0332991 in glioblastoma xenograft cells. Neuro Oncol, 2012. **14**(7): p. 870-81.

188. de Rooij, J.D., et al., NUP98/JARID1A is a novel recurrent abnormality in pediatric acute megakaryoblastic leukemia with a distinct HOX gene expression pattern. Leukemia, 2013. **27**(12): p. 2280-8.

189. van Zutven, L.J., et al., Identification of NUP98 abnormalities in acute leukemia: JARID1A (12p13) as a new partner gene. Genes Chromosomes Cancer, 2006. **45**(5): p. 437-46.

190. Troy JD, A.E., Geyer JT, Saber W, Myelodysplastic syndromes in the United States: an update for clinicians. Ann Med, 2014.

191. Flachbartova, Z. and B. Kovacech, Mortalin - a multipotent chaperone regulating cellular processes ranging from viral infection to neurodegeneration. Acta Virol., 2013. **57**(1): p. 3-15.

192. Lelliott, C.J., et al., Ablation of PGC-1beta results in defective mitochondrial activity, thermogenesis, hepatic function, and cardiac performance. PLoS Biol, 2006. **4**(11): p. e369.

193. Kasahara, A., et al., Mitochondrial fusion directs cardiomyocyte differentiation via calcineurin and Notch signaling. Science, 2013. **342**(6159): p. 734-7.

194. Chen H, D.S., Ewald AJ, Griffin EE, Fraser SE, Chan DC, Mitofusins Mfn1 and Mfn2 coordinately regulate mitochondrial fusion and are essential for embryonic development. J Cell Biol., 2003. **160**(2): p. 189-200.

195. Rahn JJ, S.K., Chan SS, Opa1 is required for proper mitochondrial metabolism in early development. PLoS One, 2013. **8**(3): p. 1-13.

196. Crabtree, G.R., Calcium, calcineurin, and the control of transcription. J Biol Chem, 2001. **276**(4): p. 2313-6.

197. Folmes, C.D., et al., Somatic oxidative bioenergetics transitions into pluripotency-dependent glycolysis to facilitate nuclear reprogramming. Cell Metab, 2011. **14**(2): p. 264-71.

198. Xu, X., et al., Mitochondrial regulation in pluripotent stem cells. Cell Metab, 2013. **18**(3): p. 325-32.

199. Panopoulos, A.D., et al., The metabolome of induced pluripotent stem cells reveals metabolic changes occurring in somatic cell reprogramming. Cell Res, 2012. **22**(1): p. 168-77.

200. Andrew B. Lassar, B.M.P., Harold Weintraub, Transfection of a DNA locus that mediates the conversion of 10T1/2 fibroblasts to myoblasts. Cell, 1986. **47**(5): p. 649 - 656.

201. Tapscott SJ, D.R., Thayer MJ, Cheng PF, Weintraub H, Lassar AB, MyoD1: a nuclear phosphoprotein requiring a Myc homology region to convert fibroblasts to myoblasts. Science, 1988. **242**(4877): p. 405-11.

202. Munson R Jr, C.K., Glaser L, Multiple controls for the synthesis of muscle-specific proteins in BC3H1 cells. J Cell Biol, 1982. **92**(2): p. 350 - 356.

203. Helen M. Blau, C.J.E., Manipulation of myogenesis in vitro: Reversible inhibition by DMSO. Cell, 1979. **17**(1): p. 95- -108.

204. Fattaey AR1, H.K., Dembski MS, Dyson N, Harlow E, Vuocolo GA, Hanobik MG, Haskell KM, Oliff A, Defeo-Jones D, et al., Characterization of the retinoblastoma binding proteins RBP1 and RBP2. Oncogene, 1993. **8**(11): p. 1349-56.

205. Guha, M. and N.G. Avadhani, Mitochondrial retrograde signaling at the crossroads of tumor bioenergetics, genetics and epigenetics. Mitochondrion, 2013. **13**(6): p. 577-91.

206. S., D., Pathogenesis and treatment of mitochondrial myopathies: recent advances. Acta Myol., 2010. **29**(2): p. 333 - 338.

207. Kane, C.D., et al., Molecular characterization of novel and selective peroxisome proliferator-activated receptor alpha agonists with robust hypolipidemic activity in vivo. Mol Pharmacol, 2009. **75**(2): p. 296-306.

208. Chatterjee, A., E. Mambo, and D. Sidransky, Mitochondrial DNA mutations in human cancer. Oncogene, 2006. **25**(34): p. 4663-74.

209. Pagliarini, D.J., et al., A mitochondrial protein compendium elucidates complex I disease biology. Cell, 2008. **134**(1): p. 112-23.

APPENDIX

UIC UNIVERSITY OF ILLINOIS AT CHICAGO

January 31, 2013

Elizaveta Benevolenskaya
Biochemistry & Molecular Genetics
M/C 669

Office of Animal Care and
Institutional Biosafety Committees (MC 672)
Office of the Vice Chancellor for Research
206 Administrative Office Building
1737 West Polk Street
Chicago, Illinois 60612-7227

Dear Dr. Benevolenskaya:

The protocol indicated below has been reviewed in accordance with the Institutional Biosafety Committee Policies of the University of Illinois at Chicago on 11/15/2012. *The protocol was not initiated until final clarifications were reviewed and approved on* ***1/31/2013. Protocol expires 3 years from the date of review (11/15/2015). This protocol replaces protocol 09-094 which has been terminated.***

Title of Application: Role of RB Pathway in Differentiation

IBC Number: 12-085

Highest Biosafety Level: 2

Condition of Approval: The enclosed report indicates the training status for bloodborne pathogen (BBP) training and IATA shipping training. Only those personnel who have been trained and whose training has not expired are approved for work that may involve exposure to bloodborne pathogens and shipping potentially infectious material. Please note that federal regulations require yearly training for BBP; AND biennial training for IATA.

You may forward this letter of acceptable IBC verification of your research protocol to the funding agency considering this proposal. **Please be advised that investigators must report significant changes in their research protocol to the IBC office via a letter addressed to the IBC chair prior to initiation of the change. If a protocol changes in such a manner as to require IBC approval, the change may not be initiated without IBC approval being granted.**

Thank you for complying with the UIC's Policies and Procedures.

Sincerely,

Randal C. Jaffe, Ph.D.
Chair, Institutional Biosafety Committee

RCJ/mbb

Enclosures

Cc: IBC file

VITA

NAME: Michael L. Beshiri

EDUCATION: Bachelor of Arts, Biology
Assumption College, Worcester MA, 1999

Ph.D., Biochemistry and Molecular Genetics
University of Illinois, Chicago, IL, 2014

PUBLICATIONS: **Beshiri ML**, Islam A, DeWaal DC, Richter WF, Love J, Lopez-Bigas N, Benevolenskaya EV. Genome-wide analysis using ChIP to identify isoform-specific gene targets. *J Vis Exp.* 7;(41), pii: 2101 (2010).

Lin W, Cao J, Liu J, **Beshiri ML**, Fujiwara Y, Francis J, Cherniack AD, Geisen C, Blair LP, Zou MR, Shen X, Kawamori D, Liu Z, Grisanzio C, Watanabe H, Minamishima YA, Zhang Q, Kulkarni RN, Signoretti S, Rodig SJ, Bronson RT, Orkin SH, Tuck DP, Benevolenskaya EV, Meyerson M, Kaelin WG Jr, Yan Q. Loss of the retinoblastoma binding protein 2 (RBP2) histone demethylase suppresses tumorigenesis in mice lacking Rb1 or Men1. *Proc Natl Acad Sci U S A*. 108(33), 13379-86 (2011).

Beshiri ML, Holmes KB, Richter WF, Hess S, Islam AB, Yan Q, Plante L, Litovchick L, Gévry N, Lopez-Bigas N, Kaelin WG Jr, Benevolenskaya EV. Coordinated repression of cell cycle genes by KDM5A and E2F4 during differentiation. *Proc Natl Acad Sci U S A*. 109(45), 18499-504 (2012).

ABSTRACTS: **M.L. Beshiri**, Q. Yang, W.G. Kaelin, Jr, and E.V. Benevolenskaya. 2010. The Dynamic Role of RBP2 During Differentiation. Cold Spring Harbor Laboratory Meeting on Mechanisms & Models of Cancer. Abstracts of papers presented: 34.

Cao, J., J. Liu, **M.L. Beshiri**, E.V. Benevolenskaya, W.G. Kaelin, Jr., Q. Yan. 2010. Loss of histone demethylase RBP2 suppresses tumorigenesis. Cold Spring Harbor Laboratory Meeting on Mechanisms & Models of Cancer. Abstracts of papers presented: 239.

Beshiri, M.L., A.B.M.M.K. Islam, E.V. Benevolenskaya. 2012. Studying the histone demethylase RBP2 during RB-mediated differentiation. UIC Cancer Center Research Forum.

Benevolenskaya, E.V., **M.L. Beshiri**, A.B.M.M.K. Islam, N. Lopez-Bigas.. 2012. pRB function during differentiation is linked to epigenetic mechanisms. Cold Spring Harbor Laboratory Meeting on Mechanisms & Models of Cancer. Abstracts of papers presented: 24.

Beshiri, M.L., K.B Holmes, W.F Richter, A.B.M.M.K. Islam, L. Plante, L. Litovchick, N. Gévry, N.Lopez-Bigas, W.G. Kaelin Jr., E.V. Benevolenskaya. 2012. Coordinated repression of cell cycle genes by KDM5A and E2F4 during differentiation. Cold Spring Harbor Laboratory Meeting on Mechanisms & Models of Cancer. Abstracts of papers presented: 26.

Beshiri, M.L, Richter W.F., Abul B.M.M.K. Islam, Nuria Lopez-Bigas, and Elizaveta V. Benevolenskaya. pRB function during differentiation is linked to epigenetic mechanisms. UIC College of Medicine Research Forum.

Beshiri, M.L., A.B.M.M.K. Islam, E.V. Benevolenskaya. Studying the Histone Demethylase RBP2 During RB-Mediated Differentiation. UIC College of Medicine Research Forum.

Beshiri, M.L., Abul B.M.M.K. Islam, N.Lopez-Bigas, E.V. Benevolenskaya. October 12, 2012. The function of the tumor suppressor pRB during differentiation is linked to epigenetic mechanisms. 10th Annual CBC Symposium. Northwestern University, Chicago.

Beshiri, M.L., Abul B.M.M.K. Islam, N.Lopez-Bigas, E.V. Benevolenskaya. October 29-31, 2012. pRB function during differentiation is linked to epigenetic mechanisms. Cell Symposia Hallmarks of Cancer Meeting. Westin Market, San Francisco. Abstracts of papers presented: Breaking News.